UNIVERSITÀ
DEGLI STUDI
DI PADOVA

Sede Amministrativa: Università degli Studi di Padova
Sede Consorziata: Consiglio Nazionale delle Ricerche (CNR)

Dipartimento di Biologia

SCUOLA DI DOTTORATO DI RICERCA IN: BIOSCIENZE E BIOTECNOLOGIE
INDIRIZZO: BIOCHIMICA E BIOFISICA
CICLO XXIV

# BIOPHYSICAL ANALYSIS OF THE MODULATION OF CLC-K CHANNELS BY EXTRACELLULAR LIGANDS

**Direttore della Scuola:** Ch.mo Prof. Giuseppe Zanotti
**Coordinatore d'indirizzo:** Ch.mo Prof. Catia Sorgato
**Supervisore:** Ch.mo Prof. Ildikò Szabò

**Dottoranda:** Antonella Gradogna

# Table of Contents

# Summary

CLC proteins form a family of voltage-gated homodimeric $Cl^-$ transporters comprising both $Cl^-$ channels (ClC-0, ClC-1, ClC-2, ClC-Ka, ClC-Kb) and $Cl^-/H^+$-exchangers (ClC-3 to ClC-7) (Accardi & Miller, 2004; Picollo & Pusch, 2005; Scheel et al, 2005). They are involved in important physiological processes, such as transepithelial transport, membrane excitability, cell volume regulation, and luminal acidification of the endosomal-lysosomal system (Zifarelli & Pusch, 2007). CLC proteins are found in all phyla; in particular in humans there are nine CLC genes. The role of these proteins is highlighted by the diseases associated with mutations in CLC protein encoding genes (myotonia, Dent's disease, Bartter's syndrome, osteopetrosis) (Zifarelli & Pusch, 2007; Jentsch, 2008). The human $Cl^-$ channels ClC-Ka and ClC-Kb, as their murine orthologues ClC-K1 and ClC-K2, are expressed in the kidney and in the inner ear where they are involved in NaCl reabsorption (Kieferle et al, 1994) and in the endolymph production (Estévez et al, 2001), respectively. CLC-K channels are associated with a small $\beta$-subunit called barttin (Birkenhäger et al, 2001; Estévez et al, 2001). Mutations in ClC-Kb and barttin cause Bartter's syndrome, a kidney disease characterized by severe salt wasting and hypokalemia (Simon et al, 1997; Birkenhäger et al, 2001).

Because of their important physiological function, CLC-K channels are a potential pharmacological target. Among several chemical compounds that modulate CLC-K channels, niflumic acid (NFA), a known $Cl^-$ channel inhibitor, aroused our interest because of its unexpected effect on CLC-Ks. NFA blocks ClC-K1(Liantonio et al, 2004; Picollo et al, 2007), but surprisingly it increases ClC-Kb currents, and modulates ClC-Ka in a biphasic manner (Liantonio et al, 2006). To identify the residues responsible for the potentiating effect of NFA on ClC-Ka, we performed an extensive site-directed mutagenesis of ClC-Ka and voltage clamp measurements of the mutants expressed in *Xenopus* oocytes. The result of this work was the identification of three residues (L155, G345, and A349) which are involved in the potentiation by NFA (Zifarelli et al, 2010).

Extracellular calcium and protons modulate CLC-K channels in the physiological concentration range. In particular, the channels are activated by extracellular calcium and blocked by extracellular protons (Gradogna et al, 2010). Since the kidney has an

important role in calcium reabsorption and in the maintenance of acid-base balance (Frick & Bushinsky, 2003; Jeck et al, 2005), calcium and proton regulation of CLC-K channels is potentially of physiological relevance. We performed a detailed biophysical analysis of $Ca^{2+}$ and proton modulation of human CLC-K channels expressed in *Xenopus* oocytes. Experimental data showed an allosteric modulation of CLC-Ka for both, $Ca^{2+}$ and protons. Modeling predicted a two state (blocked/unblocked) mechanism for proton modulation, while a four-state mechanism could properly describe $Ca^{2+}$ modulation. An extensive mutagenic screen of ClC-Ka combined with voltage clamp measurements allowed us to identify two mutations, E261Q and D278N, which reduced calcium sensitivity of ClC-Ka. The proximity of the residues, E261 and D278, from different subunits suggested that they likely form an intersubunit $Ca^{2+}$ binding site. In fact the double mutant E261D/D278N was completely $Ca^{2+}$-insensitive. Moreover we identified a histidine, H497 responsible for the block of CLC-K channels at acidic pH (Gradogna & Pusch, 2010). We next decided to study the calcium effect on the other CLC-K channels. Human ClC-Kb displays a similar behaviour as ClC-Ka, while rat ClC-K1 is more calcium sensitive than the human CLC-Ks. The high sequence identity and the conserved calcium sensitivity suggested that the calcium binding site is a characteristic shared by all CLC-K channels. The double mutant E261Q/D278N of ClC-Kb and ClC-K1 completely abolished the calcium sensitivity supporting this hypothesis. To investigate the specificity of the $Ca^{2+}$ binding site I studied the effect of various divalent cations ($Zn^{2+}$, $Mg^{2+}$, $Ba^{2+}$, $Sr^{2+}$, $Mn^{2+}$) on ClC-Ka, ClC-K1, and ClC-Kb. Both WT ClC-Ka and the double mutant E261Q/D278N, were blocked by 5 mM $Zn^{2+}$ suggesting that $Zn^{2+}$ affects the channel interacting with a separate binding site. $Mg^{2+}$ did not activate CLC-K channels at concentrations up to 50 mM. In contrast, CLC-Ka and ClC-Kb were activated by $Ba^{2+}$, $Sr^{2+}$, and $Mn^{2+}$ with a rank order of potency $Ca^{2+}$>$Ba^{2+}$>$Sr^{2+}$. Interestingly, ClC-K1 showed an altered rank order $Ca^{2+}$> $Sr^{2+}$>> $Ba^{2+}$. Furthermore, the $Ca^{2+}$ insensitive double mutant, E261/D278, was also insensitive to $Ba^{2+}$ and $Sr^{2+}$ (Gradogna et al, 2010; Gradogna & Pusch, 2010) demonstrating the specificity of the mechanism of activation of CLC-K channels by $Ca^{2+}$ and the other divalent cations.

Finally, in collaboration with the group of Prof. Ildikò Szabò from the University of Padua, we tested the functional expression of the putative channel *sll0993* from the cyanobacterium *Synechocystis* sp. PCC6803 (Kaneko et al, 1996). The coding sequence of the protein and that of a C-terminal EGFP-fusion protein were inserted in vectors optimized for the expression in *Xenopus* oocytes and tested for functional expression in oocytes. Oocytes injected with EGFP-fusion protein yielded a significant level of fluorescence demonstrating that the protein was produced. Unfortunately, for neither construct, we could detect any currents above those seen in non-injected oocytes using the voltage clamp technique.

In summary, we have provided an extensive biophysical and molecular characterization of the mechanisms of regulation of CLC-K chloride channels by extracellular ligands. All experiments have been executed at the Institute of Biophysics of the Italian National Research Council in Genoa, Italy in the group of Dr. Michael Pusch.

# Riassunto

Le proteine CLC sono una famiglia di trasportatori del cloruro voltaggio dipendenti, omodimerici comprendenti sia canali del cloruro (ClC-0, ClC-1, ClC-2, ClC-Ka, ClC-Kb) che $Cl^-/H^+$scambiatori (da ClC-3 a ClC-7) (Accardi & Miller, 2004; Picollo & Pusch, 2005; Scheel et al, 2005). Essi sono implicati in importanti processi fisiologici come il trasporto epiteliale, l'eccitabilità di membrana, la regolazione del volume cellulare e l'acidificazione del lume del sistema endosomale-lisosomiale (Zifarelli & Pusch, 2007). Le proteine CLC sono espresse in tutti i phyla, in particolare nell'uomo ci sono nove geni che codificano proteine CLC. Il ruolo di queste proteine è messo in luce dalle malattie associate con mutazioni in corrispondenza dei geni codificanti proteine CLC (miotonia, malattia di Dent, sindrome di Bartter, osteopetrosi) (Zifarelli & Pusch, 2007; Jentsch, 2008). I canali del cloruro ClC-Ka e ClC-Kb, come i loro ortologhi murini ClC-K1 e ClC-K2, sono espressi nel rene e nell'orecchio interno dove essi sono rispettivamente coinvolti nel riassorbimento di NaCl (Kieferle et al, 1994) e nella produzione di endolinfa (Estévez et al, 2001). I canali CLC-K sono associati con una piccola subunità β chiamata barttin (Birkenhäger et al, 2001; Estévez et al, 2001). Mutazioni in ClC-Kb e barttin determinano la sindrome di Bartter, una malattia caratterizzata da perdita di sali ed ipokalemia (Simon et al, 1997; Birkenhäger et al, 2001). A causa della loro importante funzione fisiologica, i canali CLC-K rappresentano un potenziale bersaglio farmacologico. Tra i molti composti chimici che modulano i CLC-K, l'acido niflumico, un noto inibitore dei canali del cloruro, destava il nostro interesse a causa del suo inaspettato effetto sui CLC-K. NFA blocca ClC-K1(Liantonio et al, 2004; Picollo et al, 2007), ma sorprendentemente esso attiva le correnti di CLC-Kb e modula in modo bifasico CLC-Ka (Liantonio et al, 2006). Per identificare i residui aminoacidici responsabili dell'effetto attivatorio di NFA su ClC-Ka, noi eseguivamo una estensiva mutagenesi sito specifica di ClC-Ka e misure di voltage clamp dei mutanti espressi in oociti di Xenopus. Il risultato di questo lavoro era l'identificazione di tre residui (L155, G345, and A349) che sono coinvolti nel potenziamento attraverso NFA (Zifarelli et al, 2010).

Calcio extracellulare e protoni modulano i canali CLC-K in un intervallo di concentrazione fisiologica. In particolare i canali sono attivati da aumento di calcio

extracellulare e bloccati da pH acido extracellulare (Gradogna et al, 2010). Poichè il rene ha un ruolo importante nel riassorbimento di calcio e nel mantenimento dell'equilibrio acido-base (Frick & Bushinsky, 2003; Jeck et al, 2005), la regolazione da parte del calcio e dei protoni dei canali CLC-K è potenzialmente di rilevanza fisiologica. Noi eseguivamo una dettagliata analisi biofisica della modulazione da parte del $Ca^{2+}$ e dei protoni dei canali CLC-K dell'uomo espressi in oociti di *Xenopus*. I dati sperimentali mostravano che sia $Ca^{2+}$ che protoni modulano CLC-Ka in modo allosterico. Studi di modellistica indicavano un meccanismo a due stati (bloccato/non bloccato) per la modulazione dei protoni, mentre un modello comprendente quattro stati poteva descrivere in modo appropriato la modulazione da parte del calcio. Una estensiva analisi mutagenica combinata con misure di voltage clamp ci consentiva di identificare due mutazioni E261Q e D278N che riducevano la sensibilità al calcio di ClC-Ka. La vicinanza dei residui E261 e D278 appartenenti a differenti subunità suggeriva che probabilmente essi formano un sito di legame per il calcio intersubunità. Infatti il doppio mutante E261Q/D278N era completamente insensibile al calcio. Inoltre noi identificavamo una istidina, H497 responsabile per il blocco dei canali CLC-K causato dal pH acido (Gradogna & Pusch, 2010). Quindi decidevamo di studiare l'effetto del calcio sugli altri CLC-K. ClC-Kb presenta un comportamento simile a ClC-Ka, mentre ClC-K1 è più sensibile al calcio dei canali CLC-K dell'uomo. L'alta identità di sequenza e il fatto che la sensibilità al calcio è conservata tra i CLC-K suggeriva che il sito di legame per il calcio è una caratteristica condivisa da tutti i CLC-K. Il doppio mutante E261Q/D278N di ClC-Kb e ClC-K1 perdevano completamente la sensibilità al calcio confermando questa ipotesi. Per determinare la specificità del sito di legame del $Ca^{2+}$ studiavo l'effetto di vari cationi divalenti ($Zn^{2+}$, $Mg^{2+}$, $Ba^{2+}$, $Sr^{2+}$, $Mn^{2+}$) su ClC-Ka, ClC-K1e ClC-Kb. Sia ClC-Ka WT che il doppio mutante E261Q/D278N erano bloccati da 5 mM $Zn^{2+}$ suggerendo che lo ione $Zn^{2+}$ ha effetto sul canale interagendo con un sito di legame distinto. Lo ione $Mg^{2+}$ non attivava i canali CLC-K a concentrazioni fino a 50 mM. Invece ClC-Ka e ClC-Kb erano attivati da $Ba^{2+}$, $Sr^{2+}$e $Mn^{2+}$ con un ordine di potenziamento: $Ca^{2+}$>$Ba^{2+}$>$Sr^{2+}$. E' interessante osservare che ClC-K1 presentava un ordine di potenziamento modificato: $Ca^{2+}$> $Sr^{2+}$>> $Ba^{2+}$. Inoltre il doppio mutante E261Q/D278N, insensibile al $Ca^{2+}$, era anche insensibile al $Ba^{2+}$ and $Sr^{2+}$ (Gradogna

et al, 2010; Gradogna & Pusch, 2010) dimostrando la specificità del meccanismo di attivazione dei canali CLC-K attraverso lo ione calcio e gli altri cationi divalenti.
Infine, in collaborazione con il gruppo della Prof. Ildikò Szabò dell'Università di Padova, noi provavamo l'espressione funzionale del canale putativo *sll0993* del cianobatterio *Synechocystis* sp. PCC6803 (Kaneko et al, 1996). La sequenza codificante della proteina e quella della proteina con EGFP al C-terminale erano inserite in vettori ottimizzati per l'espressione in oociti di *Xenopus* e testati per quanto riguarda l'espressione funzionale. Oociti iniettati con la proteina fusa con EGFP presentavano un consistente livello di fluorescenza dimostrando che la proteina era prodotta. Sfortunatamente, per nessuno dei due costrutti, con la tecnica del voltage clamp, potevamo rilevare correnti superiori rispetto a quelle viste in oociti non iniettati.
Riassumendo, noi abbiamo effettuato una dettagliata caratterizzazione biofisica e molecolare dei meccanismi di regolazione dei canali del cloruro CLC-K attraverso ligandi extracellulari. Tutti gli esperimenti sono stati eseguiti presso l'Istituto di Biofisica del Consiglio Nazionale delle Ricerche a Genova (Italia) nel gruppo del Dott. Michael Pusch.

# 1 Introduction

## 1.1 Mechanisms of membrane transport

All living cells are surrounded by a lipid bilayer that protects the cell components from the outside environment; moreover eukaryotic cells contain additional internal lipid bilayers that delimit the intracellular organelles. Because of its fatty nature, the lipid bilayer allows passive movement of hydrophobic substances, while it is an insurmountable barrier for the passage of charged or polar molecules. Nevertheless, the exchanges of matter between the intracellular and the extracellular environment are essential for the cellular life. In fact nutrients and waste products continuously have to enter and leave the cell, respectively. Therefore the lipid bilayer is crossed by a variety of different ion-transporting proteins that allow the selective passage of inorganic ions and organic molecules (Hille, 2001; Zifarelli & Pusch, 2007). Traditionally, the transport mechanisms were grouped in two classes, carriers and pores. A carrier was thought as a ferryboat that moves across the membrane carrying ions and molecules, whereas a pore was thought as a water-filled hole that allows the passage of ions and molecules small enough to cross it (Hille, 2001). Currently, physiologists think that small movements within a carrier are enough to expose the binding site(s) for the substrate alternatively to the intracellular and extracellular side (Hille, 2001). On a thermodynamic ground, transport mechanisms can be divided into passive and active transporters. Passive transporters lower the free energy barrier associated with the diffusion of ions and small molecules across the lipid bilayer (Zifarelli & Pusch, 2007). Consequently, the flux of ions is very fast, often more than $1 \times 10^6$ $s^{-1}$. These passive transporters, ion channels, show high substrate selectivity, allowing only selected ions to flow passively down their electrochemical gradient. Moreover, ion channels generally respond to some stimulus of electrical, mechanical or chemical kind, which leads to the opening or closing of the ion pore. This important property of the channels is called “gating” (Hille, 2001). In spite of the high selectivity ion channels are extraordinary devices able to transport ions across the membrane with a rate close to the diffusion limit.

They are usually classified based on the main ion which they are selective for, for example $Na^+$ channels, $Cl^-$ channels, etc.

On the contrary, active transporters move ions or molecules against their electrochemical gradient. This process requires energy usually provided by ATP hydrolysis (primary active transport) or, alternatively, by the dissipation of concentration gradients previously established (secondary active transport). In the secondary transports, the "uphill" movement of ions or organic molecules happens by coupling this transport to a "downhill" movement of another ion. The capture and the release of the substrate at the opposite sides of the membrane require a cycle of conformational changes of the transporter and the overcoming of a higher barrier of energy compared to that of a typical ion channel. Consequently, the ion flux through transporters is slower than in ion channels (generally $< 1 \times 10^3$ $s^{-1}$). Another feature of active transport is the strict stoichiometry of the species moved.

These are the main characteristics attributed to the passive and active transporters. However, this distinction is not absolute. There are passive transporters with a low rate of passage of ions and, vice versa, active transporters with a high rate. The weakness of this distinction was confirmed by the discovery that the family of CLC proteins comprises both channels and active transporters with a very similar architecture (Accardi & Miller, 2004; Picollo & Pusch, 2005; Scheel et al, 2005).

New knowledge about the mechanisms of membrane transport can come from crystal structures. However, crystallizing membrane proteins is not trivial. In fact their isolation from the membrane, with which they maintain tight interactions, usually leads to a loss of the native three-dimensional structure (Baker, 2010). Nevertheless, prokaryotic membrane proteins are generally more stable than eukaryotic membrane proteins and nowadays many of them have been crystallized successfully. Crystal structures of bacterial membrane proteins often are good models to start studying the respective eukaryotic homologous proteins. Recently, the use of new detergents and alternative strategies (e.g. the introduction of stability-boosting mutations) allowed crystallizing even several eukaryotic membrane proteins (Baker, 2010). The crystal structures can be used in combination with functional electrophysiological studies to significantly increase the knowledge on ion channels and transporters.

## 1.2 CLC proteins

Chloride is the most abundant physiological anion (Hille, 2001). In most animal cells it is present at a low concentration in the cytoplasm and at a high concentration in the extracellular environment. For example, in mammalian skeletal muscle the intracellular chloride concentration is 4.2 mM whereas in general the extracellular chloride concentration is around 120 mM (Hille, 2001). As a result of its distribution, $E_{Cl}$, the chloride equilibrium potential is very negative and close to the resting potential of the cell. Consequently, $Cl^-$ channels tend to oppose the excitability of nerve and muscle cells, stabilizing a negative membrane potential (Hille, 2001; Zifarelli & Pusch, 2007). Several classes of proteins transport $Cl^-$ ions. In this introduction, I will only mention some examples of them before treating extensively the family of CLC proteins. In mammalian nerve cells, GABA receptors and glycine receptors are the most important anion channels. In the adult CNS, these receptors are in charge of fast inhibitory neurotransmission, while they have excitatory function in the developing nervous system when the neurons have an unusual high intracellular $Cl^-$ concentration (Jentsch et al, 2002; Zifarelli & Pusch, 2007). The "cystic fibrosis transmembrane conductance regulator", CFTR is a voltage-independent $Cl^-$ channel belonging to the class of ABC transporters that is expressed in the membrane of several epithelia (Jentsch et al, 2002; Zifarelli & Pusch, 2007). Mutations in the gene coding for CFTR are responsible for cystic fibrosis (Riordan et al, 1989), an inherited chronic disease that affects the lungs and digestive system. $Ca^{2+}$ activated $Cl^-$ channels, CaCCs, are found in many cell types including epithelia, smooth muscle, and sensory receptors (Ferrera et al, 2010). CaCC activation leads to membrane depolarization (Hartzell et al, 2005; Ferrera et al, 2010). For many years it was tried to find out the proteins associated with CaCC activity, but only quite recently TMEM 16A was identified as a component of CaCCs (Caputo et al, 2008; Schroeder et al, 2008; Yang et al, 2008). These are just few examples of the vast and variegated world of the chloride channels being present in mammalian cells.

The first knowledge of the CLC proteins occurred by chance in the course of experiments that Miller and coworkers performed to investigate the acetylcholine-gated cation channels (White & Miller, 1979). They added membrane vesicles from

the electric organ of *Torpedo californica* to planar phospholipid bilayer. The voltage-clamp measurements performed on this prepared revealed a voltage-dependent anion selective conductance (White & Miller, 1979). Further studies showed that the plasma membranes of the electrocytes from *Torpedo* are extremely rich in a specific kind of $Cl^-$ channel (later called ClC-0). Interestingly, single channel measurements showed three different, equally spaced levels of conductance. This unusual behavior suggested that the channel was a dimer with two identical and independent $Cl^-$ diffusion pathways (Miller & White, 1980; Miller, 1982; Hanke & Miller, 1983). Moreover, the channel exhibited alternating periods of activity (bursts) with periods of no activity suggesting that the two conduction pathways (called protochannels) were not independent. It was believed that there is an additional mechanism that closes both protochannels simultaneously (Miller & Richard, 1990). These hypotheses have been confirmed by the following works on the CLC proteins (Zifarelli & Pusch, 2007). Despite the importance of these first studies, it was the cloning of the channel from *Torpedo marmorata*, called ClC-0 (Jentsch et al, 1990), that gave the determining boost to the knowledge about chloride channels. In fact, several other CLC proteins belonging to all phyla were identified by homology screening based on the sequence of the *Torpedo* chloride channel (Jentsch et al, 1999; Maduke et al, 2000).

For the following introduction of the CLC protein family, I partially used the introduction from the following review article:

Gradogna A, Pusch M. (2010) Molecular pharmacology of kidney and inner ear CLC-K chloride channels. Frontiers in Pharmacology 1:130, pp. 1-2.

The contents was expanded where it was believed to be useful for the general understanding.

CLC proteins form a family of voltage-gated $Cl^-$ channels and $Cl^-/H^+$-exchangers involved in important physiological processes, including transepithelial transport, membrane excitability, cell volume regulation and luminal acidification of the endosomal-lysosomal system (Zifarelli & Pusch, 2007). They are expressed in all phyla, in particular mammal express nine CLC proteins (Jentsch, 2008). Based on sequence homology, these proteins are grouped into three branches. The first branch comprises $Cl^-$ channels (ClC-1, ClC-2, ClC-Ka and ClC-Kb) that localize to the

plasma membrane, while the members of the two other branches (ClC-3 to ClC-5), and (ClC-6 and ClC-7) are $Cl^-/H^+$-exchangers and reside in the membranes of the endosomal/lysosomal system (Jentsch et al, 2002; Jentsch, 2008). Knockout mouse models and human diseases have provided insights into the physiological role of CLC proteins. Mutations in four of the nine human CLC genes underlie inherited diseases. CLC-1 mutations cause myotonia; mutations in CLC-Kb and in *BSDN*, the gene encoding barttin, determine different forms of Bartter's syndrome with renal salt loss; CLC-5 mutations are responsible for Dent's disease; mutations of CLC-7 lead to osteopetrosis (Zifarelli & Pusch, 2007; Jentsch, 2008). Here I shortly list the known human CLC proteins with a very brief comment. ClC-1 is a 994 amino acid protein that shows 54% sequence identity with the *Torpedo* ClC-0 channel (Steinmeyer et al, 1991). It is predominantly expressed in skeletal muscle where it is important for repolarizing the membrane voltage after an action potential and for stabilizing the resting membrane potential. Mutations in the gene encoding ClC-1 cause myotonia, a disease characterized by muscle hyperexcitability (Jentsch, 2008). ClC-2 is a 907 amino acid protein that shares 49% identity with ClC-0. It is broadly expressed in the plasma membrane of epithelia, neurons, glia, and heart (Thiemann et al, 1992). ClC-2 currents are activated by membrane hyperpolarization, cell swelling, and moderately acidic extracellular pH (Zifarelli & Pusch, 2007; Jentsch, 2008). Despite the broad distribution of this channel, its role is still unclear. *Clcn2*$^{-/-}$ mice show retinal and testicular degeneration (Bösl et al, 2001), and leukoencephalopathy, a widespread vacuolation of the white matter in the brain and spinal cord (Blanz et al, 2007). ClC-K channels will be treated in detail later. The members of the second homology branch of the CLC family (ClC-3, ClC-4, ClC-5) are $Cl^-/H^+$ antiporters expressed in the membranes of the endocytic system; ClC-3 is additionally found in synaptic vesicles. The knowledge about the functional properties of these proteins mainly arises from their ability to reach the plasma membrane upon heterologous expression. The almost exclusive intracellular localization of ClC-3 did not allow a detailed biophysical characterization of its currents (Li et al, 2000). Even though ClC-3 is broadly expressed in many tissues, its role is not clear (Jentsch, 2008). There are no human diseases associated with ClC-3 mutations; however Clcn3$^{-/-}$ mice showed degeneration of the hippocampus and loss

of the photoreceptors (Stobrawa et al, 2001). In addition to this, other phenotypes have been reported making difficult to establish the role of ClC-3 (Jentsch, 2008). Unlike ClC-3, ClC-4 and ClC-5 reach the plasma membrane upon heterologous expression allowing their electrophysiological analysis. Both of them yield strongly outwardly rectifying currents. ClC-4 is broadly expressed in many tissues, mainly in brain, liver and kidney, while ClC-5 is found in the epithelia of the kidney and intestine. The physiological role of ClC-4 is still unclear (Zifarelli & Pusch, 2007; Jentsch, 2008). The fact that mutations of ClC-5 cause Dent disease, an X-linked hereditary disorder associated with proteinuria and kidney stones, highlights the involvement of ClC-5 in the reabsorption of small proteins at level of the proximal tubule in the kidney (Fisher et al, 1994; Lloyd et al, 1996). The third branch of CLC proteins comprises ClC-6 and ClC-7. ClC-6 is expressed in the nervous system (Poët et al, 2006), while ClC-7 colocalizes with the β-subunit Ostm1 in late endosomes/lysosomes of many tissues, in particular it is highly expressed in osteoclasts, the cells responsible for bone degradation. There are no human diseases associated with ClC-6, however $Clcn6^{-/-}$mice revealed a lysosomal storage disease with lipofuscin accumulation (Poët et al, 2006). In contrast, mutations of the gene *CLCN7* encoding ClC-7 cause osteopetrosis (Kornak et al, 2001). The exclusive intracellular localization of ClC-6 and ClC-7/Ostm1did not allow their biophysical characterization. However, recently ClC-7/Ostm1expression in plasma membrane was obtained by disrupting some leucines belonging to the lysosomal sorting motifs in the N-terminus of ClC-7 (Stauber & Jentsch, 2010). Based on this strategy, strongly outwardly rectifying currents from ClC-7 were measured and a basic characterization of ClC-7 was performed (Leisle et al, 2011).

All CLC proteins share several basic features. Structurally, they share the same homodimeric architecture (Ludewig et al, 1996; Middleton et al, 1996; Weinreich & Jentsch, 2001), in which each of two identical subunits contains an independent anion permeation pathway (‘double-barreled channel’); even though some CLC proteins require small *β*-subunits (barttin and ostm1) for proper function (Estévez et al, 2001; Waldegger et al, 2002; Lange et al, 2006), the basic mechanisms of ion conduction are mostly dependent of the CLC α-subunits. So far all CLC proteins that have been functionally investigated, appear to be practically completely

impermeable to cations (except protons, see below). The open probability of the CLC channels is regulated by two distinct gating mechanisms: a 'protopore gate' or 'fast gate' (in CLC-0) closes individual pores, an additional, slow (or common) gate closes both pores simultaneously. If similar gating mechanisms are present also in CLC transporters, like the human CLC-5 $Cl^-/H^+$ antiporter or the plant CLC-a $NO_3^-/H^+$ antiporter, is still unclear (De Angeli et al, 2006; Zdebik et al, 2008; Alekov & Fahlke, 2009; De Angeli et al, 2009; Zifarelli & Pusch, 2009b; Picollo et al, 2010). Important structural and functional information was provided by the crystal structures of bacterial CLCs (Dutzler et al, 2002; Dutzler et al, 2003). Each monomer consists of 18 intramembrane α-helices (labelled A-R) and exhibits a complex topology. Each subunit presents an internal pseudo-twofold symmetry with the two halves spanning the membrane in opposite directions. Each subunit bears three distinct $Cl^-$ binding sites which can be occupied simultaneously, called $S_{int}$, $S_{cen}$, $S_{ext}$ (Dutzler et al, 2002; Dutzler et al, 2003; Lobet & Dutzler, 2006; Picollo et al, 2009). In the crystal structure of CLC-ec1, $S_{ext}$ was found to be occupied by the side chain of the conserved glutamate 148. When E148 was mutated to alanine or glutamine the same site was occupied by a $Cl^-$ ion and the ion conduction pathway was open (Dutzler et al, 2003). In fact, in most CLC proteins, selective conduction and gating are intimately coupled: the permeant ions directly affect gating (Pusch et al, 1995) and the critical E148 is the main determinant of the 'fast gate' (Dutzler et al, 2003). Interestingly, in contrast to most CLC-channels and CLC-transporters, CLC-K channels have a hydrophobic residue (valine) in place of the critical glutamate (Waldegger & Jentsch, 2000; Zifarelli & Pusch, 2007; Jentsch, 2008). The common characteristics of CLC proteins initially led to the implicit assumption that the family is composed of only $Cl^-$ channels. Surprisingly, Accardi and Miller (2004) discovered that CLC-ec1 is a $Cl^-/H^+$ exchanger. Subsequent studies have shown that also several eukaryotic CLC proteins are anion/proton antiporters (Picollo & Pusch, 2005; Scheel et al, 2005; De Angeli et al, 2006; Neagoe et al, 2010), demonstrating that two different transport mechanisms can be based on the same molecular architecture. In contrast to the bacterial CLC-ec1, all eukaryotic and some prokaryotic CLC proteins have large C-terminal intracellular domains which bear two so-called CBS domains (Estévez & Jentsch, 2002). These domains have been

found to bind adenine nucleotides in isolated CLC-5 and CLC-2 C-terminals fragments (Scott et al, 2004; Wellhauser et al, 2006; Meyer et al, 2007) and adenine nucleotides affect the function of CLC-1 (Bennetts et al, 2005; Bennetts et al, 2007; Tseng et al, 2007), CLC-5 (Zifarelli & Pusch, 2009b), and the plant atCLC-a (De Angeli et al, 2009). However, the CBS domains of CLC-Ka do not appear to bind nucleotides (Markovic & Dutzler, 2007), and no consistent effects of intracellular nucleotides on CLC-K function have been described so far. Recently, two groups independently determined the crystal structure of two CLC proteins: a CLC $Cl^-/H^+$ antiporter from the cyanobacterium *Synechocystis* sp. PCC6803 (Jayaram et al, 2011), and a $Cl^-/H^+$ antiporter from the thermophilic red alga *Cyanidioschyzon merolae* (Feng et al, 2010). The availability of these new structures will increase the insight about the CLC family, in particular the structure of the eukaryotic CLC protein will supply information regarding the large intracellular portions of CLC proteins.

## 1.3 CLC-K channels

### *1.3.1 Cloning and basic knowledge*

Since the cloning of ClC-0 from the electric organ of *Torpedo marmorata* (Jentsch et al, 1990), in short time homologous chloride channels from several species were isolated. Since the electric organ derives from skeletal muscle, initially the researchers focused on mammalian muscle and could clone the rat muscle $Cl^-$ channel, ClC-1 (Steinmeyer et al, 1991). Extending the research to other tissues, ClC-2 was isolated from rat heart and brain (Thiemann et al, 1992). In the kidney there is a massive reabsorption of NaCl, consequently the renal epithelium was expected to have several chloride conductances. The first CLC-K channel, rClC-K1 was cloned by a reverse transcription-polymerase chain reaction (RT-PCR) strategy using rat kidney mRNA (Uchida et al, 1993). A rat kidney cDNA library screen with PCR fragments led to identify ClC-K1 (Uchida et al, 1993). The amino acid identity is 39% with the Torpedo channel (ClC-0), 41% with ClC-1, and 43% with ClC-2 (Uchida et al, 1993). By a similar strategy, based on sequence homology, rat ClC-K2 and the human ClC-Ka and ClC-Kb were cloned from rat and human kidney, respectively (Kieferle et al, 1994). The membrane topology and thus the protein architecture of ClC-K channels are similar to that of other members of the CLC protein family. Compared with ClC-0, -1, and -2, CLC-K channels are smaller proteins of 687 amino acids (Kieferle et al, 1994). Human ClC-Ka and ClC-Kb share 90% of identity in nucleic acid and amino acids sequences whereas they have 80% identity to rodent ClC-K1 and ClC-K2 (Kieferle et al, 1994). As both CLC-K genes are located next to each other at chromosome 1p36 and have high degree of homology, it can be supposed that they were created by gene duplication from a common ancestor (Kobayashi et al, 2002). Moreover the functional correspondence between the rat and the human channels was established in transgenic mice. The authors showed that the promoter of the human ClC-Kb gene could drive the reporter gene expression (green fluorescence protein gene, EGFP) in the specific cell types where expression of ClC-K2 was reported. These results confirmed that ClC-Kb is the human homologue of rat and mouse ClC-K2 (Kobayashi et al, 2002). CLC-K channels are expressed in the kidney and in the inner ear where they co-assemble

with the β-subunit barttin (Uchida et al, 1993; Kieferle et al, 1994; Birkenhäger et al, 2001; Estévez et al, 2001). This subunit was, however, discovered only in 2001 (see below). The exact location of CLC-K channels was established by immunohistochemistry using polyclonal CLC-K channels antibodies. However, the antibodies cannot distinguish between the various CLC-K isoforms. Therefore the different distribution of these isoforms along the rat nephron was deduced by reverse transcription (RT-PCR) strategy on rat kidney mRNA (Uchida et al, 1993; Kieferle et al, 1994). In the kidney, rat/mouse ClC-K1 (probably corresponding to human ClC-Ka) is found in the thin ascending limb of Henle's loop of the nephron, whereas ClC-K2 (corresponding to ClC-Kb) is only expressed in the basolateral membranes of epithelial cells in the thick ascending limb (TAL), connecting tubule, distal convoluted tubule and intercalated cells (Uchida et al, 1995; Kobayashi et al, 2001). Reverse transcription of mRNA and immunofluorescence data from the inner ear revealed that in the inner ear both isoforms are expressed in basolateral membranes of marginal cells of the stria vascularis and in dark cells of the vestibular organ (Estévez et al, 2001). Analysis of DNA samples of patients affected by Bartter's syndrome, an inherited renal disease, demonstrated that this phenotype could be associated with mutations in the gene *CLCNKB* coding for ClC-Kb (Simon et al, 1997).

### *1.3.2 Bartter'syndrome and the discovery of barttin*

Bartter's syndrome is an autosomal recessive disease characterized by defective renal reabsorption of sodium chloride in the thick ascending limb (TAL) of Henle's loop. Previously, it had been associated with loss-of-function mutations in two genes encoding transporters from this segment of the nephron, the Na-K-2Cl cotransporter and the ROMK potassium channel (Simon et al, 1996a; Simon et al, 1996b). Since several subjects affected by Bartter's syndrome did not show mutations in these proteins, the research was extended also to the chloride channels ClC-Ka and ClC-Kb. DNA screening identified deletions, non-sense and missense mutations in ClC-Kb able to cause Bartter's syndrome type III (Simon et al, 1997). Further studies identified a gene locus of a fourth variant of Bartter's syndrome, called *BSDN,* mapped to chromosome 1p32. *BSDN* encodes an integral membrane protein, barttin,

formed of 320 amino acids with two putative transmembrane α-helices (Birkenhäger et al, 2001). Barttin acts as an essential β-subunit for ClC-K channels, with which it co-localizes in basolateral membranes of renal tubules and of potassium-secreting epithelia of the inner ear (Estévez et al, 2001). Deletions, truncations, and missense mutations in the N-terminal part of barttin are associated with Bartter's syndrome type IV characterized by congenital deafness and renal failure (Birkenhäger et al, 2001). To date, human diseases associated with ClC-Ka mutations have not been described. However, mice in which the *Clcnk1* gene coding ClC-K1 was deleted, develop nephrogenic diabetes insipidus, (Matsumura et al, 1999). Moreover a digenic defect in the genes encoding ClC-Ka and ClC-Kb results in a phenotype that mimics Bartter's syndrome with deafness arising from defects in barttin. This suggests a mutual compensation of CLC-K channels in the cells of the inner ear that co-express ClC-Ka (ClC-K1) and ClC-Kb (ClC-K2) (Schlingmann et al, 2004).

### *1.3.3 ClC-K channel functions in the kidney*

Two main locations were found for CLC-K channels: the kidney and the inner ear. Basic information on these organs is useful to understand the role of CLC-K channels in these sites. The kidneys filter the blood, excreting waste products of the metabolism (e.g. urea). Moreover they fulfill homeostatic functions such as the regulation of ion concentrations, the maintenance of acid-base balance, and the regulation of blood pressure. The kidneys also are responsible for the reabsorption of water, glucose, and amino acids, which are freely filtered at the glomerulus. They work in concert with the endocrine system and they themselves produce hormones (calcitriol and erythropoietin) and the enzyme renin. The kidney's functions are accomplished by mechanisms of filtration, reabsorption, and secretion, which take place in the nephron, the basic functional component of the kidney. As a consequence of the process of filtration at the level of the Bowman's capsule, the kidney generates 180 liters of filtrate per day. The homeostasis of the organism is kept by a massive, diversified reabsorption of ions and water which takes place in the various segments of the nephron. The result of these combined processes is the generation of only 2 liters of urine per day. Consequently, the renal tubule epithelial cells are polarized cells specialized in the movement of solutes and water from the

tubular lumen to the blood and vice versa. Because of their function, they require a matching system of transporters targeted specifically to the apical or basolateral membranes (facing the tubular lumen and the interstitial space, respectively). Since NaCl reabsorption occurs in the kidney, this organ is the preferential expression site for several CLC channels and exchangers. ClC-K1 (ClC-Ka) is found in the thin ascending limb of Henle's loop of the nephron, whereas ClC-K2 (ClC-Kb) is only expressed in the basolateral membranes of epithelial cells in the thick ascending limb of Henle's loop (TAL), connecting tubule, distal convoluted tubule (DCT) and intercalated cells from collecting duct system (CCD) (Uchida et al, 1995; Kobayashi et al, 2001). In particular the thick ascending limb of Henle's loop (TAL) is a major site of NaCl reabsorption in the kidney. Here the basolateral Na/K-ATPase pump establishes an electrochemical $Na^+$ gradient. Exploiting this gradient, the apical Na-K-2Cl co-transporter (NKCC2) transports $Na^+$, $K^+$, and $Cl^-$ from the tubular lumen into the epithelial cell. The recycling of the co-transported $K^+$ ions takes place by the apical $K^+$ channel (ROMK). While $Na^+$ is secreted over the basolateral membrane by the Na/K-ATPase, $Cl^-$ leaves the cell trough the basolateral ClC-Kb/barttin $Cl^-$ channels (Jentsch, 2008) (Fig. 1.1).

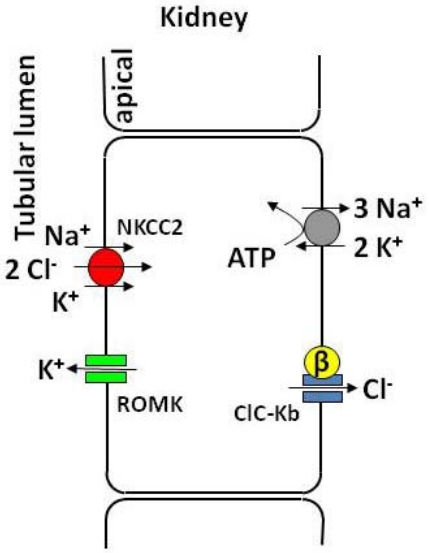


**Fig. 1.1 Transport model for NaCl reabsorption in the TAL** (from Gradogna and Pusch, 2010).

The concerted action of several transporters allows NaCl reabsorption also in the distal convoluted tubule (DCT). As in the TAL, the $Na^+$ gradient generated by the Na/K-ATPase is utilized by a cotransporter (NCCT) to move $Na^+$, $Cl^-$ ions into the epithelial cells. $Cl^-$ ions are released via ClC-Kb/barttin channels (Jeck et al, 2005). Because ion transport mechanisms are tightly connected to each other, mutations affecting the transporters involved in NaCl reabsorption underlie several types of the Bartter syndrome with renal salt wasting and secondary hypokalemia. The $K^+$ wasting resulting in low $K^+$ concentration in the blood is the most serious feature of this disease. The failure of the NaCl reabsorption in the TAL causes an increased reabsorption at the level of the collecting duct (CCD). Consequently, in the CCD, $K^+$ ions are released into the tubular lumen to compensate the intracellular $Na^+$ increase. As a consequence of hypokalemia patients can develop metabolic alkalosis. In fact, the direct effects of low $K^+$ concentration include stimulation of proximal tubule $HCO_3^-$ reabsorption and ammoniagenesis, proton secretion in the CCD, and inhibition of aldosterone secretion. Another feature of Bartter's syndrome is the low blood pressure resulting from the renal salt wasting. Hypotension activates the renin-angiotensin-aldosterone system whose function is the regulation of the blood pressure. Nevertheless, in Bartter's syndrome patients this system cannot adjust the pressure because it works only partially. The release of renin and the production of angiotensin are maintained, but the secretion of aldosterone is dampened by potassium depletion (Deschenes & Fila, 2011).

### *1.3.4 $Ca^{2+}$ reabsorption in the kidney*

Several mechanisms regulate $Ca^{2+}$ homeostasis. Bone, intestine, and kidney determine the plasma $Ca^{2+}$ concentration that normally ranges from 2.25 to 2.65 mM. In the plasma, calcium is protein bound, complexed with bicarbonate and other anions, and only ~50% is "free" in solution (the free concentration is 1.2-1.3 mM), and thus filterable at the renal glomerulus (Vargas-Poussou et al, 2002). $Ca^{2+}$ reabsorption happens at the level of the proximal tubule (PT) (~70% of filtered calcium), at the thick ascending limb of Henle's loop (TAL) (~20%), with the remaining at the more distal segments. In the PT and TAL $Ca^{2+}$ reabsorption occurs through paracellular routes, driven by the lumen positive voltage. In particular in the

TAL, $Na^+$, $K^+$, $Cl^-$ transport from the tubular lumen into the cell mediated by NKCC2 cotransporter matched with $K^+$ recycling into the luminal fluid results in a positive voltage in the luminal fluid. Instead, at the level of the distal tubule and of the connecting tubule, calcium transport occurs via transcellular mechanisms. Calcium ions enter the cell from the luminal fluid via an apical calcium channel, while they are actively transported into the interstitial space by a $Ca^{2+}$-ATPase and a $Na^+/Ca^{2+}$ exchanger (Frick & Bushinsky, 2003). An impairment of NaCl transport leads to an abnormal $Ca^{2+}$ absorption suggesting that $Ca^{2+}$ reabsorption and CLC-K function can be interrelated.

### *1.3.5 The role of the kidney in the acid-base regulation - briefly*

The processes of the metabolism normally generate excess acid equivalents. That happens directly by the oxidation of amino acids or indirectly via the generation of carbon dioxide, $CO_2$. In fact $CO_2$ rapidly reacts with water to form carbonic acid and then hydrogen and bicarbonate ions according the reaction:

$$CO_2 + H_20 \leftrightarrow H_2CO_3 \leftrightarrow HCO_3^- + H^+ \quad (1.1)$$

Since hydrogen ions can combine with the negatively charged and basic side chains of the proteins modifying their function, several mechanisms act to maintain the pH in the normal range (plasma pH =7.35 to 7.45). The weak carbonic acid and bicarbonate, its conjugate base, represent the most important buffering system in the body. Other buffers are hydrogen phosphate, ammonia, proteins such as albumin and hemoglobin that binds $CO_2$ and $H^+$. Acid-base imbalances can be rapidly compensated by changing the rate of ventilation. This reduces the concentration of carbon dioxide in the blood, restoring also pH. Besides the respiratory system, the kidney can regulate the pH of the organism by several mechanisms (the reabsorption of bicarbonate, $H^+$ secretion, and the production (ammoniagenesis) and excretion of $NH_4^+$). In particular, since bicarbonate ions are freely filtered by the glomerulus, $HCO_3^-$ reabsorption and $H^+$ secretion continuously take place into the tubular lumen to prevent the depletion of the buffering capacity and the acidosis of the blood. According to the reaction (1.1), in the tubular lumen, filtered bicarbonate combines with secreted hydrogen ions forming $CO_2$ and water. $CO_2$ can diffuse into the epithelial cells and here the inverse reaction (1.1) between $CO_2$ and $H_2O$ takes place

leading to $HCO_3^-$ regeneration. Finally bicarbonate ions exit from the cell across the basolateral membrane via a $3HCO_3^-/Na^+$ symporter and return into the blood, while $H^+$ are secreted into the tubular lumen by $Na^+/H^+$ antiporter and $H^+$-ATPase. $HCO_3^-$ reabsorption is found mainly at the proximal tubule, but also at the thick ascending limb of Henle's loop and, at the more distal segments of the nephron (Koeppen, 2009). Keeping in mind the involvement of the kidney in pH regulation, it is likely that the modulation of CLC-K channels by pH is of physiologic relevance.

### *1.3.6 ClC-K channel functions in the inner ear*

The ear translates air pressure variations, sound, into fluid movements and finally into electrical nerve impulses sent to the brain. Moreover it plays a major role in sensing balance and body position. To fulfill its functions the ear shows a refined architecture with specialized areas and peculiar strategies. In particular, I would like to focus on the portion of the inner ear, the cochlea, where the last step of this process of signal translation occurs. The cochlea is formed by three different regions: the scala media filled with the endolymph, the scala vestibuli and the scala tympani both containing the perilymph. Initially, sound is transmitted to the perilymph, then it propagates to the endolymph by the vibrations of the basilar membrane located between the scala tympani and the scala media. Perilymph has normal characteristics of an extracellular fluid, whereas the endolymph is unusually rich in $K^+$ (~140 mM) and is held at a positive potential of ~80 mV with respect to the normal extracellular space (Rickheit et al, 2008; Zdebik et al, 2009). Both properties are generated by the multilayered epithelium of the stria vascularis in the lateral wall of the scala media. Here, several transporters contribute to maintain these factors (high $K^+$ concentration and high potential), which are essential for the stimulation of hair cells and sound transmission (Fig. 1.2) (Gradogna & Pusch, 2010).

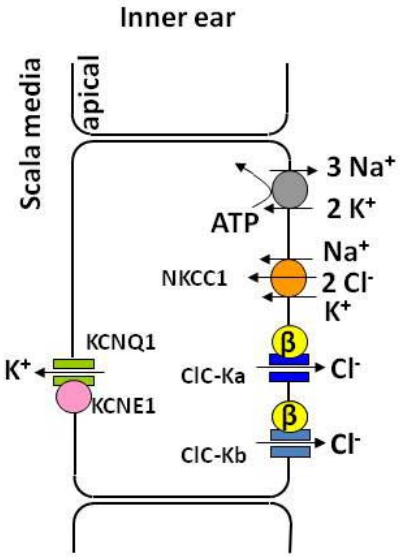


**Fig. 1.2 Transepithelial $K^+$ transport model for in the inner ear** (from Gradogna and Pusch, 2010).

Potassium ions are actively taken up from the intrastrial space into the marginal cells through the $Na^+/K^+$-ATPase and the $Na^+/K^+/2Cl^-$ cotransporter NKCC1. $K^+$ ions are released into the endolymph via apical KCNQ1/KCNE1 $K^+$ channels, while chloride ions are recycled at the basolateral membrane by ClC-Ka/barttin and ClC-Kb/barttin channels (Rickheit et al, 2008; Zdebik et al, 2009) (Fig. 1.2).

The transduction of the mechanical signal to an electrical signal happens at the level of the organ of Corti. This contains the sensory hair cells and the outer hair cells whose function is the signal amplification. Inner and outer hair cells, supplied with stereocilia, rest on the basilar membrane and lie under the tectorial membrane. Sound-induced motions of the basilar membrane cause deflections of the stereocilia embedded in the tectorial membrane. In response to this mechanical stimulus, $K^+$ channels open, $K^+$ ions enter and the hair cell is depolarized. Depolarization leads to the opening of voltage-gated $Ca^{2+}$ channels, and then to the release of neurotransmitter (glutamate) at the synapses on to the afferent neuron (Forge & Wright, 2002). In this way, the sound wave is transduced into a nervous stimulus. Interestingly, the hair cell depolarization is caused by $K^+$ ions, instead $Na^+$ ions as in nerve and muscle. This is a convenient solution, because in this way the organ of Corti does not need to extrude continuously $Na^+$ by the energy-consuming $Na^+/K^+$-ATPase (Rickheit et al, 2008; Zdebik et al, 2009). Impaired ion transport across the

stria vascularis might cause deafness. In particular, mutations in barttin, the β-subunit of CLC-K channels, cause Bartter's syndrome type IV with deafness (Estévez et al, 2001). Similarly, simultaneous mutations in ClC-Ka and ClC-Kb cause Bartter's syndrome IV with the same phenotype (Schlingmann et al, 2004). In order to establish the mechanism leading to deafness, Rickheit et al. (2008) generated a mouse model in which barttin is deleted in the inner ear, but not in the kidney. Similar to patients with Bartter IV, these mice displayed congenital deafness. Interestingly, the potassium concentration of the endolymph was maintained, while the endocochlear potential was reduced. This drastic decrease reduced the driving force for $K^+$ entry into hair cells causing degeneration of hair cells and deafness (Rickheit et al, 2008). CLC-K/barttin $Cl^-$ channels are also expressed in $K^+$-secreting dark cells of the vestibular organ (Estévez et al, 2001). The structural and functional arrangement of the vestibular system is similar to the cochlea. As in the cochlea, the vestibular endolymph is rich in $K^+$. The dark cells are essentially identical morphologically and functionally to the marginal cells of the stria (Forge & Wright, 2002). Nevertheless, the lack of CLC-K/barttin in mouse model does not cause vestibular hair cell degeneration and a strong vestibular phenotype (Rickheit et al, 2008).

### *1.3.7 Functional expression of CLC-K channels*

When the cDNA of CLC-K channels was isolated (Uchida et al, 1993; Kieferle et al, 1994), functional expression of these proteins was tested in *Xenopus* oocytes. This strategy was already successfully used for the other CLC proteins cloned (ClC-0 from *Torpedo*, mammalian ClC-1 and ClC-2 (Jentsch et al, 1990; Steinmeyer et al, 1991; Thiemann et al, 1992).) Uchida *et al*. reported that expression of rat ClC-K1 in *Xenopus* oocytes induced chloride currents (Uchida et al, 1993). Two-electrode voltage clamp measurements revealed that ClC-K1 was activated instantaneously by both hyperpolarizing and depolarizing voltage (Fig. 1.3A). Steady-state currents plotted versus voltage showed a slight outwardly rectifying current-voltage relationship (Uchida et al, 1993). Based on the current measured at the same potential after partial replacements of extracellular chloride by other anions, the conductance sequence was $Br^- > NO_3^- \geq Cl^- > I^-$ (Uchida et al, 1993; Waldegger &

Jentsch, 2000). Instead an anion permeability sequence $Cl^- > Br^- > NO_3^- > I^-$ was calculated based on reversal potential measurements upon substitution of $Cl^-$ with different anions using a modified Goldmann equation (Waldegger & Jentsch, 2000).

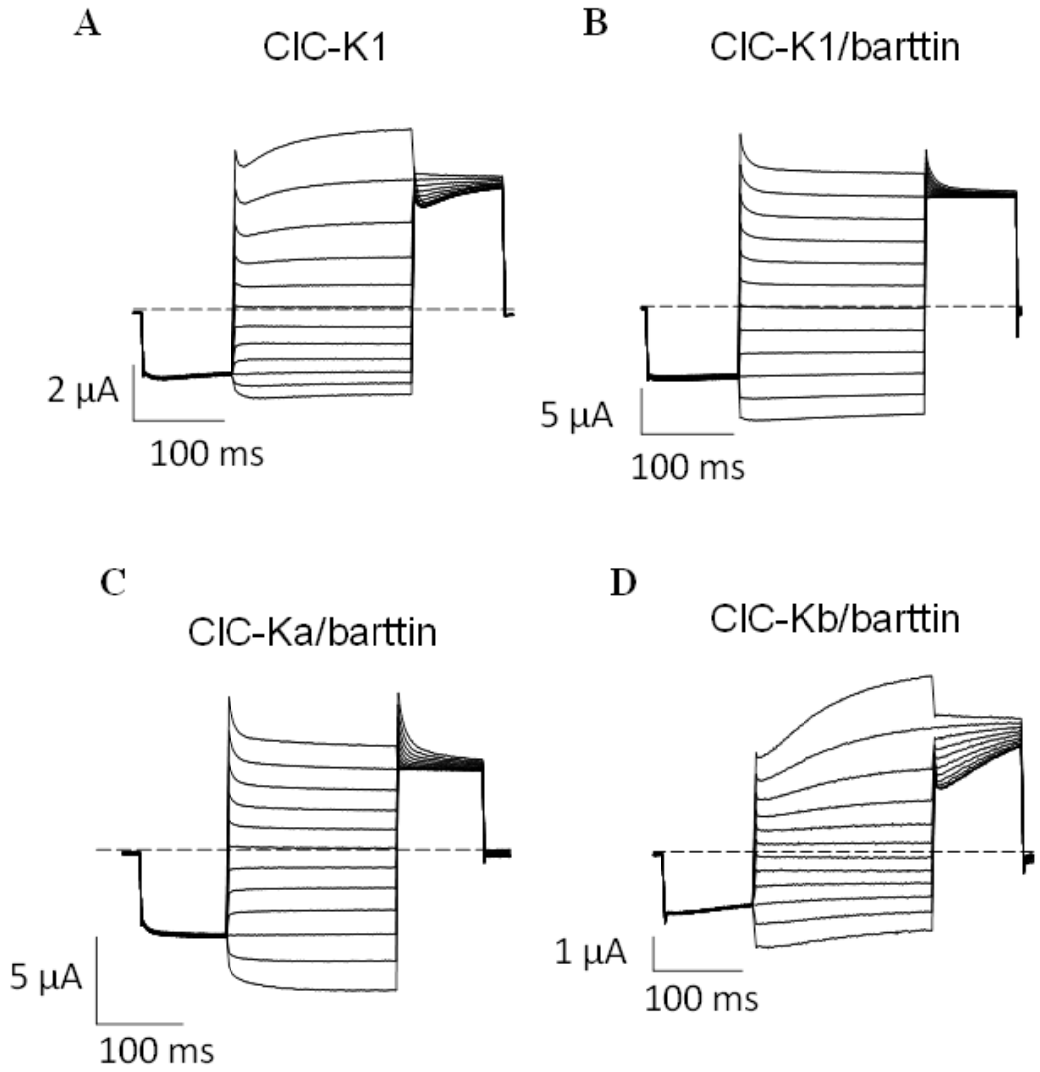


**Fig. 1.3 Typical currents mediated by ClC-K1 (A), ClC-K1/barttin (B), ClC-Ka/barttin (C), ClC-Kb/barttin (D).**

The effect of extracellular pH and calcium on the expressed current was determined. Lowering extracellular pH from 7.5 to 5.9 dramatically reduced the current, while alkalinization to pH 8 increased the current amplitude (Uchida et al, 1995; Waldegger & Jentsch, 2000). Removal of extracellular calcium reduced the current (Uchida et al, 1995; Waldegger & Jentsch, 2000). In contrast to that shown for rClC-K1, injection of cRNA of rClC-K2, hClC-Ka, and hClC-Kb in *Xenopus* oocytes did

not induce chloride currents (Kieferle et al, 1994; Waldegger & Jentsch, 2000). That was quite surprising, since they are approximately 90% identical to rClC-K1. In order to identify protein regions that may be necessary for the functional expression of these channels, chimeras ClC-Kb/ClC-K1 were prepared. Only chimeras in which the C-terminal part of ClC-Kb was replaced by rClC-K1 segments yielded currents (Waldegger & Jentsch, 2000). The solution of the mystery of the lack of expression of human CLC-K in heterologous system came from genetic studies. A new gene, *BSND* encoding the protein barttin was identified by linkage mapping in patients affected by Bartter's syndrome with additional deafness. Mutations in this gene cause Bartter's syndrome type IV (Birkenhäger et al, 2001). Since no currents were observed in oocytes injected with hCLC-K channels or barttin alone, it was hypothesized that CLC-K channels may need a β-subunit and that just barttin is that subunit (Estévez et al, 2001). Indeed, when barttin was co-expressed with ClC-Ka and ClC-Kb in *Xenopus* oocytes, $Cl^-$ currents were observed (Estévez et al, 2001). In particular, expression of ClC-Ka together with barttin resulted in large instantaneous currents with voltage-dependent activation at negative voltage below -80 mV (Estévez et al, 2001; Waldegger et al, 2002) (Fig. 1.3C). ClC-Kb/barttin yielded small but significant currents with voltage-dependent activation in the positive voltage range and inactivation in the negative voltage range (Estévez et al, 2001; Waldegger et al, 2002) (Fig. 1.3D). Permeability sequences were $Cl^- \geq Br^- > NO_3^- > I^-$ for ClC-Ka/barttin, and $Cl^- > Br^- = NO_3^- \geq I^-$ for ClC-Kb/barttin (Estévez et al, 2001). Similarly to rClC-K1 currents, ClC-Ka/barttin and ClC-Kb/barttin currents decreased upon extracellular acidification and removal of extracellular calcium (Estévez et al, 2001; Waldegger et al, 2002). A dramatic increase in current amplitude was observed after expression of ClC-K1 together with barttin (Waldegger et al, 2002) (Fig. 1.3B). Moreover the presence of the accessory subunit barttin modifies the voltage dependence of rClC-K1 currents. In the absence of barttin, rClC-K1 currents activated upon depolarization. When coexpressed with barttin, rClC-K1 currents activated upon hyperpolarization and deactivated upon depolarization (Fischer et al, 2010). Comparable to ClC-K1, ClC-K1/barttin showed currents which are rapidly and reversibly decreased upon extracellular acidification and removal of extracellular calcium (Waldegger et al, 2002). By truncations and

mutagenesis of barttin, a short proline-rich segment (a putative PY motif) essential for barttin function was identified (Estévez et al, 2001). PY motives were previously found in the epithelial Na channel subunits. Mutations in these motives induced an increase in Na channel activity (Schild et al, 1996). Similarly when the critical tyrosine residue from the PY motif of barttin was mutated (Y98A), stimulation of ClC-Ka and ClC-Kb currents by barttin was enhanced (Estévez et al, 2001). Barttin Y98A and CLC-K cRNA co-injection led to a high functional expression of all CLC-K channels, even ClC-Kb (Estévez et al, 2001). Several studies showed that barttin exerts multiple effects on the function of CLC-K channels. Certainly barttin enhances the surface expression (Estévez et al, 2001), but it seems involved in protein stability and voltage-dependent gating of CLC-K channels (Scholl et al, 2006; Fischer et al, 2010; Lang, 2010).

### *1.3.8 Pharmacological characterization of CLC-K channels*

For this section I partially used the text from:

Gradogna, M. Pusch 2010. Molecular pharmacology of kidney and inner ear CLC-K chloride channels. Frontiers in pharmacology 1:130, pp.3-6

The contents was slightly modified for a better general understanding.

After the cloning and heterologous expression of the ClC-K1 channel, the effect of several known chloride channel inhibitors was studied. Extracellular DIDS and 9-AC (9-antracene carboxylic acid) inhibited ClC-K1 channel (Uchida et al, 1993). Moreover the effects of known drugs that modulate transcellular chloride transport in the TAL were investigated. Furosemide inhibited the chloride currents, while NEM (N-ethyl-maleimide) activated ClC-K1 channel. Both of these effects were reversible (Uchida et al, 1995). Before the discovery of barttin (Estévez et al, 2001), only the rat CLC-K1 could be functionally expressed in heterologous systems (Uchida et al, 1993). To explore the functional properties of the human CLC-K homologs, Waldegger & Jentsch constructed chimeras between rat CLC-K1 and human CLC-Kb (Waldegger & Jentsch, 2000). One of these chimeras was used by Liantonio et al. in a first pharmacological investigation (Liantonio et al, 2002). These authors tested various derivatives of CPP (p-chloro-phenoxy-propionic acid) (Fig. 1.4A) as potential CLC-K inhibitors. CPP, a blocker of the skeletal muscle $Cl^-$ conductance

(De Luca et al, 1992), had previously been shown to block CLC-0 and CLC-1 from the intracellular side (Aromataris et al, 1999; Pusch et al, 2000). While CPP itself was ineffective (from the outside), bis-phenoxy derivatives of CPP (e.g. GF-100, Fig. 1.4B) were shown to be relatively potent inhibitors of the CLC-K chimera and of wild-type CLC-K1 co-expressed with barttin when applied from the outside ($K_D$ ~ 100 μM) (Liantonio et al, 2002). Following this pioneering work, Liantonio et al. (Liantonio et al, 2004) performed a structure-activity relationship (SAR) analysis based on the GF-100 molecule, using rat CLC-K1 co-expressed with barttin. Among several molecules tested, 3-phenyl-CPP (Fig. 1.4C) had an elevated blocking potency ($K_D$ ~ 100 μM) (Liantonio et al, 2004). The rapid onset and reversibility of the block suggested that the binding site must be exposed to the extracellular side of the channel. Moreover, the block by 3-phenyl-CPP was slightly voltage-dependent and was significantly increased in low $[Cl^-]_{ext}$ (Liantonio et al, 2004). This finding suggested that the binding site is located in or close to the $Cl^-$ ion conducting pathway.

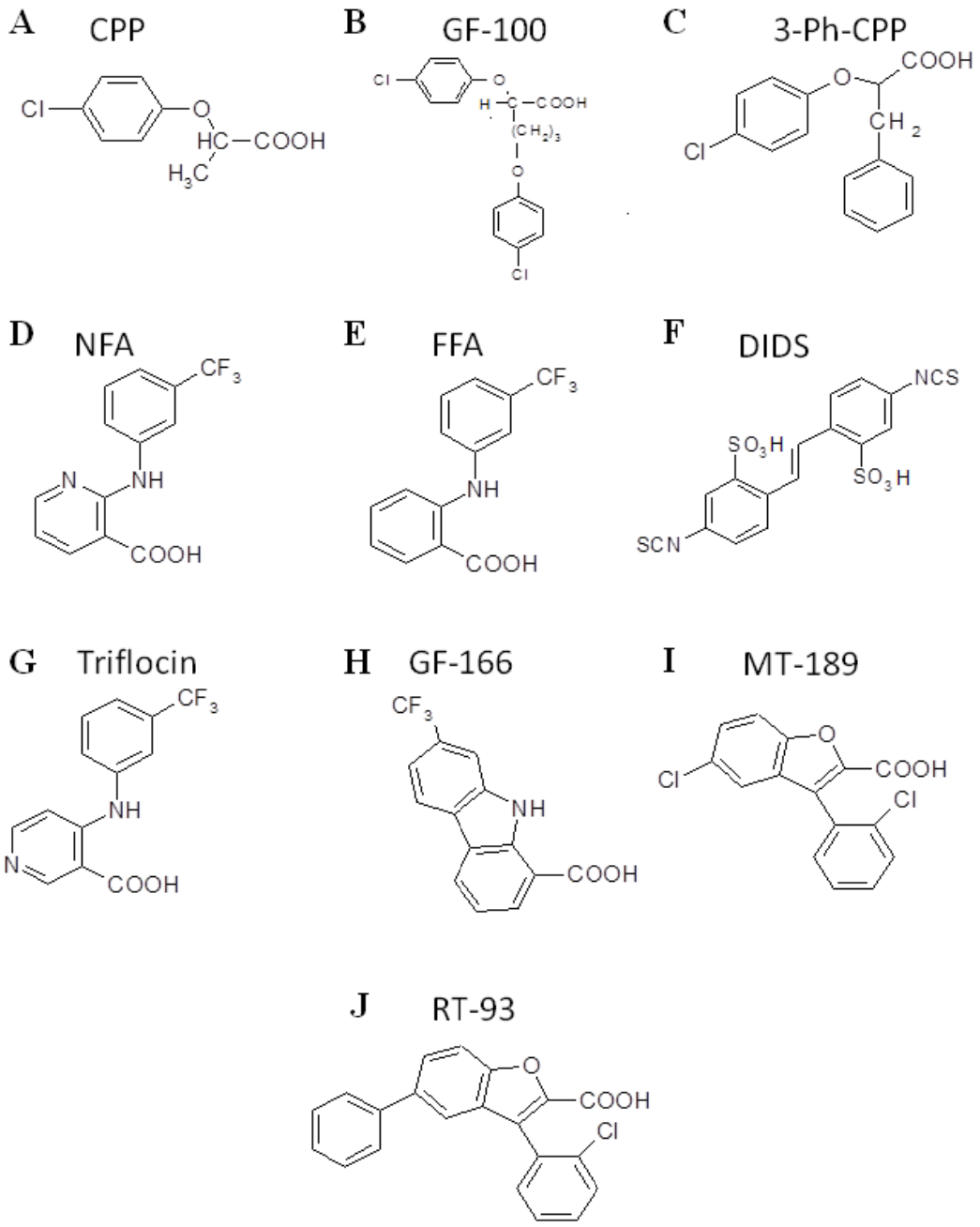


**Fig. 1.4 Chemical structures of various substances that inhibit or activate CLC-K channels.** (A) CPP, p-chloro-phenoxy-propionic acid; (B) GF-100 (proper name); (C) 3-Ph-CPP, 3-phenyl-CPP; (D) NFA, niflumic acid; (E) FFA, flufenamic acid; (F) DIDS, 4,4'-Diisothiocyanato-2,2'-stilbenedisulfonic acid; (G) Triflocin; (H) GF-166 (proper name); (I) MT-189 (proper name); (J) RT-93 (proper name) (from Gradogna and Pusch, 2010).

Among several "classical" $Cl^-$ channel blockers, CLC-K1 was found to be quite sensitive to extracellular application of 5-Nitro-2-(3-phenylpropylamino)benzoic

acid (NPPB, $K_D$ ~ 230 µM), niflumic acid (NFA, $K_D$ ~ 250 µM), and 4,4'-Diisothiocyanato-2,2'-stilbenedisulfonic acid (DIDS, $K_D$ ~ 150 µM) (Liantonio et al, 2004). In following studies it was found that the human homolog CLC-Ka, co-expressed with barttin, showed a similar sensitivity to 3-phenyl-CPP (Fig. 1.4C) and DIDS (Fig. 1.4F) as the rat CLC-K1 (Picollo et al, 2004). Surprisingly, human CLC-Kb, despite a more than 90% sequence identity with CLC-Ka, was significantly less sensitive to both compounds (Fig. 1.5A) (Picollo et al, 2004).

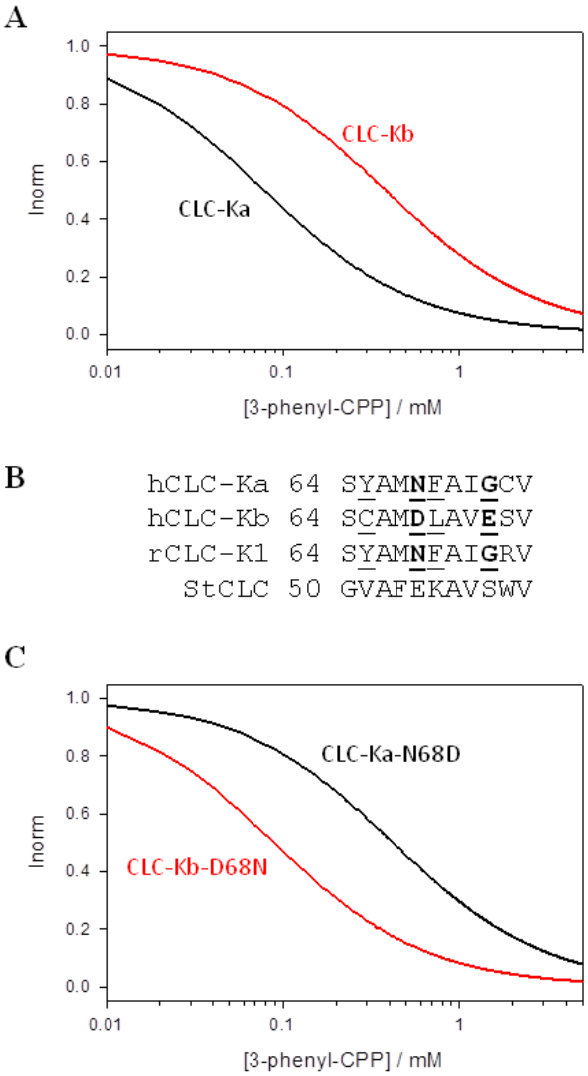


**Fig. 1.5 Effect of 3-phenyl-CPP on CLC-Ka, CLC-Kb, and mutants.** (**A**) The blocking effect of 3-phenyl-CPP on CLC-Ka and CLC-Kb. (**B**) A sequence alignment of a short stretch of residues of CLC-Ka, CLC-Kb, CLC-K1, and StCLC, a bacterial homolog (Dutzler et al, 2002). (**C**) Schematically the blocking effect of 3-phenyl-CPP of mutants CLC-Ka-N68D and CLC-Kb-D68N. Plots were generated based on data from (Picollo et al, 2004) (from Gradogna and Pusch, 2010).

By comparing the sequences of CLC-K1, CLC-Ka, and CLC-Kb, and based on the structure of bacterial CLC-homologs (Dutzler et al, 2002; Dutzler et al, 2003) four residues of helix B (Fig. 1.5B) were selected as candidates that are responsible for the differential block of CLC-Ka and CLC-Kb by 3-phenyl-CPP and DIDS (Picollo et al, 2004). In particular, Asn 68 was essential for 3-phenyl-CPP sensitivity of ClC-Ka (Fig. 1.5B,C) (Picollo et al, 2004). Asn 68 and Gly 72 contribute to DIDS sensitivity of ClC-Ka (Picollo et al, 2004). Since these residues are substituted by the negatively charged Asp68 and Glu72, ClC-Kb is less sensitive to both compounds.

Recently, benzofuran derivatives of 3-phenyl-CPP were found to block CLC-K channels (Liantonio et al, 2008). The two most potent molecules were MT-189 (Fig. 1.4I) and RT-93 (Fig. 1.4J) that block ClC-Ka with apparent $K_D$ values of 7 μM. Both compounds had a significantly reduced potency on the CLC-Ka-N68D mutant, suggesting that they bind to the same site as 3-phenyl-CPP and DIDS. MT-189 had also a reduced affinity for CLC-Kb, while the more hydrophobic compound RT-93 was equally effective on CLC-Kb as on CLC-Ka (Liantonio et al, 2008). This compound represents thus the most potent blocker of CLC-Kb described so far. In addition, this result suggests that it is probably difficult to develop drugs that are highly specific for one of the human CLC-K homologs.

Niflumic acid (NFA) (Fig. 1.4D) and flufenamic acid (FFA) (Fig. 1.4E) belong to a class of fenamates usually used as non-steroidal anti-inflammatory drugs. However, in particular NFA, is also known as a classical $Cl^-$ channel inhibitor. In fact, CLC-K1 was found to be blocked by NFA with an apparent $K_D$ of ~ 100 μM (Liantonio et al, 2004; Picollo et al, 2007) (Fig. 1.6A). It was therefore rather surprising the behavior of human CLC-K homologs. CLC-Ka is activated by sub-millimolar concentrations of NFA, while it is blocked by higher concentrations (above ~ 1 mM) with a biphasic concentration dependence (Fig. 1.6B) (Liantonio et al, 2006). In contrast, CLC-Kb is potentiated by NFA at all concentrations tested (Liantonio et al, 2006) (Fig. 1.6C). The quick activation of the currents by NFA points to an extracellular binding site for this compound (Liantonio et al, 2006; Picollo et al, 2007).

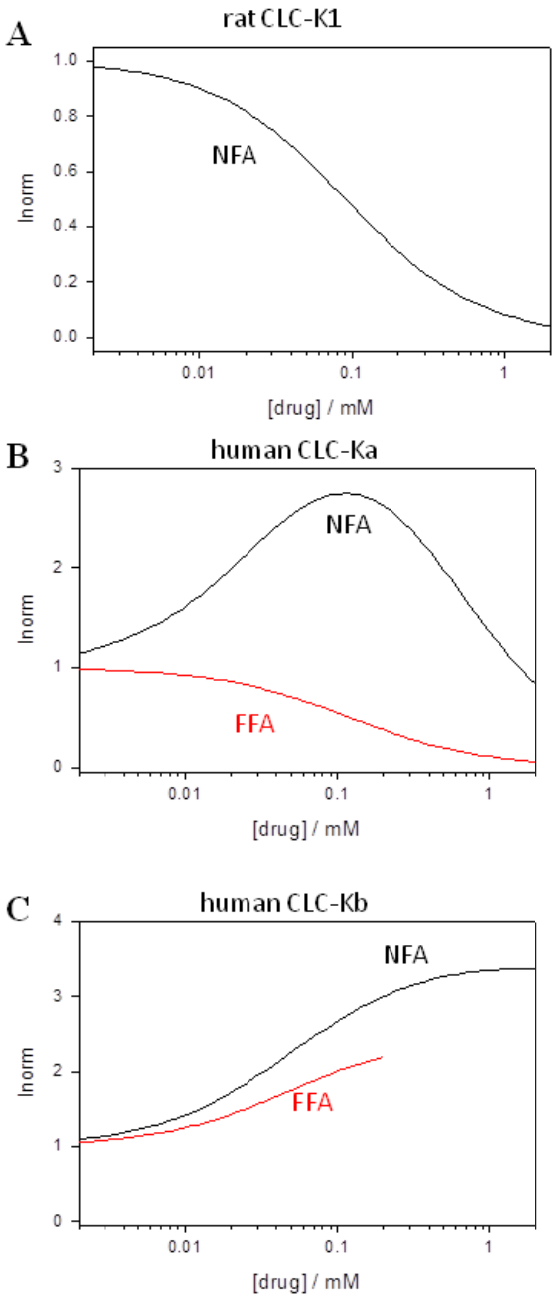


**Fig. 1.6 Blocking and potentiating effects of NFA and FFA on various CLC-K homologs (A: CLC-K1, B: CLC-Ka, C: CLC-Kb).** The effect of NFA is schematically drawn in black, whereas the effect of FFA is shown in red (from Gradogna and Pusch, 2010).

Interestingly, flufenamic acid (FFA, Fig. 1.4E), whose structure seems to be very similar to that of NFA (see Fig. 1.4D, E), does not activate CLC-Ka, but rather induces channel block.

The FFA block is probably mediated by the same pore binding site as 3-phenyl-CPP block (see above) because the mutant CLC-Ka-N68 was much less sensitive to FFA (Liantonio et al, 2006). However, the block of CLC-Ka by NFA at higher concentrations (Fig. 1.6B) and the block of CLC-K1 by NFA (Fig. 1.6A) is probably not mediated by the same binding site, because it is unaltered by the N68D mutation (Picollo et al, 2007). CLC-Kb appears somewhat more susceptible to the potentiating effect of fenamates in that also FFA enhances currents (Liantonio et al, 2006) (Fig. 1.6C).

The striking difference between the effects of NFA (activating) and FFA (blocking) on CLC-Ka could be explained by a fundamental difference between these two molecules: NFA has a rather rigid structure in which the aromatic rings are strictly co-planar. In contrast, the blockers FFA and 3-phenyl-CPP have a flexible, non co-planar conformation. This hypothesis (Liantonio et al, 2006) was nicely confirmed by designing a "flexible, non-coplanar version" of NFA, triflocin (Fig. 1.4G), and similarly by designing a "rigid, co-planar version" of FFA, GF-166 (Fig. 1.4H) (Liantonio et al, 2008). In agreement with the above mentioned hypothesis, triflocin induces block of CLC-Ka at all concentrations tested (Liantonio et al, 2008). On the other hand, GF-166 showed an activating effect on CLC-Ka at concentrations below 200 μM (Liantonio et al, 2008).

## 1.4 A bacterial putative $K^+$ channel: SynCaK

### *1.4.1 Synechocystis: a model organism*

Cyanobacteria are believed to have been the first organisms able to perform the oxygenic photosynthesis. They were essential to change the primordial reducing and anaerobic atmosphere of the earth into the present one rich in oxygen. Even now they contribute to maintain the biosphere. Moreover, according to the endosymbiotic theory, chloroplasts originated from ancestors of cyanobacteria. Because of their lower complexity compared to higher plants, they are model organisms for the study of the photosynthesis.

In particular, the peculiar characteristics of the unicellular cyanobacterium Synechocystis sp. PCC 6803 make it an excellent model organism. Synechocistis sp. PCC 6803 is able to adapt to very different ambient conditions: in the light it is photoautotroph, while it becomes heterotroph in the dark. By homologous recombination, this cyanobacterium can spontaneously integrate exogenous DNA into its genome. This feature makes genetic studies easy. In 1996 Kaneko et al. completed the sequencing of the genome of Synechocistis sp. PCC 6803 (Kaneko et al, 1996). By an analysis of open reading frames (ORFs) combined with a similarity search in gene databases, several putative genes were identified and grouped according their biological function (Kaneko et al, 1996). The availability of the entire genome boosted several studies aimed at identifying new genes and characterizing new proteins.

### *1.4.2 SynCaK: a putative $Ca^{2+}$ activated $K^+$ channel*

Using the highly conserved amino acid sequence of the selectivity filter (T-X-G-[Y-F-L]-G-D) (Hille, 2001) as a query sequence in a homology search, five putative potassium channels were identified in Synechocistis sp. PCC 6083. To establish the channel nature of these proteins, their functional properties had to be established. At the present time one of these putative $K^+$ channels (*slr 0498*), also called SynK, was cloned and expressed in mammalian cells (CHO) in fusion with a fluorescent

protein, EGFP. Confocal microscopy detected SynK expression in the plasma membrane, while patch clamp measurements revealed a voltage-gated outwardly rectifying $K^+$ channel (Zanetti et al, 2010). Another putative $K^+$ channel, corresponding to the gene *sll0993* (Kaneko et al, 1996) and called SynCaK, is subject of study by the group of Prof. Ildikò Szabò from the University of Padua. This putative $K^+$ channel, 365 amino acids long, is thought to have two transmembrane segments and to be activated by $Ca^{2+}$. In fact it shares with the eukaryotic BK channels and the majority of prokaryotic $Ca^{2+}$ activated $K^+$ channels the sequence of a C-terminal ligand-binding RCK domain that regulates the conductance of $K^+$ (Jiang et al, 2001). In particular SYNCAK shows a primary sequence that is very similar to the prokaryotic MthK, a $Ca^{2+}$-gated $K^+$ channel from *Methanobacterium autotrophicum*. Using a similar approach to that adopted for the SynK channel, the same researchers from the University of Padua cloned and expressed a SynCaK-EGFP fusion protein in mammalian cells (CHO). Patch clamp measurements revealed a voltage-gated outwardly rectifying $Ca^{2+}$ activated $K^+$ channel.

### *1.4.3 The $K^+$ channel signature sequence*

$K^+$ channels are found in all phyla. They conduct $K^+$ ions across the plasma membrane carrying out several important cellular functions such as cell volume regulation, hormone secretion, and maintenance of the resting membrane potential (MacKinnon, 2003). Despite the many different classes being characterized mainly by different mechanisms that control channel opening, $K^+$ channels share some important characteristics. They are tetramers formed by four subunits that encircle a central ion conducting pore. $K^+$ channel amino acid sequences share a highly conserved segment named $K^+$ channel signature sequence (TXGYG) (Heginbotham et al, 1994; Doyle et al, 1998). This sequence forms the selectivity filter of the channel, i.e. the structural element that allows the $K^+$ conduction and prevents the passage of other similar ions like $Na^+$ (Doyle et al, 1998; MacKinnon, 2003). By crystal structure of KcsA, a $K^+$ channel from *Streptomyces lividans*, Doyle et al. (1998) demonstrated that dehydrated $K^+$ ions can enter the pore interacting with the

main chain carbonyl oxygen atoms from the residues of the signature sequence. These oxygens simulate the water shell of the hydrated $K^+$ ion allowing its dehydration. $Na^+$ ions are not allowed to cross the membrane because of their smaller radius compared to $K^+$ ion (Doyle et al, 1998). Finally, the fact that the selectivity filter contains more than one ion causes repulsion between the ions and the quick movement of them (Doyle et al, 1998).

### *1.4.4 RCK domains*

First insight about the structure of RCK domains came from the crystal structure of the cytoplasmic domain of an *Escherichia coli* $K^+$ channel (Jiang et al, 2001). The RCK domain is an α/β protein with a core formed by a common structural motif, the Rossmann fold, that can bind a small molecule or metal ion. In some cases RCK domains contain a conserved sequence, the glycine motif (GXGXXG…D) that binds nucleotides ($NAD^+$ or ATP) (Jiang et al, 2001). Following crystallography studies performed on MthK, a $Ca^{2+}$-gated $K^+$ channel from *Methanobacterium autotrophicum*, provided further information on this domain and its function (Jiang et al, 2002; Dong et al, 2005; Pau et al, 2011). MthK is formed by four subunits, each of which bearing two transmembrane segments that form the pore and an intracellular RCK domain. In MthK there are eight RCK domains that form a gating ring at the intracellular side. Four RCK domains are joined at the pore, while the other four are co-expressed and co-assembled in the cytoplasm. $Ca^{2+}$ binding leads to conformational changes of the gating ring that in turn causes channel opening (Dong et al, 2005). The isolated RCK domains form a bilobed homodimer containing three $Ca^{2+}$ binding sites, each of which can bind two $Ca^{2+}$ ions (Pau et al, 2011). The crystal structure allowed to visualize $Ca^{2+}$ binding at the site 1 located at the bottom of the fissure between the two lobes. $Ca^{2+}$ is coordinated by carboxylates of acidic residues (glutamate and aspartate) and oxygen atoms from water molecules (Dong et al, 2005). The other two sites are localized at the interface of the subunits that form the homodimer. In totally the MthK channel can bind 24 $Ca^{2+}$ ions (Pau et al, 2011).

# 2 Materials and methods

## 2.1 Molecular biology

During this thesis I performed site-directed mutagenesis comprising more than 100 point mutations of CLC-K channels.

Mutations were introduced by recombinant polymerase chain reaction (PCR). Initially, two "mutated" primers (forward and reversal), containing the mutation, were synthesized. Additionally, two external primers were also prepared, one forward and upstream of the mutation and one reverse and downstream of the mutation. Two separate PCR reactions (PCR1 and PCR2) were performed using as a template the non mutated DNA and the high fidelity Pfu polymerase. The reaction products are two partially overlapping DNA fragments containing the mutation. A third PCR reaction (PCR3) was performed with the external primers, using as templates the PCR1 and PCR2 products. The result was the fragment of DNA mutated included between the external primers. This fragment and the vector plasmid used for the cloning were cut by the same two restriction enzymes which restriction sites are upstream and downstream of the mutation. The mutated fragment and the cut vector were joined by T4 Ligase. Finally, the plasmid DNA containing the mutation was amplified in *XL1-blue E.coli* bacteria, extracted, and sequenced (Fig. 2.1).

The cDNAs encoding CLC-K channels were inserted in the pTLN vector optimized for the oocyte system (Lorenz et al, 1996). In particular, this vector uses the *Xenopus* β-globin untranslated regions to boost expression of the proteins in oocytes (Lorenz et al, 1996).

The CLC-K and barttin constructs were linearized with MluI and NotI, respectively. Capped cRNA of CLC-K channels was transcribed *in vitro* using SP6 RNA polymerase, while capped cRNA of barttin was transcribed with T7 RNA polymerase (mMessage Machine Kit, Ambion). For the expression of CLC-K channels I co-injected cRNA of barttin and CLC-K channels in oocytes.

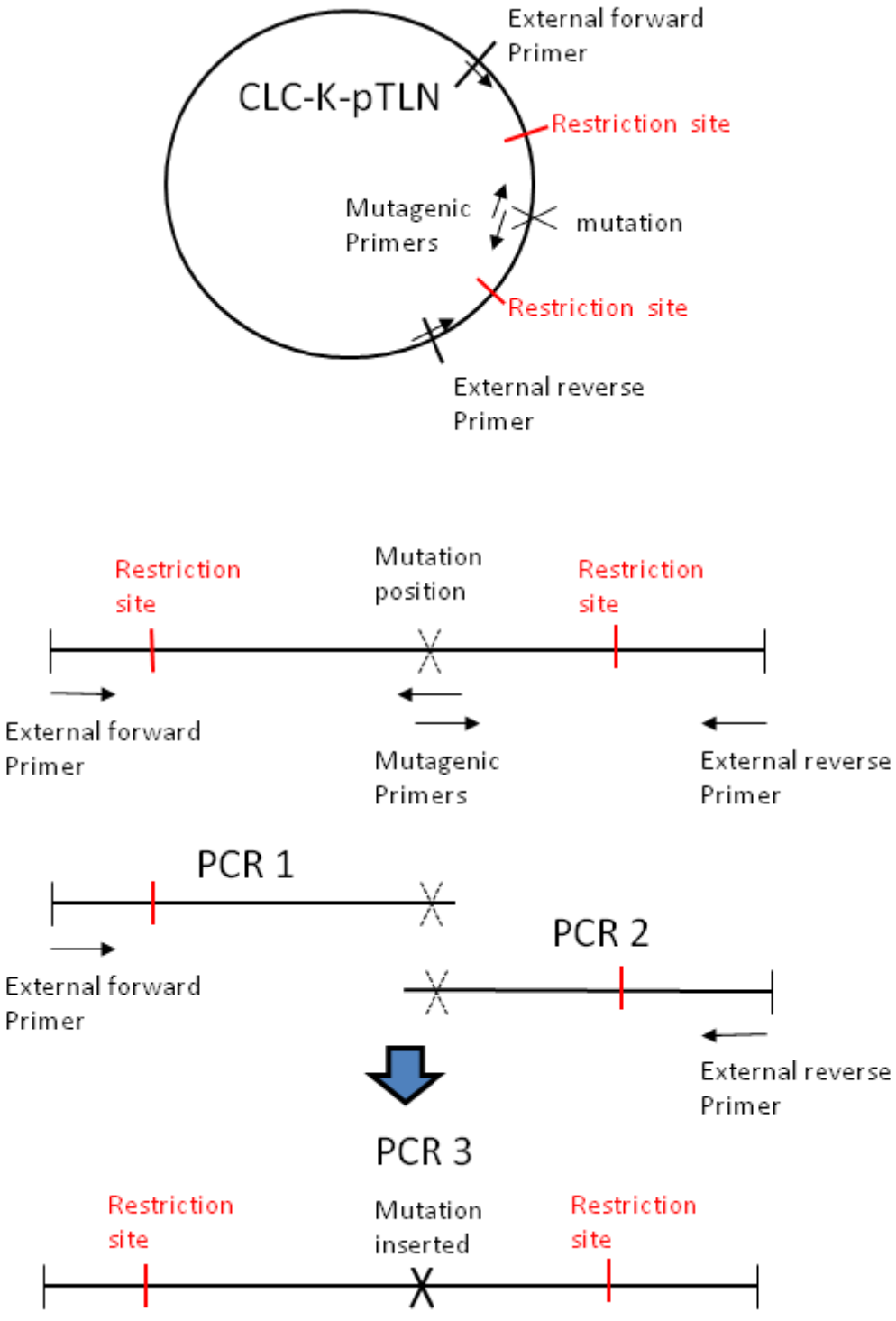


**Fig. 2.1 PCR based mutagenesis.** (See text above for the description).

## 2.2 Oocytes maintaining solution (pH 7.5)

| | |
|---|---|
| 90 mM | NaCl |
| 10 mM | Hepes |
| 1 mM | $MgCl_2$ |
| 1 mM | $CaCl_2$ |
| 2 mM | KCl |

## 2.3 Preparation of oocytes

The *Xenopus* oocyte expression system was developed for studying acetylcholine receptors in a controlled *in vivo* environment by Miledi and coworkers (Barnard et al, 1982; Miledi et al, 1982). Afterwards, this expression system has been widely used to obtain the biophysical characterization of ion channels. Since *Xenopus* oocytes contain only very few endogenous voltage activated channels and are relatively large (about 1 mm diameter), they are a very useful system to study heterologously expressed ion channels. In particular I used them to study CLC-K channels and all the constructs used in this work.

An appropriate amount of ovarian tissues was surgically extracted from a *Xenopus leavis* frog under anesthesia (30 min in a 1.5-2 g/l Tricaine methane sulfonate solution). The follicular cell layer enveloping the oocytes was removed by 2 hours incubation under shaking in a collagenase solution. To stop the enzymatic reaction oocytes isolated and defolliculated were extensively washed in the maintaining solution. Oocytes between stage IV and VI were micro-injected with ~46 nl of solution containing different concentrations of cRNAs, depending on the expression level of the construct in oocytes. For the expression of CLC-K channels I had to co-inject barttin cRNA and CLC-K cRNA. The injection pipettes were pulled using a standard pipette puller (List-Medical Electronic, L/M-3P-A, Darmstadt, Germany).

The tips of the pipettes were broken under a microscope until they had an opening diameter of about 20 μm. To avoid that the rough rim damages the oocytes, the tip was fire polished and pulled by approaching the injection pipette with a heated microfilament. After the injection the oocytes were washed in maintaining solution containing gentamycin at a concentration of 0.1g/l. The injected oocytes were incubated at 18°C in maintaining solution for 1 to 5 days to allow expression of the protein. Finally, the oocytes were placed in the measuring chamber containing the appropriate medium for the electrophysiological experiment. All voltage-clamp experiments were performed at room temperature (20-25 °C).

## 2.4 Electrophysiological methods

The plasma membrane is an insulating lipid bilayer that separates two conductors, the intracellular and the extracellular solution. Consequently, it is a capacitor able to store charges and characterized by a capacitance (symbolized C). Moreover, the membrane is crossed by passive and active transporters that allow the ion flow between the intracellular and extracellular compartment. Hence, the membrane has its conductance (symbolized G) arising from the sum of the conductances (g) of all the transporters being in it. The cell membrane can be thought as an RC circuit with a resistor and a capacitor connected in parallel (Hille, 2001). The total current that flows across the membrane is the sum of several components: the ion current ($I_{ION}$) associated with ion channels, the capacitive current ($I_C$) that flows transiently following a change in membrane potential, the leak current ($I_L$) arising from ions flowing through the non perfect junction between electrode and membrane. Actually, the ion channel associated current comprises two current components: the gating current ($I_G$) resulting from molecular rearrangements of the protein in the electric field and the ionic current ($I_{ION}$), coming from ion flow across the pore.

$I= I_G+I_{ION}+I_C+I_L= I_G+I_{ION}+C(dV/dt)+I_L$

since $C=dV/dq$ and $I=dq/dt$.

$I_G$ can be neglected because it is transient and very small in comparison to $I_{ION}$. Also $I_C$ flows only transiently at the edge of the pulse, hence it can be ignored, since for the present results only the stationary currents are relevant. Instead the contribution of $I_L$ must be subtracted to evaluate the true ionic current. This is especially

important in heterologous expression systems where $I_L$ can be caused by recording electrodes and endogenous currents. For this purpose all experiment were concluded applying a specific blocker of the channel studied (see below). All the experiments done during this thesis were performed by two-electrode voltage clamp technique. Additional patch clamp experiments were performed for the kinetic analysis of the effect of calcium ion and protons on ClC-Ka channel and for the noise analysis. For these few experiments see the descriptions in the methods from the articles (Gradogna et al, 2010; Zifarelli et al, 2010).

## 2.5 Two-electrode voltage clamp (TEVC)

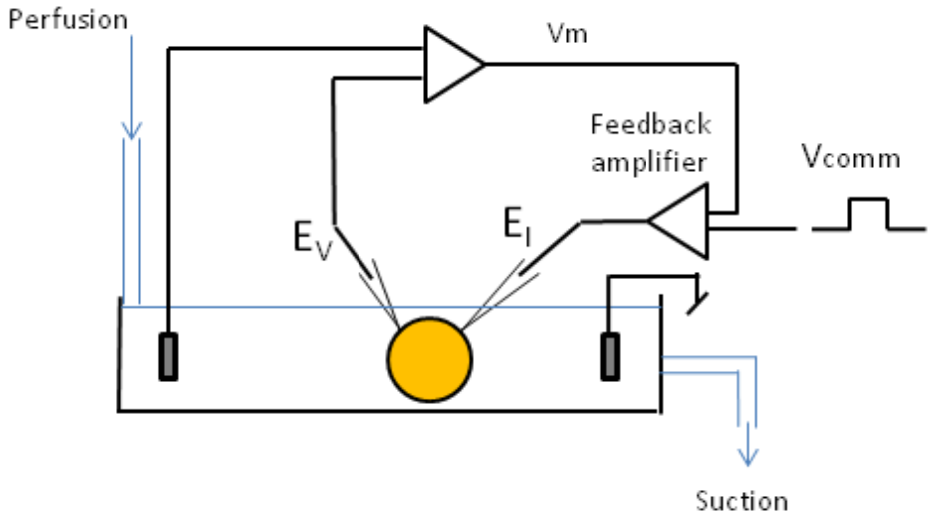


**Fig. 2.2 Schematic diagram of the main components of a two-electrode voltage clamp.** Vm (the difference in potential between the bath and the potential electrode $E_V$) is compared to the command potential, Vcomm by a feedback amplifier. The current electrode $E_I$ injects the current sufficient to reset to zero the difference Vcomm-Vm.

The voltage clamp technique was developed by Marmont (1949) and Hodgkin et al. (1952) to measure currents from the squid giant axon (Marmont, 1949; Hodgkin et al, 1952). Since then, this technique has been used widely to study ion channels in cell membranes from all kinds of tissues. Many variants of the voltage clamp have been developed; in particular, the two-electrode voltage clamp is used for studies of channels expressed in *Xenopus* oocytes. During TEVC experiments two electrodes are inserted into the oocyte. One electrode records the membrane potential (voltage

electrode), and the other electrode (current electrode) injects the amount of current needed to keep the desired potential using a feedback circuit (Fig. 2.2).

The parameter measured from the experimenter is the current that passes through the current electrode; this current arises from the discrepancy between the membrane potential and the command potential. A feature that has to be considered in the voltage clamp experiments is the series resistance $R_S$. $R_S$ is the sum of the resistances of the elements that the injected current has to traverse: the bath, the electrodes and the cytoplasm. $R_S$ causes a discrepancy between the measured membrane potential and the true potential difference across the membrane. If $R_S$ is known, the size of the error is easily estimated by $V=IxR_s$. This error is particularly relevant when large currents are measured; we decided to perform $R_S$ compensation for currents larger than 10 μA. For this purpose, the series resistance was measured by applying a step change in current during the experiment in current clamp mode. Based on this, the $R_S$ compensation was performed offline using a feature of the analysis program ANA.

The voltage clamp set-up was formed by a support system of the cell, two mechanical micromanipulators to control the movements of the potential and the current electrodes, and a microscope (inverted microscope Olympus SZ30 magnification 0.9X to 4X). A gravity perfusion system allowed changing up to ten solutions by mechanical valves. The stimulation protocols and data recordings were controlled by an Acer Aspire T180 QB7Z computer. It was connected to a National Instruments AD/DA converter that changes the digital signal into the analogical signal and vice versa, and finally to a voltage-clamp amplifier (Turbo TEC-03X, npi electronics, Tamm, Germany). Borosilicate glass capillaries (Harvard 1.5 mm O.D. x 0.86 mm I.D.) were pulled in a 2 steps vertical puller (List-Medical Electronic, L/M-3P-A, Darmstadt, Germany) to obtain the voltage clamp pipettes.

Voltage clamp data were acquired using the custom acquisition program GePulse (available at http://www.ge.ibf.cnr.it/~pusch.ibf/programs-mik.htm).

## 2.6 Stimulation protocols

The membrane was kept at a holding potential between -40 and -20 mV corresponding to the resting membrane potential in our conditions. At this potential the current flowing through the chloride channels is small because it is close to the chloride equilibrium potential. To evaluate the currents at different potentials, we used the following protocols of stimulation. After a prepulse to -100 mV for 100 ms, channels were stimulated with voltages ranging from -140 to 80 mV with 20 mV increments for 200 ms. Pulses ended with a tail pulse to 60 mV for 100 ms (Fig. 2.3A, B) (Gradogna et al, 2010).

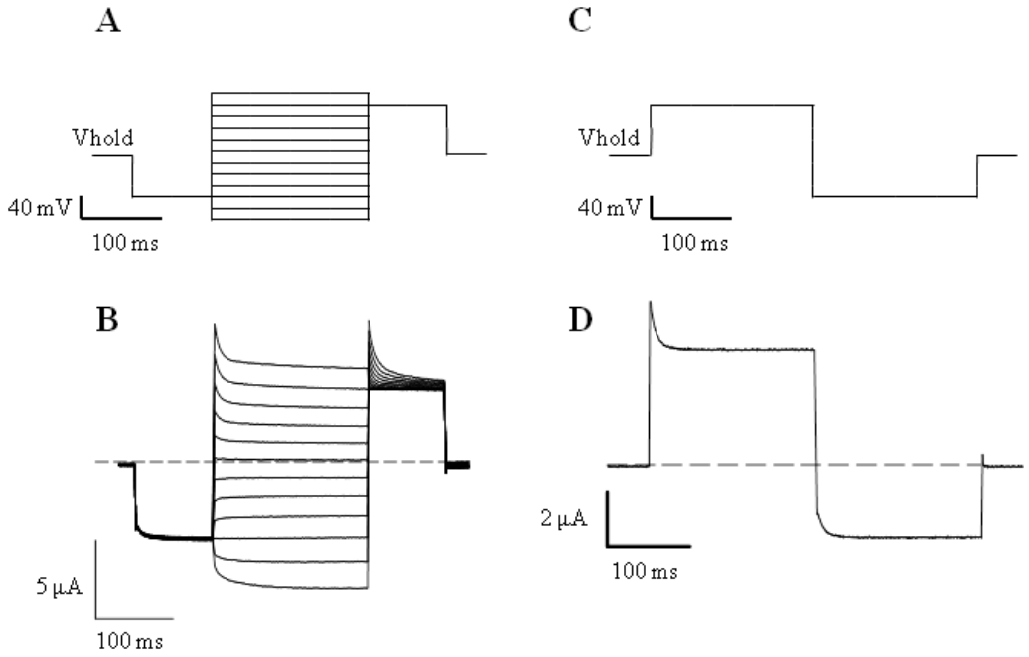


**Fig. 2.3 Stimulation protocols and corresponding currents recorded. A)** IV protocol. **B)** Current responses of CLC-Ka to the protocol of the panel A. **C)** Protocol to evaluate the substance effect. **D)** Current responses to the protocol of the panel C.

An alternative stimulation protocol comprised a prepulse to 60 mV for 100 ms followed by steps to values from -140 to 80 mV for 200 ms, and a tail pulse to -100 mV (Zifarelli et al, 2010). The effect of niflumic acid, divalent cations, and pH on CLC-K channels was evaluated by applying repetitive pulses to 60 mV of 200 (or 100) ms duration with a stimulation interval of 1 s (Fig. 2.3C, D). During this protocol the solutions were continuously applied until steady state was reached.

Reversibility was always checked by returning to the standard solution (Gradogna et al, 2010; Zifarelli et al, 2010).

## 2.7 Experimental solutions

In all voltage clamp experiments the standard bath solution contained 10 mM $Ca^{2+}$ and had pH 7.3. However, because in our studies we employed various different solutions, a detailed description can be found in the Methods of the published articles (Gradogna et al, 2010; Zifarelli et al, 2010). Here, I only report the list of the solutions used in the last, unpublished experiments.

To study the effect of the divalent cations on ClC-K channels I used the following standard bath solution containing (in mM): 92 NaCl, 10 $CaCl_2$, 10 HEPES at pH 7.3 (osmolarity: 224 mosm). The concentration of $CaCl_2$ was varied between 0 and 50 mM in parallel varying the NaCl concentration to maintain fixed the chloride concentration (112 mM). In particular, the osmolarity of the solution containing 50 mM $CaCl_2$ was increased by adding 40 mM sucrose. The solutions of the other divalent cations (barium, strontium, magnesium, manganese, zinc) were prepared in a similar way replacing $CaCl_2$ with $BaCl_2$, $SrCl_2$, $MgCl_2$, $MnCl_2$, $ZnCl_2$, respectively. Because zinc and manganese tended to form precipitates, the highest concentrations tested were 5 mM $ZnCl_2$ and 10 mM $MnCl_2$.

To estimate the contribution of endogenous currents and leak, I applied a solution containing (in mM): 100 NaI, 5 $MgSO_4$, 10 Hepes at pH 7.3 that specifically blocks CLC-K channels, but not endogenous currents (Picollo et al, 2004).

## 2.8 Data analysis

Voltage clamp data were analyzed using the custom analysis program ANA (available at http://www.ge.ibf.cnr.it/~pusch.ibf/programs-mik.htm).

Most of the experiments of this thesis were performed to evaluate the effect of compounds or ions on the currents of CLC-K channels. The stimulation protocol for this purpose is been described in section 2.6 and shown in Fig. 2.3C, an example of the current response is shown in Fig. 2.3D. For the data analysis, we evaluated the mean currents collected at 60 mV in steady-state. Because the level of functional expression of the channels can vary substantially in different batches of oocytes, and

even in oocytes belonging to same batch, mean currents were normalized to the steady-current measured in the standard bath solution, i.e., 10 mM $Ca^{2+}$, pH 7.3. Leak currents, estimated by replacing extracellular chloride by iodide (see experimental solutions), were subtracted. Normalized currents of CLC-K channels were plotted versus divalent ion concentration and pH.

## 2.9 Kinetic modeling

In the course of my thesis I performed a detailed dose-response analysis of the effect of $Ca^{2+}$, $H^{+}$, and other divalent ions on CLC-K channels. Based on these experimental data we could speculate about the mechanisms of ion-channel binding and modeling the ion modulation of CLC-Ka channel.

The simplest case was the proton modulation of CLC-Ka. Because high proton concentrations completely block CLC-Ka, we hypothesized a two-state model as shown below.

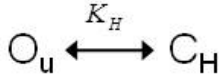


i.e., the channel can be in two states: $O_u$ (unbound open state) or $C_H$ (bound closed state). $H^{+}$ binding is governed by the equilibrium dissociation constant $K_H$. At equilibrium, the probability $p_u$ of the channel of not being blocked by a proton was:

$$p_u = \frac{1}{1+\left(\frac{[H]}{K_H}\right)^n}$$

where *[H]* is the proton concentration, $K_H$ the apparent binding constant, and *n* the Hill coefficient. Since our experimental data were normalized to the current in standard conditions (pH 7.3, 10 mM $Ca^{2+}$), the equation used to fit the pH dependence at 60 mV was the ratio between $p_u[H]/ p_u(7,3)$. For the best fit curve of experimental data and the corresponding $K_H$ and *n* values found see Figure 2 and the paragraph *Modeling pH and $Ca^{2+}$ modulation of ClC-Ka* pp. 316-317 from the article: Gradogna A, Babini E., Picollo A., Pusch M. 2010. A regulatory calcium-binding site at the subunit interface of CLC-K kidney chloride channels. J.Gen. Physiol. 136:3.

Interestingly, the Hill coefficient *n* is 1.6. Since Hill coefficient indicates the degree of cooperativity of binding, i.e., the number of ligands able to saturate the channel, *n* > 1 suggests that more than one proton (most likely two) is necessary to block the channel.

Another more complicated case was $Ca^{2+}$ activation of CLC-Ka. Because even in the absence of $Ca^{2+}$ ClC-Ka yields currents, we supposed an allosteric model composed of four states as shown below.

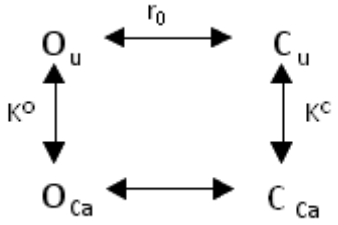


Where $O_U$ and $O_{Ca}$ indicate unbound and Ca-bound open states, $C_U$ and $C_{Ca}$ unbound and Ca-bound closed states of the channel. $Ca^{2+}$ binding to the open state is governed by the dissociation constant $K^O$, whereas $Ca^{2+}$ binding to the closed state is described by the dissociation constant $K^C$. $r_0$ is the ratio between the probability of being in states $C_u$ and $O_u$ ($r_0=p(C_u)/p(O_u)$).

Under the assumption of the microscopic reversibility (i.e. in a system at equilibrium, any molecular process and the reverse of that process occur, on the average, at the same rate), we wrote the four equations that describe the probability of the channel being in the different states in function of the dissociation constants $K^O$, $K^C$ and $[Ca^{2+}]$:

$$p0_u + pC_u + p0_{Ca} + pC_{Ca} = 1$$

$$\frac{pC_u}{pO_u} = r_0$$

$$\frac{pC_{Ca}}{pC_u} = \frac{[Ca]}{K^C}$$

$$\frac{pO_{Ca}}{pO_u} = \frac{[Ca]}{K^O}$$

Based on these with simple mathematical passages, we could determine the probability of the channel being in the open state $p_o$:

$$p_o = \frac{1 + \frac{[Ca]}{K^O}}{1 + r_0 + \frac{[Ca]}{K^O} + r_0 \frac{[Ca]}{K^C}}$$

The equation used to fit the calcium dependence at 60 mV was the ratio between the open probability varying calcium concentration and the open probability at the standard concentration, i.e., $p_u[Ca]/ p_u(10)$. For the best fit curve of experimental data and the corresponding $K^O$, $K^C$ and $r_0$ values see Figure 1 and the paragraph *Modeling pH and $Ca^{2+}$ modulation of ClC-Ka* pp. 316-317 from the article: Gradogna A, Babini E., Picollo A., Pusch M. 2010. A regulatory calcium-binding site at the subunit interface of CLC-K kidney chloride channels. J.Gen. Physiol. 136:3.

In the last experiments I studied the effect of several divalent cations on CLC-K currents. In particular, we established that $Ba^{2+}$ activates CLC-Ka in a similar manner as $Ca^{2+}$, even if it is less potent. To investigate if $Ba^{2+}$ has a reduced affinity or a reduced efficacy compared to $Ca^{2+}$, we performed a dose-response analysis and modeling of $Ca^{2+}$ and $Ba^{2+}$ modulation. We hypothesized an allosteric model composed of six states as shown below.

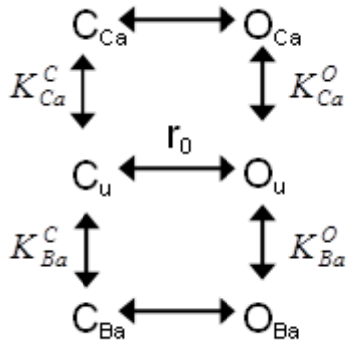


With the usual symbols: $O_U$, $O_{Ca}$ and $O_{Ba}$ indicate unbound, Ca-bound and Ba-bound open states, $C_U$ , $C_{Ca}$ and $C_{Ba}$ unbound, Ca-bound and Ba-bound closed states of the channel. $Ca^{2+}$ and $Ba^{2+}$ binding to the open state are governed by the dissociation constants $K^O_{Ca}$ and $K^O_{Ba}$, respectively, whereas $Ca^{2+}$ and $Ba^{2+}$ binding to the closed state are described by the dissociation constants $K^C_{Ca}$ and $K^C_{Ba}$, respectively. $r_0$ is here the ratio between the probability of being in states $O_u$ and $C_u$ ($r_0$=p($O_u$) /p ($C_u$)).

From the six equations that describe the probability of the channel being in the different states as a function of the dissociation constants $K_{Ca}^{O}, K_{Ca}^{C}, K_{Ba}^{O}, K_{Ba}^{C}$, and $[Ca^{2+}]$ and $[Ba^{2+}]$, with some mathematical passages we obtained the equation that describes the probability of the channel being open:

$$p_0 = \frac{1 + \frac{[Ca]}{K_{Ca}^{0}} + \frac{[Ba]}{K_{Ba}^{0}}}{1 + \frac{1}{r_0} + [Ca]\left(\frac{1}{r_0 K_{Ca}^{C}} + \frac{1}{K_{Ca}^{0}}\right) + [Ba]\left(\frac{1}{r_0 K_{Ba}^{C}} + \frac{1}{K_{Ba}^{0}}\right)}$$

The equations used to fit the calcium dependence and the barium dependence at 60 mV were the ratio between the open probability varying calcium concentration and the open probability at 10 $Ca^{2+}$ in absence of barium and the ratio between the open probability varying barium concentration and the open probability at 10 $Ba^{2+}$ in absence of calcium, respectively. For the best fit curves of the experimental data, the dissociation constants and $r_0$ values, and our conclusions see Fig. 3.7A in the section 3.3.2 “Specificity of the calcium-binding site in ClC-Ka”.

# 3 Results

## 3.1 Identification of sites involved in ClC-Ka potentiation by NFA

CLC-K channels contribute to the mechanism of water diuresis and NaCl reabsorption in the kidney. Moreover, they are involved in the endolymph production in the inner ear. For their important physiological function, they are a potential pharmacological target. In section 1.3.8 ("Pharmacological characterization of CLC-K channels"), I reported the identification of several chemical compounds that modulate CLC-K channels. Among these, niflumic acid (NFA) aroused interest because of its unexpected effect on CLC-Ks. NFA is a known inhibitor of $Cl^-$ channels. In fact it blocks ClC-K1(Liantonio et al, 2004; Picollo et al, 2007). Surprisingly it increases ClC-Kb currents, and modulates ClC-Ka in a biphasic manner (Liantonio et al, 2006). Low NFA concentrations activate ClC-Ka, while concentrations $\gtrsim$ 1 mM block this channel (Liantonio et al, 2006). It was proposed that two different sites are responsible for NFA-induced block and potentiation of ClC-Ka (Picollo et al, 2007). Interestingly, despite the similar structure of NFA and FFA (see Fig. 1.4D,E), FFA only blocks ClC-Ka. Moreover, the residue (N68) responsible for ClC-Ka block by FFA and CPP derivatives is not involved in the ClC-Ka block by NFA (Liantonio et al, 2006). Because of its peculiarity the interaction between CLC-K channel and NFA is an interesting topic of study concerning both the characterization of the channel and pharmacological aims.

In this work we intended to identify the residues responsible for the potentiating effect of NFA on ClC-Ka. Based on the structure of a bacterial CLC homolog, we performed an extensive site-directed mutagenesis of ClC-Ka. Some criteria were applied to select the amino acids to mutate. Because NFA effect takes place very quickly (Liantonio et al, 2006; Picollo et al, 2007), the binding site(s) is likely exposed to the outside. Moreover, since ClC-K1 is not potentiated by NFA, initially we mutated all external residues conserved in the human CLC-Ks, but not in ClC-K1. Since ClC-K1 could have a "vestigial" potentiating site, we mutated other external residues based on their exposure to the extracellular side. We performed voltage clamp measurements of these mutants expressed in *Xenopus* oocytes. The

result of this work was the identification of five mutations that abolish the NFA-induced potentiation. Keeping in mind that NFA potentiates ClC-Ka by increasing its open probability (Picollo et al, 2007), we had to exclude that the lack of potentiation results from an unspecific modification of the gating. In fact two of the mutations identified, G167A and F213A, probably affect the NFA potentiation modifying the gating properties of the channel. Both these mutants yielded much larger currents than WT and lacked the typical time-dependent relaxations of WT currents. Moreover non-stationary noise analysis revealed a drastically increased $p_{open}$ compared to WT. Instead the other three mutants identified, L155A, G345S, and A349E did not yielded increased functional expression and, with the exception of A349E, they showed similar current relaxations to those of WT. Moreover, the L155A mutant had an unaltered $p_{open}$ respect to WT. All this suggested that L155, G345, and A349 residues are involved in the potentiation by NFA. Interestingly, L155A, G345S, and A349E mutants lacked the potentiation, but kept the blocking effect of NFA. These results confirmed the hypothesis that two different binding sites are responsible for the opposite effects of NFA on ClC-Ka.

In the following pages I insert the article:

Zifarelli G, Liantonio A, Gradogna A, Picollo A, Gramegna G, De Bellis M, Murgia AR, Babini E, Camerino DC & Pusch M. 2010. Identification of sites responsible for the potentiating effect of niflumic acid on ClC-Ka kidney chloride channels. *Br J Pharmacol 160:1652-61*

BJP BRITISH JOURNAL OF PHARMACOLOGY

BPS BRITISH PHARMACOLOGICAL SOCIETY

British Journal of Pharmacology (2010), 160, 1652–1661

0007-1188/10
www.brjpharmacol.org

RESEARCH PAPER

# Identification of sites responsible for the potentiating effect of niflumic acid on ClC-Ka kidney chloride channels

G Zifarelli[1], A Liantonio[1,2], A Gradogna[1], A Picollo[1]*, G Gramegna[1,2], M De Bellis[1,2], AR Murgia[1], E Babini[1], D Conte Camerino[2] and M Pusch[1]

[1]*Istituto di Biofisica, Consiglio Nazionale delle Ricerche, Genova, Italy, and* [2]*Sezione di Farmacologia, Dipartimento Farmacobiologico, Via Orabona 4, Università di Bari, Bari, Italy*

**Background and purpose:** ClC-K kidney $Cl^-$ channels are important for renal and inner ear transepithelial $Cl^-$ transport, and are potentially interesting pharmacological targets. They are modulated by niflumic acid (NFA), a non-steroidal anti-inflammatory drug, in a biphasic way: NFA activates ClC-Ka at low concentrations, but blocks the channel above ~1 mM. We attempted to identify the amino acids involved in the activation of ClC-Ka by NFA.
**Experimental approach:** We used site-directed mutagenesis and two-electrode voltage clamp analysis of wild-type and mutant channels expressed in *Xenopus* oocytes. Guided by the crystal structure of a bacterial CLC homolog, we screened 97 ClC-Ka mutations for alterations of NFA effects.
**Key results:** Mutations of five residues significantly reduced the potentiating effect of NFA. Two of these (G167A and F213A) drastically altered general gating properties and are unlikely to be involved in NFA binding. The three remaining mutants (L155A, G345S and A349E) severely impaired or abolished NFA potentiation.
**Conclusions and implications:** The three key residues identified (L155, G345, A349) are localized in two different protein regions that, based on the crystal structure of bacterial CLC homologs, are expected to be exposed to the extracellular side of the channel, relatively close to each other, and are thus good candidates for being part of the potentiating NFA binding site. Alternatively, the protein region identified mediates conformational changes following NFA binding. Our results are an important step towards the development of ClC-Ka activators for treating Bartter syndrome types III and IV with residual channel activity.
*British Journal of Pharmacology* (2010) **160,** 1652–1661; doi:10.1111/j.1476-5381.2010.00822.x

**Keywords**: CLC-K channels; Bartter syndrome; diuretic; chloride channel; niflumic acid; kidney
**Abbreviations**: NFA, niflumic acid

## Introduction

ClC-K proteins (ClC-Ka and -Kb in humans, and their rodent orthologues ClC-K1 and -K2) (Uchida *et al.*, 1993; Adachi *et al.*, 1994; Kieferle *et al.*, 1994) are $Cl^-$ channels forming a distinct branch of the CLC protein family (Zifarelli and Pusch, 2007) that are expressed in the kidney and the inner ear (Jentsch, 2005; Uchida and Sasaki, 2005). They both co-express with an auxiliary β subunit, barttin (Estévez *et al.*, 2001), which regulates their plasma membrane localization and modulates their functional properties (Estévez *et al.*, 2001; Waldegger *et al.*, 2002; Scholl *et al.*, 2006).

From the insurgence of diabetes insipitus in ClC-K1 knock-out mice (Matsumura *et al.*, 1999; Akizuki *et al.*, 2001), it has been inferred that ClC-Ka is a crucial component in the countercurrent system that preserves a correct urine concentration, even though, to date, no mutation in ClC-Ka has been reported to cause a defect in the ability to concentrate urine in humans. Loss-of-function mutations in ClC-Kb result in Bartter syndrome type III (Simon *et al.*, 1997), characterized by massive salt loss due to impaired NaCl reabsorption in the thick ascending limb. In the inner ear, ClC-K channels are important for $K^+$ secretion into the scala media (Rickheit *et al.*, 2008). This is the reason why patients affected by Bartter syndrome type IV, caused by loss-of-function mutations in barttin, present both renal dysfunction (more severe than in

Correspondence: M Pusch, Istituto di Biofisica, Consiglio Nazionale delle Ricerche, Via de Marini 6, I-16149 Genova, Italy. E-mail: pusch@ge.ibf.cnr.it
*Present address: Department of Anesthesiology, Weill Cornell Medical School, 510 East 70th Street, New York, NY 10021, USA.
Received 2 February 2009; revised 2 March 2010; accepted 9 March 2010

Bartter syndrome type III) and deafness (Birkenhäger *et al*., 2001). This also occurs in patients in which both ClC-K isoforms are non-functional, but this is very rare (Schlingmann *et al*., 2004).

From a pharmacological point of view, ClC-K channels are the only members of the CLC family for which a significant advance has been achieved (Liantonio *et al*., 2002; 2004; 2006; 2008; Picollo *et al*., 2004; Pusch *et al*., 2007; Matulef *et al*., 2008). The binding site for the ClC-Ka blockers DIDS, 3-phenyl-CPP and flufenamic acid (FFA), a fenamate derivative, has been identified as being close to N68 (Picollo *et al*., 2004), located in the channel pore. Recently, niflumic acid (NFA), a drug belonging to a class of fenamates used as non-steroidal anti-inflammatory drugs, has been shown to have a very peculiar effect on ClC-K channels. NFA potentiates ClC-Ka currents at concentrations up to ~1 mM, whereas at higher concentrations it has an inhibitory effect (Liantonio *et al*., 2006). NFA is far from being a specific modulator of ClC-K channels. In fact, NFA or other fenamates are able to interact with both $Cl^-$ channels (Qu and Hartzell, 2001; Coyne *et al*., 2007; Greenwood and Leblanc, 2007; Verkman and Galietta, 2008) and Shaker-like cation channels (Busch *et al*., 1994; Abitbol *et al*., 1999; Malykhina *et al*., 2002; Greenwood and Leblanc, 2007; Fernandez *et al*., 2008; Cheng and Sanguinetti, 2009; Foster *et al*., 2009). Detailed studies on HCN hyperpolarization of activated cation channels suggested an interaction of NFA with positive residues of the S4 segment, which leads to an alteration of voltage sensing (Cheng and Sanguinetti, 2009), whereas an interaction motif in the S3–S4 linker was found in eag $K^+$ channels (Fernandez *et al*., 2008). $GABA_A$ receptor $Cl^-$ channels are strongly activated by mefenamic acid (Coyne *et al*., 2007). Among $Cl^-$ channels, $Ca^{2+}$-activated $Cl^-$ channels are probably the most sensitive to extracellular NFA (Qu and Hartzell, 2001; Greenwood and Leblanc, 2007). The muscle CLC $Cl^-$ channel, ClC-1, is blocked by intracellular NFA in a voltage-dependent manner (Liantonio *et al*., 2007). However, of the CLC proteins tested (ClC-1, ClC-5, ClC-K), only ClC-K channels have been shown to be sensitive to extracellularly applied NFA (Liantonio *et al*., 2006). Despite a high sequence conservation, the three ClC-K channels that have been tested for NFA modulation show a different response: rat ClC-K1 is blocked in a dose-dependent manner; human ClC-Kb is activated at concentrations up to 2 mM (Liantonio *et al*., 2006); ClC-Ka is potentiated at low concentrations (<~1 mM), but blocked at higher concentrations (Liantonio *et al*., 2006; Picollo *et al*., 2007). Such a different effect on channels that are highly homologous (homology is 91% between –Ka and –Kb, and 83% between –Ka and –K1) argues for a very specific pharmacological profile. To explain the biphasic dependence of ClC-Ka on NFA, Picollo *et al*. (2007) suggested the presence of two distinct binding sites for NFA. The results from $Cl^-$ competition experiments indicated that neither of the two sites is located in the channel pore and, consistently, none of the binding sites for NFA involve N68, the blocking site for FFA and CPP derivatives.

The different action of NFA and FFA on ClC-Ka is related to the different geometrical arrangement of the two aromatic rings in the two molecules. A planar geometry, as in NFA, favours potentiation, whereas a non-planar geometry, endowed with a greater degree of flexibility (as found in FFA), favours block (Liantonio *et al*., 2008).

In order to identify the NFA binding sites, we performed extensive site-directed mutagenesis on ClC-Ka. Of the 97 mutations screened, only five eliminated the potentiating effect of NFA. Two of these (G167A and F213A) drastically altered the general gating properties, such that no conclusion can be established about their role in NFA potentiation. The three remaining mutations (L155A, G345S and A349E) greatly reduced or abolished the potentiating effect of NFA without affecting its blocking ability. L155 is located on the extracellular side of helix E, whereas G345 and A349 are in the loop connecting helices K and L. Based on the crystal structure of the bacterial CLC homologs, these two regions are expected to be exposed to the extracellular side of the channel, relatively close to each other, and are thus good candidates for being part of the potentiating NFA binding site or responsible for conformational changes that follow NFA binding leading to current potentiation.

## Methods

*Molecular biology and heterologous expression*

Mutations were introduced by recombinant PCR as previously described (Accardi and Pusch, 2003). All constructs were in the pTLN vector (Lorenz *et al*., 1996) and were co-expressed with the barttin mutant Y98A which increases expression (Estévez *et al*., 2001). RNA was prepared using the mMessage mMachine SP6 and T7 kits (Applied Biosystems Italia, Monza, Italy) and injected into *Xenopus* oocytes as previously described (Pusch *et al*., 2000).

The ion channel nomenclature used conforms to BJP's *Guide to Receptors and Channels* (Alexander *et al*., 2008).

*Electrophysiology*

Voltage clamp data were acquired at 21–25°C using the custom acquisition program Gepulse (available at http://www.ge.cnr.it/ICB/conti_moran_pusch/programs_pusch/software-mik.htm) and a TURBO TEC-03X amplifier (npi electronic, Tamm, Germany). Currents were recorded in a bath solution containing 90 mM NaCl, 1 mM $MgCl_2$, 10 mM $CaCl_2$ and 10 mM HEPES at pH 7.3. Different NFA concentrations were prepared by dissolving NFA in dimethyl sulphoxide (DMSO) and diluting the resultant solution in the bath solution. Final DMSO concentration was ≤0.2%. DMSO alone had no effect on ClC-Ka-mediated currents at this concentration. NFA and all other reagents were purchased from Sigma-Aldrich (Milan, Italy). Pulses were elicited from a holding potential corresponding to the resting membrane potential (–30 to –50 mV). The acute effect of NFA was evaluated by applying repetitive pulses to 60 mV of 100 ms duration, and calculating the ratio between the current measured in the presence of NFA and that in control conditions. ClC-K channels are efficiently blocked by extracellular iodide (Liantonio *et al*., 2002). This was exploited to estimate the contribution of endogenous currents and leak by replacing extracellular chloride by iodide and by removing extracellular calcium at the end of the protocol (this solution contained 100 mM NaI,

5 mM $MgSO_4$, 10 mM HEPES, pH 7.3). Outward currents in the presence of iodide were taken as being purely endogenous. The estimated leak currents were subtracted from the control currents in the absence and presence of NFA to calculate the ratio $I(c)/I(0)$, where $c$ is the concentration of NFA.

*Non-stationary noise analysis*

For patch clamping, the intracellular solution contained (in mM): 100 *N*-methyl-D-glucamine-Cl (NMDG-Cl), 2 $MgCl_2$, 10 HEPES, 2 EGTA, pH 7.3, whereas the extracellular solution contained 90 NMDG-Cl, 10 $CaCl_2$, 1 $MgCl_2$, 10 HEPES, pH 7.3. Patch pipettes were pulled from aluminosilicate glass capillaries (Hilgenberg, Malsfeld, Germany) and had resistances of 1–2 $\times$ $10^6$ ohm in the recording solutions. Recordings were performed in the inside-out configuration. Currents were recorded at 50 kHz after filtering at 10 kHz with an eight-pole Bessel filter. For noise analysis, 30–100 identical pulses to –100 or –140 mV were applied, and the mean response, $I$, was calculated. The variance, $\sigma^2$, was calculated from the averaged squared difference of consecutive traces. Background variance at 0 mV was subtracted, and the variance–mean plot was fitted by $\sigma^2 = iI - I^2/N$, with the single-channel current, $i$, and the number of channels, $N$, as free parameters (Pusch *et al*., 1994). The maximal open probability, $P_{max}$, was estimated by $P_{max} = I_{max}/(N * i)$, where $I_{max}$ is the maximal current.

*Statistical analysis*

Each mutant screened was expressed and analysed in at least two batches of oocytes, and measurements were performed for at least three oocytes. For all injections, control measurements were performed for wild-type (WT) ClC-Ka. Statistical analysis was performed using Student's unpaired *t*-test. The five mutants mentioned in the Abstract had a highly significantly different response to NFA at 200 μM compared to WT ($P < 0.01$), whereas none of the other mutants was significantly different ($P > 0.05$).

## Results

Application of NFA from the extracellular side of the membrane leads to a rapid potentiation of ClC-Ka (Liantonio *et al*., 2006; Picollo *et al*., 2007) (Figure 1). Therefore, the NFA binding site(s) involved in this potentiating effect are most likely accessible from the outside. Thus, in order to identify the residues involved in NFA binding, we selected several amino acids which are predicted to be accessible from the extracellular side, based on the crystal structure of the bacterial ClC-ec1 (Dutzler *et al*., 2002; 2003). This model has been useful in previous studies of drug-binding sites on human CLC channels (Estévez *et al*., 2003; Picollo *et al*., 2004). We applied several different criteria to select amino acids to mutate. Because ClC-K1 is only blocked by NFA, whereas ClC-Ka and ClC-Kb are both potentiated, we first identified amino acids that are conserved in ClC-Ka and ClC-Kb, but not in ClC-K1. However, because the homology between all ClC-K channels is very high, it is possible that ClC-K1 presents nevertheless a 'vestigial' potentiating site. Therefore, in addition, we selected

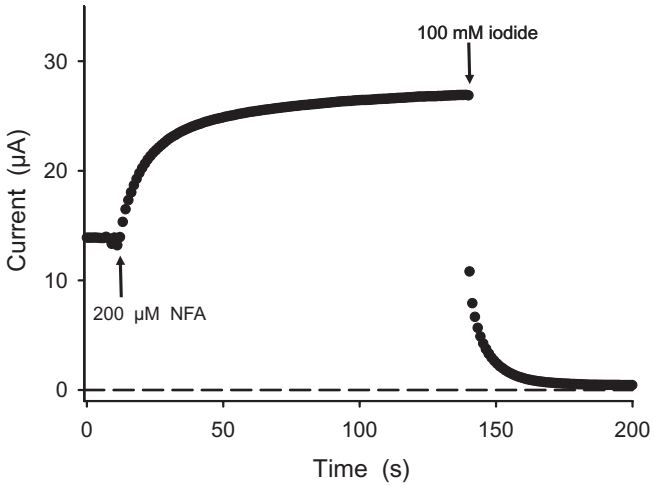


**Figure 1** Typical response of WT ClC-Ka to the application of 200 μM NFA. A 60 mV test pulse of 100 ms duration was applied about once per second, and the average current is plotted as a function of time. The current remaining after the application of 100 mM iodide was used as an estimate of endogenous/leak currents.

further residues based on their exposure to the extracellular side. In general, charged residues were neutralized, and if uncharged residues in ClC-Ka corresponded to charged residues in ClC-K1, such a mutation was introduced into ClC-Ka. Furthermore, if uncharged residues conserved in ClC-Ka and -Kb corresponded to a different uncharged residue in ClC-K1, the corresponding mutation was introduced into ClC-Ka. The residues selected are coloured in Figure 2A,B, which shows that we covered a relatively large portion of the surface-accessible part of the protein. Triggered by a recent publication on the effects of NFA on cation channels (Fernandez *et al*., 2008), we also mutated two residues that corresponded to a signature sequence of NFA binding, even though these residues are localized on the intracellular side (R182G and R184G, the latter of which did not yield functional expression).

WT ClC-Ka is robustly activated by more than twofold by 200 μM NFA (Figure 1) (Liantonio *et al*., 2006). Thus, to screen the mutations for a possible alteration of NFA-mediated potentiation, we applied 200 μM NFA to all mutants that could be functionally expressed in *Xenopus* oocytes. Currents were recorded using a test pulse to 60 mV once per second. After a stable baseline had been established in the absence of NFA, 200 μM NFA was continuously perfused, and after a steady state had been reached, we calculated the ratio of the current produced in the presence of NFA and the initial current induced in control conditions (see Figure 1 for a typical recording). Mean values of this ratio are shown in Figure 3. Most mutations only slightly altered the NFA-induced potentiation, the effect being non-significant. However, five mutations abolished the NFA-induced potentiation: L155A, G167A, F213A, G345S and A349E (shown as red bars in Figure 3).

The lack of potentiation by NFA in the presence of these mutations in principle suggests that these residues are contributing to the activating NFA binding site and/or are involved in conformational changes following NFA binding.

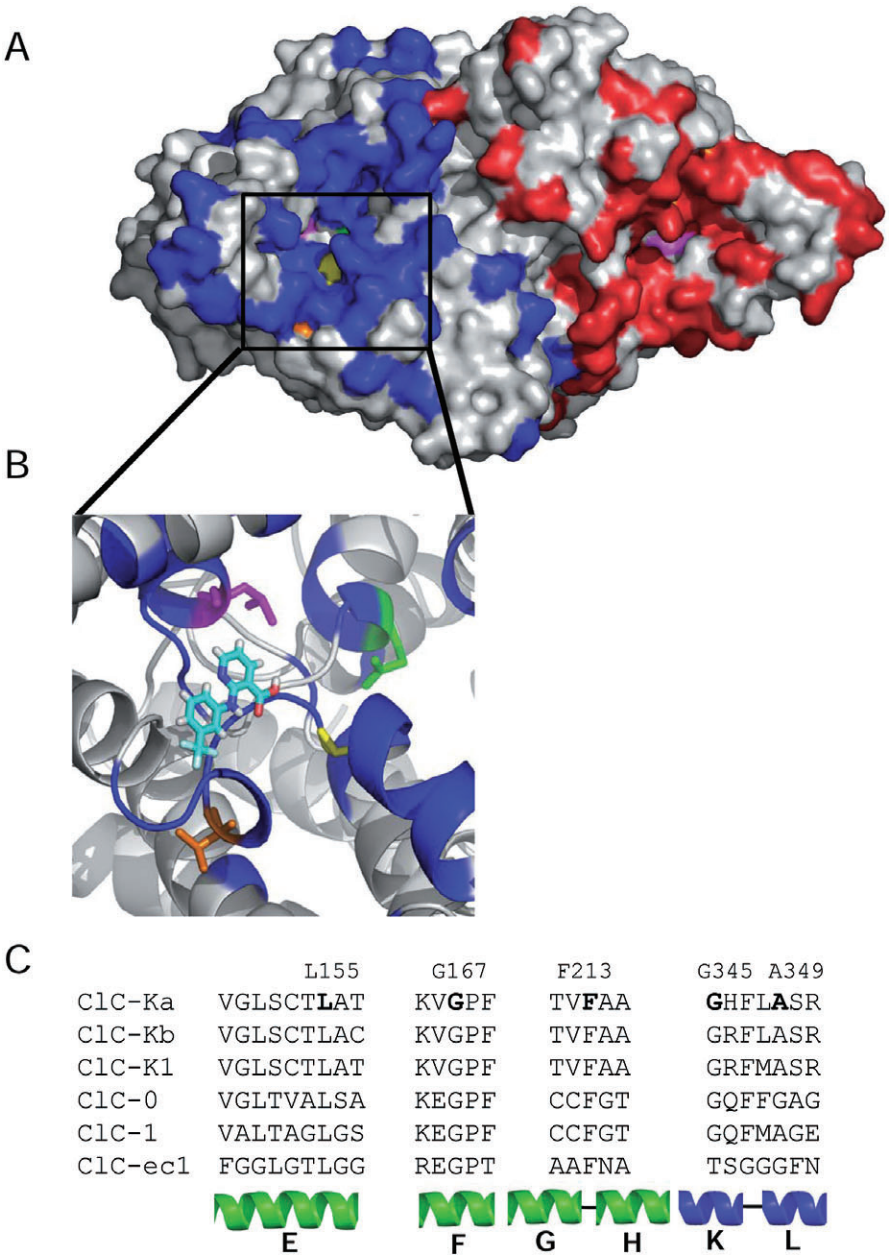


**Figure 2** Location of mutants mapped on the structure of ClC-ec1. (A) A surface representation of the bacterial ClC-ec1 (pdb entry 1OTS) viewed from the extracellular side. The central glutamate residue (E148) is coloured in green indicating the pore. The residues corresponding to those selected for mutation are shown in colour. In the left subunit, the residues that emerged as the most interesting ones are coloured in pink (L139 corresponding to L155 of ClC-Ka), orange (T312 corresponding to G345 of ClC-Ka) and yellow (G316 corresponding to A349 of ClC-Ka) respectively. (B) A zoom of the region comprising the extracellular side of helix E and the extracellular loop between helices K and L is shown in cartoon representation with the four residues L139, E148, T312, G316 highlighted as stick with colouring as in (A). An NFA molecule is shown close to the putative binding site. In (C), alignments of sequence stretches comprising the five residues (shown in bold) that affected NFA potentiation are shown.

However, further analysis is needed before such a conclusion can be reached. First of all, it has to be kept in mind that NFA potentiates ClC-Ka by increasing its open probability (Picollo *et al*., 2007). Thus, we first have to exclude that the lack of potentiation is due to an intrinsic modification of the gating properties brought about by the mutation. In fact, two of the positive hit mutants, G167A and F213A, probably affect the NFA potentiation by this mechanism.

G167 is a highly conserved residue adjacent to V166 (Figure 2C), a residue of paramount importance for the gating of all CLC proteins (Zifarelli and Pusch, 2007). The current level of G167A was significantly enhanced compared to WT: whereas WT expressed microampere-sized currents 3 days after injection, G167A-injected oocytes expressed currents after 1 day and the RNA had to be diluted at least fivefold (compared to WT) in order to obtain an expression level below 10 μA (data not shown). Moreover, the currents mediated by G167A lacked the time-dependent relaxations that characterize WT currents, consistent with a drastic effect on channel gating (Figure S1).

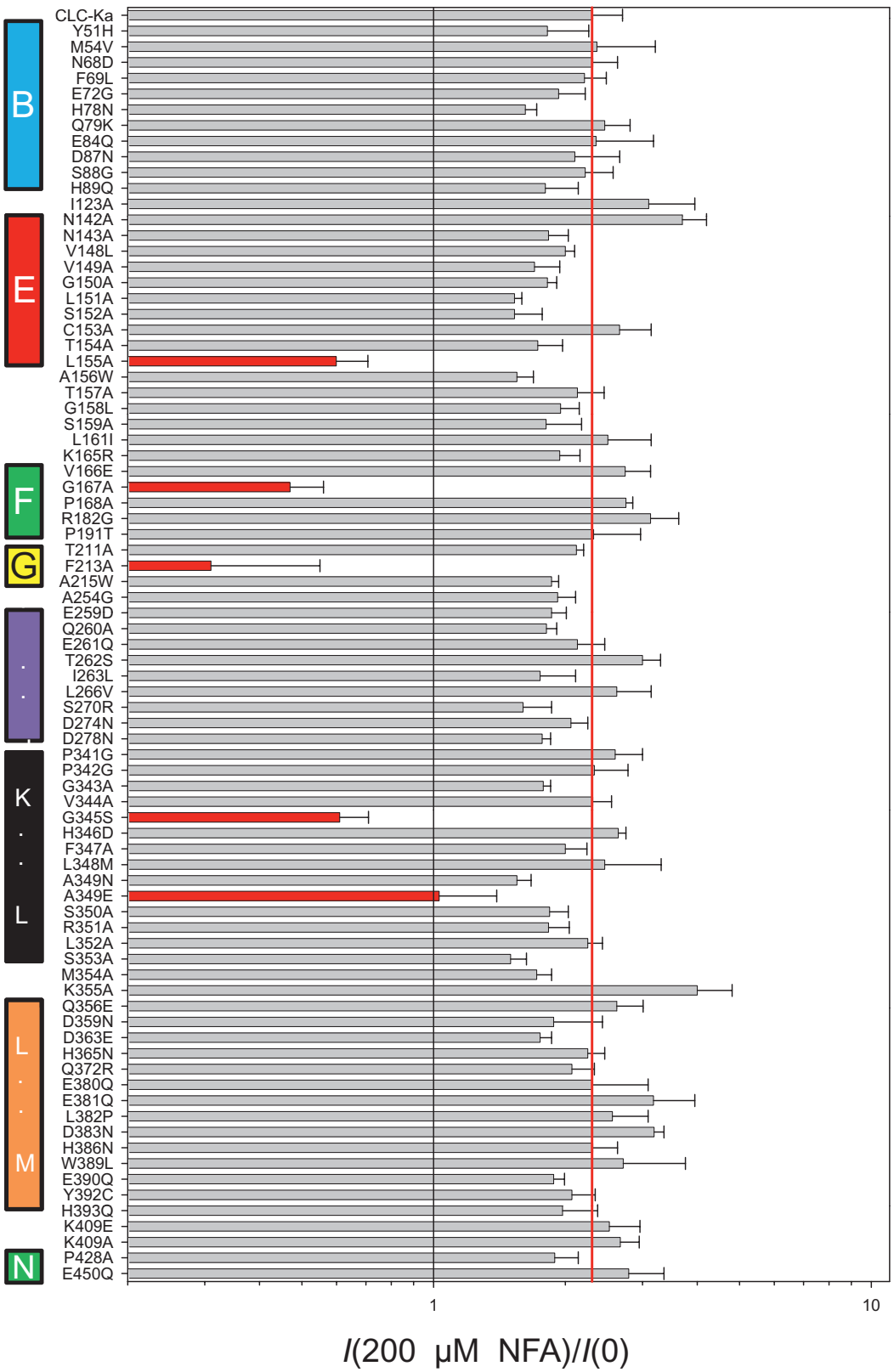


**Figure 3** Mutational analysis of NFA-mediated potentiation. The ratio of currents in the presence of 200 µM NFA and in control solution at 60 mV is plotted for the mutations that resulted in significant functional expression ($n \geq 3$; error bars indicate SEM). Mutants L155A, G167A, F213A, G345S and A349E were significantly different from WT ($P < 0.01$), whereas the remaining mutants were not significantly different ($P > 0.05$) (see Methods for statistical analysis). The red line indicates the value for WT; the black line indicates the value '1' (i.e. implying no effect of NFA on current magnitude). The mutants E281D and E442D showed very small expression not allowing a quantitative assessment of NFA effects. The following mutants showed no expression above background: T55A, Y56C, C73R, R184G, V212A, A214W, A214T, E259Q, E281Q, D363N, G424A, M427A, E442Q.

F213 is also a highly conserved residue (Figure 2C). Similar to G167A, the currents mediated by F213A are much larger than those for WT and exhibit much less voltage-dependent gating relaxations (Supporting Information Figure S1).

To assess a possible effect on gating parameters directly, we used non-stationary noise analysis to estimate the single-channel conductance and the absolute open probability ($p_{open}$) (Sigworth, 1980). However, preliminary single-channel recordings indicated that the single-channel behaviour of ClC-Ka is very flickery (Pusch, unpubl. results). Such flickery behaviour might interfere with the standard noise analysis if the fast transitions are not resolved. We therefore investigated, firstly, the influence of the filter frequency on the results. The power spectrum at –140 mV could be well fitted by the sum of three Lorentzian components (Supporting Information Figure S2A) with corner frequencies of 6.6 Hz, 208 Hz and 2.3 kHz respectively. The latter, high-frequency component, however, had a very small amplitude compared to the other two components (see legend of Supporting Information Figure S2A). Most importantly, the filter frequency did not seem to exert a large effect on the estimate of the single-channel conductance, as the largest difference for this parameter obtained at the most extreme filter frequencies tested (250 and 9000 Hz, respectively) was less than 30% (Supporting Information Figure S2B). Thus, non-stationary noise analysis appears to be a valid method to be applied to the ClC-Ka channel. WT ClC-Ka is characterized by a single-channel conductance of ~18 pS and a $p_{open}$ that is very small under the experimental conditions tested (i.e. 10 mM external calcium, pH 7.3) (Figure 4A; Table 1). In fact, if the $p_{open}$ is less than ~0.1, noise analysis is not suitable for determining the absolute value. Moreover, the application of this technique is somehow problematic for F213A and even more so for G167A, as the lack of current kinetics (Figure 4B,C; left panels) only allows a very limited range of the parabola in the variance–mean plot to be resolved (Figure 4B,C; right panels), rendering the independent estimate of $p_{open}$ and of the single-channel current unreliable. Nevertheless, the noise analysis is compatible with a single-channel conductance similar to that of WT ClC-Ka and a greatly increased $p_{open} \geq 0.5$ (fits in Figure 4B,C; Table 1). Thus, although not conclusive, several pieces of evidence suggest that G167A and F213A have altered gating properties and a drastically increased $p_{open}$ compared to WT. This thwarts any kind of conclusion about the modification of NFA action on these mutants.

Currents elicited by the mutant L155A were found to be similar to WT with respect to both magnitude and kinetics (Figure 5A,B), suggesting that the overall gating characteristics are similar. In fact, non-stationary noise analysis indicated that this mutant is characterized by an open probability that is significantly smaller than 0.1, similar to WT (Figure 4C; Table 1); 200 μM NFA decreased the current in this mutant ($I_{NFA}/I_{control} = 0.43$). L155 is located on the extracellular side of helix E and is very much conserved among CLC proteins (Figure 2C). Interestingly, several other mutations in helix E (L151A, S152A, A156W; see Figure 2) appeared to reduce the NFA-mediated potentiation of the current, but this effect was not significant.

G345 and A349 are located on the extracellular loop connecting helices K and L, and they are also conserved, although

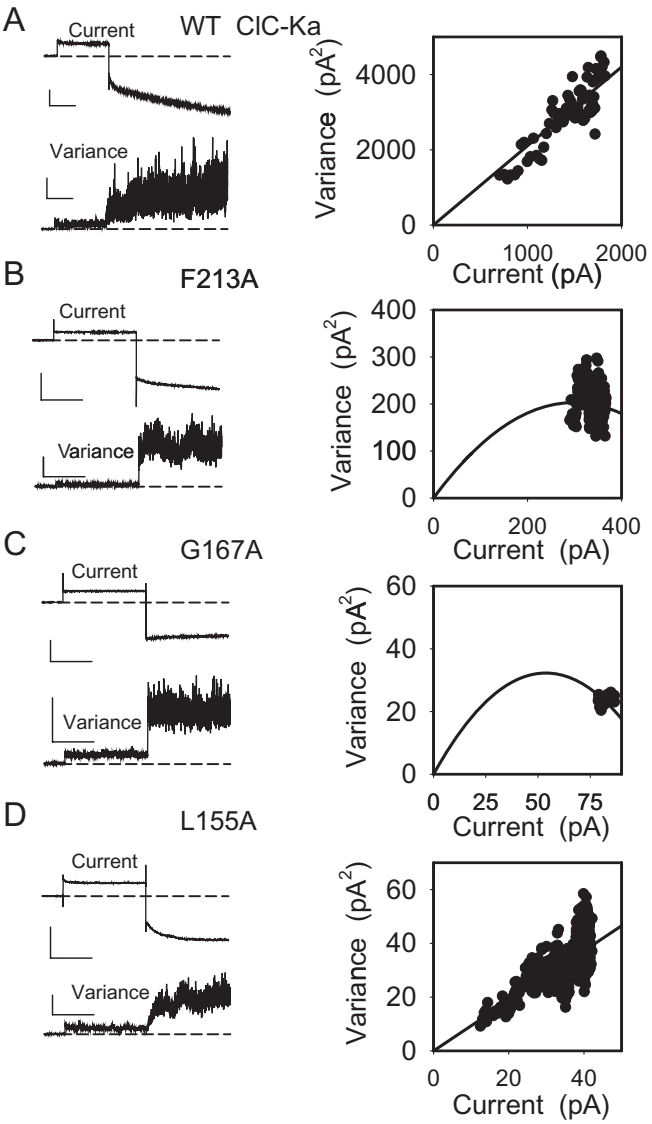


**Figure 4** Noise analysis revealed gating alterations. Typical results of non-stationary noise analysis of WT ClC-Ka (A), mutant F213A (B), mutant G167A (C) and mutant L155A (D) are shown. The mean (upper trace) and the variance (lower trace) are shown on the left, while the right shows the variance plotted versus the mean (symbols) and fitted with a parabola (line) as described in Methods. The parameters obtained by the fit are: (A): $i = 2.1$ pA, $P_{max} < 0.1$; (B): $i = 1.4$ pA, $P_{max} = 0.61$; (C): $i = 1.2$, $P_{max} = 0.81$; (D): $i = 0.93$, $P_{max} < 0.1$. Horizontal scale bars indicate 100 ms; vertical scale bars indicate: (A) 500 pA, 2000 pA$^2$; (B) 200 pA, 100 pA$^2$; (C) 50 pA, 20 pA$^2$; (D) 20 pA, 20 pA$^2$. Mean values of $P_{max}$ are shown in Table 1.

to a lesser extent compared to the other residues analysed (Figure 2C). The currents elicited by G345S were smaller than those in WT, and the current relaxations that characterize the WT were almost completely absent (Figure 5C). Also for this mutant, 200 μM NFA had a blocking rather than a potentiating effect (Figure 5C). The currents mediated by the mutant A349E were very similar to WT (Figure 5D) and were unaffected by 200 μM NFA (Figure 5D). Unfortunately, the levels of the currents of the mutants A349E and G345S were too small to allow noise analysis using the patch clamp technique.

**Table 1** Average values for the maximal open probability obtained from non-stationary noise analysis

| *Construct* | $P_{max}$ |
|---|---|
| WT ClC-Ka | <0.1 ($n$ = 9) |
| F213A | 0.50 ± 0.1 ($n$ = 4) |
| G167A | 0.75 ± 0.06 ($n$ = 4) |
| L155A | <0.1 ($n$ = 5) |

Fit values obtained for WT ClC-Ka and mutant L155A are <0.1 precluding a determination of the true value using this method.

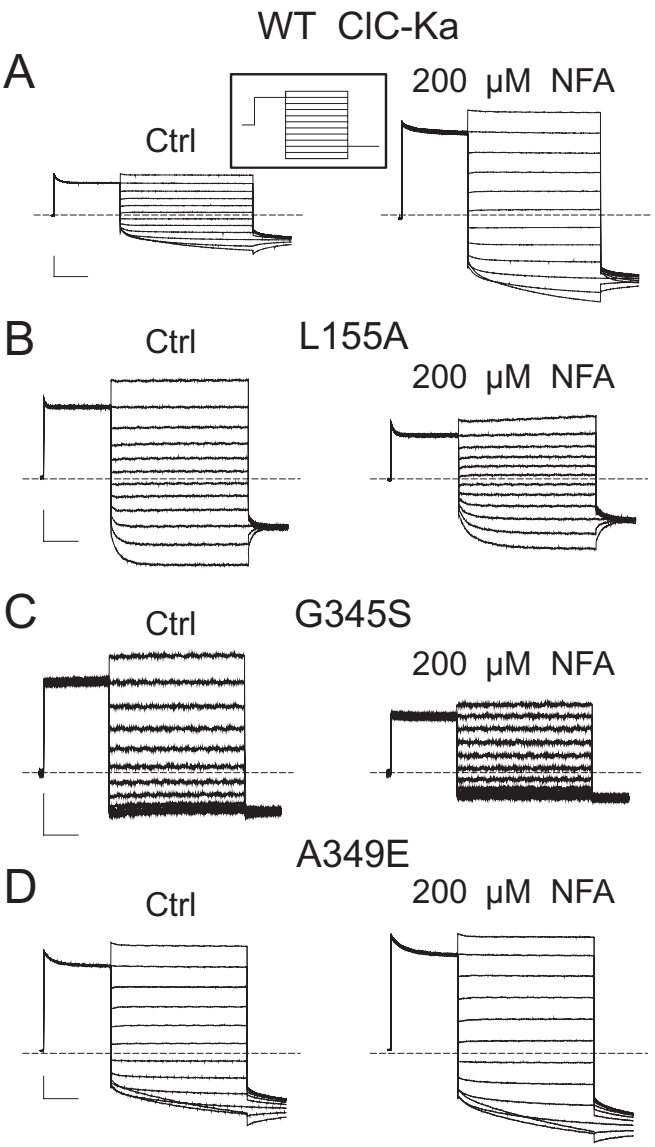


**Figure 5** Representative current traces for WT and the indicated mutants in control solution and in 200 µM NFA. Horizontal scale bars correspond to 50 ms; vertical scale bars correspond to 5 µA for WT and 1 µA for the mutants. The pulse protocol comprised a prepulse to 60 mV followed by steps to values from –140 to 80 mV, and a tail pulse to –100 mV and is depicted in (A) as an inset.

Taken together, the lack of a potentiating effect to NFA in the L155A, G345S and A349E mutants indicates that the interaction between these mutants and NFA is drastically altered compared to that in the WT. However, the results

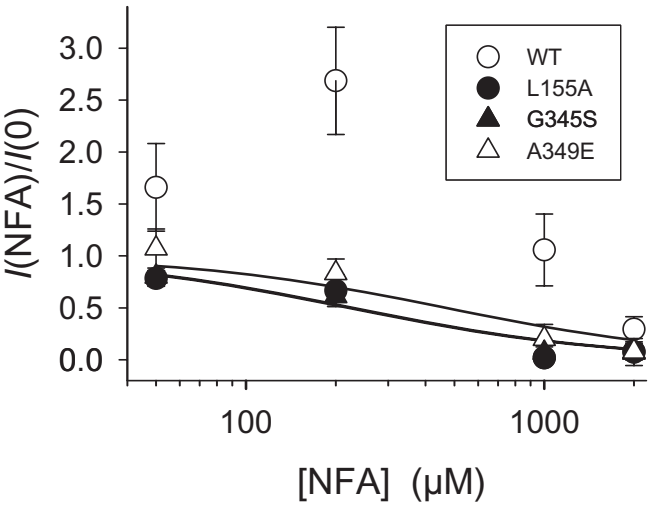


**Figure 6** Concentration dependence of the effects of NFA in WT and in the indicated mutants. Lines are fits to the equation $I([NFA])/I(0) = 1/(1 + [NFA]/K)$ with the apparent dissociation constant $K$ as the fitted parameter, resulting in values of 230 µM (L155A), 220 µM (G345S) and 460 µM (A349E) respectively.

could, in principle, be attributed to an enhanced block rather than a reduced potentiation. We therefore tested the response of these mutants to different NFA concentrations (Figure 6). In contrast to the biphasic response of WT ClC-Ka (Liantonio *et al*., 2006), all three mutants show monotonic NFA-induced inhibition with sub-millimolar $EC_{50}$ (see legend of Figure 6). Most importantly, 50 µM NFA, a concentration that leads to a significant potentiation of the WT, had only a small inhibitory effect on the mutants. These results confirm that the mutants specifically ablate the potentiating effect of NFA, but leave the NFA-induced block intact.

## Discussion and conclusions

ClC-K channels are essential components in the mechanism of water diuresis and NaCl re-absorption in the kidney and for the hearing process, and are involved in several human genetic diseases (Jentsch, 2005; Uchida and Sasaki, 2005; Zifarelli and Pusch, 2007). ClC-Kb polymorphisms have also been implicated in high blood pressure (Jeck *et al*., 2004), although recent publications contradict these findings (Kokubo *et al*., 2005; Speirs *et al*., 2005). Thus, pharmacological tools able to selectively modulate the activity of ClC-K channels can be of great interest in the treatment of several pathological conditions. Specific modulators of ClC-Ka may regulate water diuresis without affecting osmotic diuresis, mostly due to ClC-Kb (Picollo *et al*., 2004). In particular, increased water diuresis due to ClC-Ka block can be beneficial to reduce cardiac load, for example after heart failure (Fong, 2004). On the other hand, ClC-Ka potentiators might be useful to treat patients with Bartter syndrome type III or type IV, if residual channel activity is present.

NFA is a peculiar ClC-K ligand with unprecedented features; it potentiates ClC-Ka at low concentrations, but blocks the channel at high concentrations. On the basis of a kinetic model, it has been proposed that the two opposite effects of

NFA on ClC-Ka are mediated by two distinct binding sites (Picollo *et al*., 2007). N68, which is part of the blocking site for FFA and CPP derivatives (Picollo *et al*., 2004), does not appear to be part of the NFA binding site(s) (Picollo *et al*., 2007). This suggests that NFA acts on ClC-Ka by a different mechanism compared to FFA and CPP derivatives. The potentiation produced by NFA at low concentrations is caused by an augmentation of the open probability. Thus, NFA can be clearly classified as a gating modifier of ClC-K channels. Similar to its effect on ClC-Ka, NFA and other fenamates potentiate several types of cation channels (Busch *et al*., 1994; Abitbol *et al*., 1999; Malykhina *et al*., 2002; Fernandez *et al*., 2008; Cheng and Sanguinetti, 2009) modulating their open probability. On the other hand, NFA blocks various $Cl^-$ channels by binding to the ion-conducting pore, consistent with its negative charge. This appears to be the case for $Ca^{2+}$-activated $Cl^-$ channels (Qu and Hartzell, 2001) and for ClC-1, which is blocked from the intracellular side of the membrane (Liantonio *et al*., 2007). For ClC-Ka, it is still unclear whether the NFA-induced block at high concentrations reflects a pore-blocking mechanism.

In the present work, we set out to identify the NFA binding site on ClC-Ka that is responsible for the potentiating effect. The rapid current increase suggests that the binding site for potentiation is exposed to the extracellular side of the membrane. Using the bacterial ClC-ec1 structure as a guide, we screened 97 mutations and found that five mutations abolished the NFA-mediated potentiation. Interestingly, none of these mutations significantly reduced the block induced by NFA at higher concentrations. This finding is consistent with the idea that the potentiating and blocking effects are mediated by different protein regions.

Two of the residues identified (G167 and F213) are unlikely to contribute directly to the activating NFA binding site. Noise analysis of the mutants G167A and F213A, although not conclusive, is at least compatible with an increased open probability compared to WT, consistent with the presence of much larger currents. If this speculative interpretation holds, NFA would not have any effect on these mutants even in the presence of normal binding. However, in the absence of direct binding data, no firm conclusion about NFA binding can be drawn for these residues.

On the other hand, the fact that the mutants L155A, G345S and A349E did not display an increased current expression level, and, with the exception of G345S, exhibited similar current relaxations to those of WT, supports the idea that they specifically alter the NFA/channel interaction. However, an unaltered $p_{open}$ could be directly assessed only for mutant L155A, as this had a sufficient current expression level to allow non-stationary noise analysis measurements. Importantly, from the dose–response analysis, we can safely conclude that these mutations specifically eliminate the potentiating effect without significantly altering the blocking effect of NFA. This is the first direct evidence that the potentiating and blocking effects of NFA are mediated by distinct protein regions. Further studies are required to identify the blocking binding site.

Our results indicate that the extracellular side of helix E and the extracellular loop connecting helices K and L (in particular residues G345 and A349) are critical for the occurrence of the potentiating effect of NFA. In the bacterial ClC-ec1, these regions are exposed to the outside and are relatively close to each other. Given the molecular dimensions of NFA, which is shown in Figure 2 close to the putative binding site, it is possible that these residues contribute to the potentiating binding site for NFA. Because the sequence conservation between ClC-ec1 and ClC-K channels is very low (see e.g. Figure 2), it is impossible to predict the precise spatial orientation of the corresponding amino acids of ClC-Ka, and to draw specific structural conclusions regarding the NFA binding site.

Unfortunately, the NFA affinity associated with the current potentiation is rather low rendering direct ligand binding studies almost impossible. Thus, the possibility that the effect of the mutations could be due to an alteration of conformational changes that follow NFA binding cannot be excluded. Further studies are required to discriminate between these two models. In this respect, it is interesting to note that in addition to L155A, several other mutants located towards the interior helix E, reduced, but not significantly, the NFA-mediated potentiation. It may be speculated that the extracellular end of helix E is involved in direct NFA binding, while a re-arrangement of the helix is involved in the transmission of conformational changes that effectively increase the open probability.

Our results identify a protein region of ClC-Ka specifically responsible for the potentiating effect of NFA, and underscore the physical separation of protein regions responsible for the block and potentiation induced by NFA. They are fundamental for understanding the interaction between ClC-Ka and NFA at a molecular level, and therefore strongly indicate that CLC-K channels are suitable targets for drugs for the treatment of Bartter syndrome.

## Acknowledgements

We thank T.J. Jentsch for the ClC-Ka and barttin clone. This work was supported by grants from Telethon, Italy (GGP08064 to M.P.) and the Italian 'Ministero dell'Istruzione, dell'Università e della Ricerca' (MIUR PRIN 20078ZZMZW_002 to M.P., and MIUR PRIN 20078ZZMZW_003 to D.C.C.).

## Conflict of interest

None.

## References

Abitbol I, Peretz A, Lerche C, Busch AE, Attali B (1999). Stilbenes and fenamates rescue the loss of I(KS) channel function induced by an LQT5 mutation and other IsK mutants. *Embo J* **18**: 4137–4448.

Accardi A, Pusch M (2003). Conformational changes in the pore of CLC-0. *J Gen Physiol* **122**: 277–293.

Adachi S, Uchida S, Ito H, Hata M, Hiroe M, Marumo F *et al*. (1994). Two isoforms of a chloride channel predominantly expressed in

thick ascending limb of Henle's loop and collecting ducts of rat kidney. *J Biol Chem* **269**: 17677–17683.

Akizuki N, Uchida S, Sasaki S, Marumo F (2001). Impaired solute accumulation in inner medulla of Clcnk1–/– mice kidney. *Am J Physiol Renal Physiol* **280**: F79–F87.

Alexander SP, Mathie A, Peters JA (2008). *Guide to Receptors and Channels (GRAC)*, 3rd edition. *Br J Pharmacol* **153** (Suppl. 2): S1–209.

Birkenhäger R, Otto E, Schurmann MJ, Vollmer M, Ruf EM, Maier-Lutz I *et al*. (2001). Mutation of BSND causes Bartter syndrome with sensorineural deafness and kidney failure. *Nat Genet* **29**: 310–314.

Busch AE, Herzer T, Wagner CA, Schmidt F, Raber G, Waldegger S *et al*. (1994). Positive regulation by chloride channel blockers of IsK channels expressed in *Xenopus* oocytes. *Mol Pharmacol* **46**: 750–753.

Cheng L, Sanguinetti MC (2009). Niflumic acid alters gating of HCN2 pacemaker channels by interaction with the outer region of S4 voltage sensing domains. *Mol Pharmacol* **75**: 1210–1121.

Coyne L, Su J, Patten D, Halliwell RF (2007). Characterization of the interaction between fenamates and hippocampal neuron GABA(A) receptors. *Neurochem Int* **51**: 440–446.

Dutzler R, Campbell EB, Cadene M, Chait BT, MacKinnon R (2002). X-ray structure of a ClC chloride channel at 3.0 Å reveals the molecular basis of anion selectivity. *Nature* **415**: 287–294.

Dutzler R, Campbell EB, MacKinnon R (2003). Gating the selectivity filter in ClC chloride channels. *Science* **300**: 108–112.

Estévez R, Boettger T, Stein V, Birkenhäger R, Otto E, Hildebrandt F *et al*. (2001). Barttin is a $Cl^-$ channel beta-subunit crucial for renal $Cl^-$ reabsorption and inner ear $K^+$ secretion. *Nature* **414**: 558–561.

Estévez R, Schroeder BC, Accardi A, Jentsch TJ, Pusch M (2003). Conservation of chloride channel structure revealed by an inhibitor binding site in ClC-1. *Neuron* **38**: 47–59.

Fernandez D, Sargent J, Sachse FB, Sanguinetti MC (2008). Structural basis for ether-a-go-go-related gene $K^+$ channel subtype-dependent activation by niflumic acid. *Mol Pharmacol* **73**: 1159–1167.

Fong P (2004). CLC-K channels: if the drug fits, use it. *EMBO Rep* **5**: 565–566.

Foster RR, Zadeh MA, Welsh GI, Satchell SC, Ye Y, Mathieson PW *et al*. (2009). Flufenamic acid is a tool for investigating TRPC6-mediated calcium signalling in human conditionally immortalised podocytes and HEK293 cells. *Cell Calcium* **45**: 384–390.

Greenwood IA, Leblanc N (2007). Overlapping pharmacology of $Ca^{2+}$-activated $Cl^-$ and $K^+$ channels. *Trends Pharmacol Sci* **28**: 1–5.

Jeck N, Waldegger S, Lampert A, Boehmer C, Waldegger P, Lang PA *et al*. (2004). Activating mutation of the renal epithelial chloride channel ClC-Kb predisposing to hypertension. *Hypertension* **43**: 1175–1181.

Jentsch TJ (2005). Chloride transport in the kidney: lessons from human disease and knockout mice. *J Am Soc Nephrol* **16**: 1549–1561.

Kieferle S, Fong P, Bens M, Vandewalle A, Jentsch TJ (1994). Two highly homologous members of the ClC chloride channel family in both rat and human kidney. *Proc Natl Acad Sci U S A* **91**: 6943–6947.

Kokubo Y, Iwai N, Tago N, Inamoto N, Okayama A, Yamawaki H *et al*. (2005). Association analysis between hypertension and CYBA, CLCNKB, and KCNMB1 functional polymorphisms in the Japanese population – the Suita study. *Circ J* **69**: 138–142.

Liantonio A, Accardi A, Carbonara G, Fracchiolla G, Loiodice F, Tortorella P *et al*. (2002). Molecular requisites for drug binding to muscle CLC-1 and renal CLC-K channel revealed by the use of phenoxy-alkyl derivatives of 2-(*p*-chlorophenoxy)propionic acid. *Mol Pharmacol* **62**: 265–271.

Liantonio A, Pusch M, Picollo A, Guida P, De Luca A, Pierno S *et al*. (2004). Investigations of pharmacologic properties of the renal CLC-K1 chloride channel co-expressed with barttin by the use of 2-(*p*-chlorophenoxy)propionic acid derivatives and other structurally unrelated chloride channels blockers. *J Am Soc Nephrol* **15**: 13–20.

Liantonio A, Picollo A, Babini E, Carbonara G, Fracchiolla G, Loiodice F *et al*. (2006). Activation and inhibition of kidney CLC-K chloride channels by fenamates. *Mol Pharmacol* **69**: 165–173.

Liantonio A, Giannuzzi V, Picollo A, Babini E, Pusch M, Conte Camerino D (2007). Niflumic acid inhibits chloride conductance of rat skeletal muscle by directly inhibiting the CLC-1 channel and by increasing intracellular calcium. *Br J Pharmacol* **150**: 235–247.

Liantonio A, Picollo A, Carbonara G, Fracchiolla G, Tortorella P, Loiodice F *et al*. (2008). Molecular switch for CLC-K $Cl^-$ channel block/activation: optimal pharmacophoric requirements towards high-affinity ligands. *Proc Natl Acad Sci U S A* **105**: 1369–1373.

Lorenz C, Pusch M, Jentsch TJ (1996). Heteromultimeric CLC chloride channels with novel properties. *Proc Natl Acad Sci U S A* **93**: 13362–13366.

Malykhina AP, Shoeb F, Akbarali HI (2002). Fenamate-induced enhancement of heterologously expressed HERG currents in *Xenopus* oocytes. *Eur J Pharmacol* **452**: 269–277.

Matsumura Y, Uchida S, Kondo Y, Miyazaki H, Ko SB, Hayama A *et al*. (1999). Overt nephrogenic diabetes insipidus in mice lacking the CLC-K1 chloride channel. *Nat Genet* **21**: 95–98.

Matulef K, Howery AE, Tan L, Kobertz WR, Du Bois J, Maduke M (2008). Discovery of potent CLC chloride channel inhibitors. *ACS Chem Biol* **3**: 419–428.

Picollo A, Liantonio A, Didonna MP, Elia L, Camerino DC, Pusch M (2004). Molecular determinants of differential pore blocking of kidney CLC-K chloride channels. *EMBO Rep* **5**: 584–589.

Picollo A, Liantonio A, Babini E, Camerino DC, Pusch M (2007). Mechanism of interaction of niflumic acid with heterologously expressed kidney CLC-K chloride channels. *J Membr Biol* **216**: 73–82.

Pusch M, Steinmeyer K, Jentsch TJ (1994). Low single channel conductance of the major skeletal muscle chloride channel, ClC-1. *Biophys J* **66**: 149–152.

Pusch M, Liantonio A, Bertorello L, Accardi A, De Luca A, Pierno S *et al*. (2000). Pharmacological characterization of chloride channels belonging to the ClC family by the use of chiral clofibric acid derivatives. *Mol Pharmacol* **58**: 498–507.

Pusch M, Liantonio A, De Luca A, Conte Camerino D (2007). Pharmacology of CLC chloride channels and transporters. In: Pusch M (ed.). Chloride Transport across Biological Membranes*, Vol. 38*. Elsevier: Amsterdam, pp. 83–108.

Qu Z, Hartzell HC (2001). Functional geometry of the permeation pathway of $Ca^{2+}$-activated $Cl^-$ channels inferred from analysis of voltage-dependent block. *J Biol Chem* **276**: 18423–18429.

Rickheit G, Maier H, Strenzke N, Andreescu CE, De Zeeuw CI, Muenscher A *et al*. (2008). Endocochlear potential depends on $Cl^-$ channels: mechanism underlying deafness in Bartter syndrome IV. *Embo J* **27**: 2907–2917.

Schlingmann KP, Konrad M, Jeck N, Waldegger P, Reinalter SC, Holder M *et al*. (2004). Salt wasting and deafness resulting from mutations in two chloride channels. *N Engl J Med* **350**: 1314–1319.

Scholl U, Hebeisen S, Janssen AG, Müller-Newen G, Alekov A, Fahlke C (2006). Barttin modulates trafficking and function of ClC-K channels. *Proc Natl Acad Sci U S A* **103**: 11411–11416.

Sigworth FJ (1980). The variance of sodium current fluctuations at the node of Ranvier. *J Physiol* **307**: 97–129.

Simon DB, Bindra RS, Mansfield TA, Nelson-Williams C, Mendonca E, Stone R *et al*. (1997). Mutations in the chloride channel gene, *CLCNKB*, cause Bartter's syndrome type III. *Nat Genet* **17**: 171–178.

Speirs HJ, Wang WY, Benjafield AV, Morris BJ (2005). No association with hypertension of CLCNKB and TNFRSF1B polymorphisms at a hypertension locus on chromosome 1p36. *J Hypertens* **23**: 1491–1496.

Uchida S, Sasaki S (2005). Function of chloride channels in the kidney. *Ann Rev Physiol* **67**: 759–778.

Uchida S, Sasaki S, Furukawa T, Hiraoka M, Imai T, Hirata Y *et al*. (1993). Molecular cloning of a chloride channel that is regulated by dehydration and expressed predominantly in kidney medulla. *J Biol Chem* **268**: 3821–3824.

Verkman AS, Galietta LJ (2008). Chloride channels as drug targets. *Nat Rev Drug Discov* **19**: 19.

Waldegger S, Jeck N, Barth P, Peters M, Vitzthum H, Wolf K *et al*. (2002). Barttin increases surface expression and changes current properties of ClC-K channels. *Pflügers Arch* **444**: 411–418.

Zifarelli G, Pusch M (2007). CLC chloride channels and transporters: a biophysical and physiological perspective. *Rev Physiol Biochem Pharmacol* **158**: 23–76.

## Supporting information

Additional Supporting Information may be found in the online version of this article:

**Figure S1** Representative current traces for the mutants G167A (A) and F213A (B).
**Figure S2** Spectral properties of ClC-Ka.

Please note: Wiley-Blackwell are not responsible for the content or functionality of any supporting materials supplied by the authors. Any queries (other than missing material) should be directed to the corresponding author for the article.

## 3.2 A $Ca^{2+}$ binding site at the subunit interface of CLC-K channels

Previous studies demonstrated that ClC-K currents increase by increasing of extracellular $Ca^{2+}$ (Uchida et al, 1995; Sauvé et al, 2000; Waldegger & Jentsch, 2000; Estévez et al, 2001; Waldegger et al, 2002), while the channels are blocked by acid pH (Uchida et al, 1995; Waldegger & Jentsch, 2000; Estévez et al, 2001; Waldegger et al, 2002). Proton modulation is found in most CLC proteins both in $Cl^-/H^+$ antiporters and $Cl^-$ channels (Friedrich et al, 1999; Accardi & Miller, 2004; Picollo & Pusch, 2005; Zifarelli & Pusch, 2009a). The pH dependence of most CLC channels depends on the protonation/deprotonation of a "critical glutamate" that is involved in the opening of the channels (Hanke & Miller, 1983; Rychkov et al, 1996; Jordt & Jentsch, 1997; Chen & Chen, 2001; Arreola et al, 2002; Dutzler et al, 2003; Traverso et al, 2006; Zifarelli et al, 2008; Niemeyer et al, 2009; Zifarelli & Pusch, 2010). However, the "critical glutamate" is substituted by a neutral valine in ClC-K channels. Therefore a different mechanism has to mediate the pH dependence of CLC-Ks. The CLC-K modulation by $Ca^{2+}$ is a peculiar feature of these channels that is not found in other CLC proteins. Interestingly, $Ca^{2+}$ and proton modulation of CLC-K channels occur in physiological concentration ranges. Moreover, the kidney is involved in calcium reabsorption and the maintenance of acid-balance (see sections 1.3.4 "$Ca^{2+}$ reabsorption in the kidney" and 1.3.5 "The role of the kidney in the acid-base regulation-briefly", respectively). Therefore $Ca^{2+}$ and proton regulation of CLC-K channels is potentially of physiological relevance.

In this work we performed a detailed biophysical analysis of $Ca^{2+}$ and proton modulation of human CLC-K channels expressed in *Xenopus* oocytes. Voltage clamp measurements carried out varying $Ca^{2+}$ and proton concentrations indicated that hCLC-K currents increase with increasing $Ca^{2+}$ concentration without saturation up to 50 mM while they decrease at acid pH with an almost complete block at pH 6.0. Kinetic experiments, performed by patch recordings and fast solution exchange, showed an allosteric modulation of CLC-Ka for both, $Ca^{2+}$ and protons. Based on these experimental data, modeling predicted a two state (blocked/unblocked) mechanism for proton modulation. Moreover a Hill coefficient > 1 suggested that two protons are required to block the channel. Because $Ca^{2+}$ is not strictly essential for opening, a four-state mechanism could properly describe $Ca^{2+}$ modulation. To

identify the $Ca^{2+}$ binding site, we performed an extensive mutagenic screen of ClC-Ka. Based on the structure of the bacterial homologue EcClC-1, we mutated all titratable residues of ClC-Ka that are accessible from the outside. As result of this work we identified two mutations, E261Q and D278N, which reduced calcium sensitivity of ClC-Ka. The proximity of the residues, E261 and D278, from different subunits suggested that they likely form an intersubunit $Ca^{2+}$ binding site. In fact the double mutant E261D/D278N was completely $Ca^{2+}$-insensitive.

In addition to the "critical glutamate", an off-pore histidine was found to be involved in the proton modulation of ClC-2, in particular in proton induced block of this channel (Niemeyer et al, 2009). Based on this discovery, we mutated the corresponding residue of ClC-Ka, H497, in several amino acids. The only functional mutant, H497M yielded very small currents. Since the double mutant E261Q/D278N retained proton sensitivity, we prepared the triple mutant E261Q/D278N/H497M. The triple mutant completely abolished $H^+$-induced current block. We concluded that protonation of H497 is responsible for the block of CLC-K channels at acidic pH.

In the following pages I insert the article:

Gradogna A, Babini E, Picollo A & Pusch M. 2010. A regulatory calcium-binding site at the subunit interface of CLC-K kidney chloride channels. *J Gen Physiol* 136:311-23

Published August 30, 2010



# A regulatory calcium-binding site at the subunit interface of CLC-K kidney chloride channels

Antonella Gradogna, Elena Babini, Alessandra Picollo, and Michael Pusch

Istituto di Biofisica, Consiglio Nazionale delle Ricerche, 16149 Genoa, Italy

The two human CLC $Cl^-$ channels, ClC-Ka and ClC-Kb, are almost exclusively expressed in kidney and inner ear epithelia. Mutations in the genes coding for ClC-Kb and barttin, an essential CLC-K channel β subunit, lead to Bartter syndrome. We performed a biophysical analysis of the modulatory effect of extracellular $Ca^{2+}$ and $H^+$ on ClC-Ka and ClC-Kb in *Xenopus* oocytes. Currents increased with increasing $[Ca^{2+}]_{ext}$ without full saturation up to 50 mM. However, in the absence of $Ca^{2+}$, ClC-Ka currents were still 20% of currents in 10 mM $[Ca^{2+}]_{ext}$, demonstrating that $Ca^{2+}$ is not strictly essential for opening. Vice versa, ClC-Ka and ClC-Kb were blocked by increasing $[H^+]_{ext}$ with a practically complete block at pH 6. $Ca^{2+}$ and $H^+$ act as gating modifiers without changing the single-channel conductance. Dose–response analysis suggested that two protons are necessary to induce block with an apparent pK of ∼7.1. A simple four-state allosteric model described the modulation by $Ca^{2+}$ assuming a 13-fold higher $Ca^{2+}$ affinity of the open state compared with the closed state. The quantitative analysis suggested separate binding sites for $Ca^{2+}$ and $H^+$.

A mutagenic screen of a large number of extracellularly accessible amino acids identified a pair of acidic residues (E261 and D278 on the loop connecting helices I and J), which are close to each other but positioned on different subunits of the channel, as a likely candidate for forming an intersubunit $Ca^{2+}$-binding site. Single mutants E261Q and D278N greatly diminished and the double mutant E261Q/D278N completely abolished modulation by $Ca^{2+}$. Several mutations of a histidine residue (H497) that is homologous to a histidine that is responsible for $H^+$ block in ClC-2 did not yield functional channels. However, the triple mutant E261Q/D278N/H497M completely eliminated $H^+$-induced current block. We have thus identified a protein region that is involved in binding these physiologically important ligands and that is likely undergoing conformational changes underlying the complex gating of CLC-K channels.





## INTRODUCTION

In the kidney, transepithelial movement of ions and their relative reabsorption are guaranteed by the presence of channels and transporters along the nephron. In particular, Henle's loop is the nephron segment in which a large fraction of NaCl and divalent cations are reabsorbed, maintaining the body's salt equilibrium and fluid balance. In the thick ascending limb (TAL), $Cl^-$ is mainly taken up through the apical NKCC2 transporter, which works in concert with the Na-K-ATPase and the ROMK potassium channel, and is released from the basolateral membrane through ClC-Kb/barttin channels (Jentsch, 2005; Jentsch et al., 2005).

Human CLC-K channels belong to the CLC family of $Cl^-$ channels and transporters. ClC-Ka and ClC-Kb share 90% of identity in their primary structure and coassemble in the kidney and inner ear with the β subunit barttin (Uchida et al., 1993; Kieferle et al., 1994; Simon et al., 1997; Estévez et al., 2001; Jentsch, 2005; Jentsch et al., 2005). ClC-K1 (ClC-Ka) appears to be mainly expressed in the thin ascending limb of Henle's loop of the nephron, whereas ClC-K2 (ClC-Kb) is restricted to the basolateral membranes of epithelial cells in the TAL, connecting tubule, distal convoluted tubule, and intercalated cells. Both isoforms are also localized in basolateral membranes of marginal cells of the stria vascularis and in dark cells of the vestibular organ, in which they play a role in the production of the endolymph (Rickheit et al., 2008). The role of CLC-K channels is stressed by the association of mutations in the genes coding for CLC-Ks and barttin to several kidney diseases. Mutations in ClC-Kb and barttin genes are associated with the renal disease called Bartter syndrome (type III and type IV, respectively), which is characterized by renal salt wasting due to an impaired NaCl reabsorption in the TAL (Simon et al., 1997). Mutations in the gene coding for barttin also cause deafness (Birkenhäger et al., 2001). Moreover, it has been shown that mice lacking the ClC-K1 channel exhibit nephrogenic diabetes insipidus (Matsumura et al., 1999). Yet, no human

Correspondence to Michael Pusch: pusch@ge.ibf.cnr.it

A. Picollo's present address is Dept. of Anesthesiology, Weill Cornell Medical School, New York, NY 10021.

Abbreviations used in this paper: NFA, niflumic acid; TAL, thick ascending limb; WT, wild type.



The Rockefeller University Press $30.00
J. Gen. Physiol. Vol. 136 No. 3 311–323
www.jgp.org/cgi/doi/10.1085/jgp.201010455



Supplemental Material can be found at:
http://jgp.rupress.org/content/suppl/2010/08/23/jgp.201010455.DC1.html

Published August 30, 2010

disease with mutations only in the gene coding for ClC-Ka has been described yet. However, simultaneous loss of function of both ClC-Ka and ClC-Kb leads to Bartter syndrome (type IV) with deafness, similar to the effect of barttin mutations (Schlingmann et al., 2004). This result supports the idea that ClC-Ka and ClC-Kb are functionally redundant in the inner ear, but not in the kidney.

In previous reports, it has been described that human CLC-K channels, like the rodent CLC-K1, are modulated by extracellular $Ca^{2+}$ and protons in the millimolar range, and at physiological pH, respectively (Uchida et al., 1995; Estévez et al., 2001; Waldegger et al., 2002). In fact, both isoforms are enhanced by increasing $[Ca^{2+}]_{ext}$ and blocked by increasing concentration of extracellular protons. Modulation of CLC proteins by pH is very common. This is not surprising for those CLC proteins that act as $Cl^-/H^+$ antiporters because $H^+$ is one of the transported substrates (Friedrich et al., 1999; Accardi and Miller, 2004; Picollo and Pusch, 2005; Zifarelli and Pusch, 2009). However, most CLC channels are also strongly pH dependent because of the protonation/deprotonation of a conserved glutamate residue, the "gating glutamate," that is involved in the opening of the channels (Hanke and Miller, 1983; Rychkov et al., 1996; Jordt and Jentsch, 1997; Saviane et al., 1999; Chen and Chen, 2001; Arreola et al., 2002; Dutzler et al., 2003; Traverso et al., 2006; Zifarelli et al., 2008; Niemeyer et al., 2009; Zifarelli and Pusch, 2010). However, in contrast with most CLC channels, in CLC-K channels a valine residue substitutes the gating glutamate. Hence, their pH dependence cannot be mediated by the same mechanism. Recently, for ClC-2 two distinct regulatory sites for protons have been identified (Niemeyer et al., 2009): protonation of the gating glutamate activates ClC-2 in a voltage-dependent manner, whereas protonation of an off-pore histidine residue leads to channel block. Conceivably, a similar mechanism might be responsible for the $H^+$-induced block of CLC-K channels.

On the other hand, activation by extracellular $Ca^{2+}$ is unique to CLC-K channels. The concentrations at which CLC-Ks are maximally sensitive to $Ca^{2+}$ and $H^+$ are close to the physiological values found in extracellular fluids. Therefore, the modulation by these agents is likely of physiological relevance, even though there is no direct evidence for this view.

Here, we performed a detailed biophysical analysis of this modulation. Moreover, we performed a mutagenic screen and identified a histidine residue (H497) that is responsible for $H^+$-induced block as well as two residues (E261 and D278) that likely form an intersubunit $Ca^{2+}$-binding site.

## MATERIALS AND METHODS

### Molecular biology

Mutations were introduced by recombinant PCR as described previously (Accardi and Pusch, 2003). cRNA was transcribed in vitro by SP6 RNA polymerase (Applied Biosystems) after linearization with MluI. ClC-Ka and its mutants were coexpressed with human barttin Y98A to enhance the expression (Estévez et al., 2001). The barttin construct was linearized with NotI, and RNA was transcribed using T7 RNA polymerase. All cDNA constructs were provided by T. Jentsch (Leibniz-Institut für Molekulare Pharmakologie, Berlin, Germany).

### Electrophysiology

The cRNA of each construct was injected in defolliculated *Xenopus* oocytes. Oocytes were kept at 18°C in Barth's solution containing (in mM) 84 NaCl, 1 KCl, 2.5 $NaHCO_3$, 0.5 $Ca(NO_3)_2$, 0.6 $CaCl_2$, and 7.5 Tris-HCl, pH 7.4, or in a solution containing (in mM) 90 NaCl, 10 HEPES, 2 KCl, 1 $MgCl_2$, and 1 $CaCl_2$, pH 7.5. Voltage clamp data were acquired 2–4 d after the injection at room temperature using a custom acquisition program (Gepulse) and a custom-built amplifier or a TEC-03X amplifier (npi electronic). The standard bath solution contained (in mM): 112 NaCl, 10 $Ca$-Gluconate$_2$, 1 $MgSO_4$, and 10 HEPES, pH 7.3 (osmolarity: 235 mOsm). To study the effect of calcium on CLC-K currents, the concentration of $CaGluconate_2$ of the standard solution was varied between 0.1 and 50 mM (the 50-mM Ca solution had an osmolarity of 313 mOsm). The somewhat elevated osmolarity of these solutions did not lead to the unspecific activation of endogenous currents in non-injected oocytes. HEPES was replaced by MES buffer in solutions having a pH <7. The holding potential was chosen close to the resting membrane potential (∼−30 mV). To evaluate the currents at different potentials, we used the following protocols of stimulation. For Figs. 1 and 2: after a prepulse to −140 mV for 200 ms, channels were stimulated with voltages ranging from −140 to 80 mV with 20-mV increments for 500 ms. Pulses ended with a tail to 60 mV for 200 ms. For all other figures: after a prepulse to −100 mV for 100 ms, channels were stimulated with voltages ranging from −140 to 80 mV with 20-mV increments for 200 ms. Pulses ended with a tail pulse to 60 mV for 100 ms.

To evaluate $Ca^{2+}$ and pH effects on ClC-Ka wild type (WT) and all its mutants, the channels were stimulated with repetitive pulses to 60 mV for 200 ms applied at 1 Hz, and solutions with different pH and/or $[Ca^{2+}]$ were continuously applied until steady state was reached. Reversibility was always checked by returning to the standard solution. To estimate the contribution of endogenous currents, we applied a solution containing 100 mM NaI, 1 mM $MgSO_4$, and 10 mM HEPES, pH 7.3, that specifically blocks currents carried by CLC-K, but not endogenous currents (Picollo et al., 2004).

The effect of calcium and pH was quantified by calculating the ratio between the mean current at 60 mV in the specific solution and in the standard bath solution (10 mM $[Ca^{2+}]$, pH 7.3). Leak currents (i.e., currents remaining in iodide) were subtracted. Error bars in figures indicate SEM.

### Patch clamp experiments

For patch clamp recordings, the vitelline membrane of oocytes was mechanically removed during exposure to a hypertonic solution. The intracellular solution contained (in mM): 100 *N*-methyl-D-glucamine-Cl (NMDG-Cl), 2 $MgCl_2$, 10 HEPES, and 2 EGTA, pH 7.3. The standard extracellular solution contained (in mM): 90 NMDG-Cl, 10 $CaCl_2$, 1 $MgCl_2$, and 10 HEPES, pH 7.3. For some experiments, the pH was changed to 8 (keeping HEPES-buffer) or the $Ca^{2+}$ concentration was changed to 2 or 1.8 mM $CaCl_2$. For the 0 $Cl^-$ solution (Fig. 3), $Cl^-$ was exchanged by glutamate. Pipettes were pulled from aluminosilicate glass capillaries (Hilgenberg) and had resistances of 1–2 × $10^6$ Ohm in the recording solutions. Currents were recorded at 50 kHz after filtering at 10 kHz with an eight-pole Bessel filter. For the recordings shown in Fig. 3, the outside-out configuration of the patch clamp technique was used, whereas for the noise analysis experiments shown in Fig. S1, the inside-out configuration was used (Hamill et al., 1981; Stühmer, 1998).

Published August 30, 2010

For noise analysis, 30–100 identical pulses to −100 or −140 mV were applied, and the mean response, *I*, was calculated. The variance, $\sigma^2$, was calculated from the averaged squared difference of consecutive traces. Background variance at 0 mV was subtracted, and the variance-mean plot was constructed by binning as described by Heinemann and Conti (1992).

The binned variance-mean plot was fitted by $\sigma^2 = iI - I^2/N$, with the single-channel current, *i*, and the number of channels, *N*, as free parameters (Pusch et al., 1994). The single-channel conductance was calculated assuming a linear i-V relationship.

For the experiments shown in Fig. 3, a rapid solution exchanger (RSC-160; Biological Science Instruments) was used. In this instrument, three glass capillaries of 0.5-mm diameter are mounted on a rod that is rotated by a step motor. Full switching from one solution to the other requires ∼10 ms (see Fig. 3 A, inset c).

### Data analysis

Currents measured at different $[Ca^{2+}]_{ext}$ and pH were normalized to the steady-state current measured at 60 mV in the standard bath solution, i.e., 10 mM $Ca^{2+}$, pH 7.3. Normalized currents were plotted versus $[Ca^{2+}]_{ext}$ and pH.

### Online supplemental material

In Fig. S1, we show example experiments for nonstationary noise analysis done for ClC-Ka at various pH and $[Ca^{2+}]_{ext}$ conditions. In Fig. S2, we summarize the results of the effects of $[Ca^{2+}]_{ext}$ on all mutants. In Fig. S3, we summarize the results of the effects of $[pH]_{ext}$ on all mutants. Figs. S1–S3 are available at http://www.jgp.org/cgi/content/full/jgp.201010455/DC1.

## RESULTS

### Effect of extracellular calcium and protons on ClC-Ka and ClC-Kb channels

CLC-K currents, measured in the standard solution containing 10 mM $Ca^{2+}$, pH 7.3, show the following typical behavior: ClC-Ka partially deactivates at positive voltages and activates at negative voltages (Estévez et al., 2001; Picollo et al., 2004) (Fig. 1 A), whereas ClC-Kb activates at positive voltages and deactivates at negative

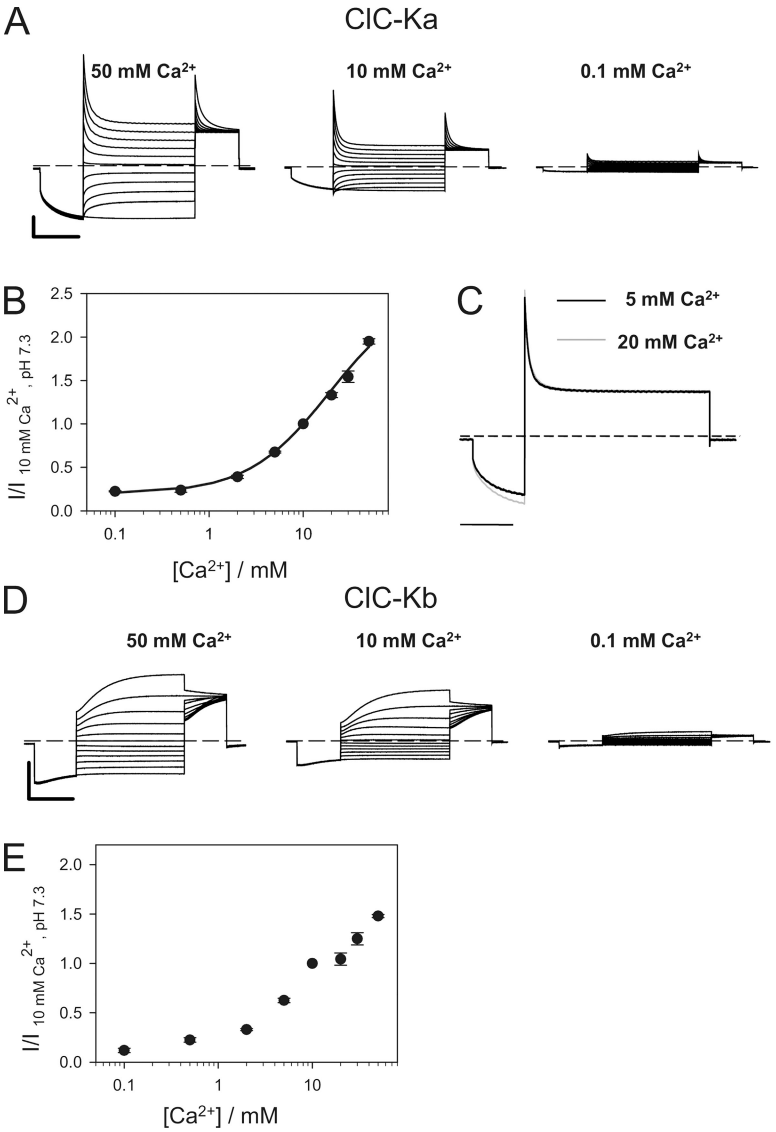


**Figure 1.** $Ca^{2+}_{ext}$ dependence of ClC-Ka and ClC-Kb. (A) Typical currents of ClC-Ka evoked by the standard IV-pulse protocol at different $Ca^{2+}$ concentrations as indicated, at pH 7.3. (B) Effect of $[Ca^{2+}]_{ext}$ on ClC-Ka (circles; $n = 9$). Current at 60 mV acquired at different conditions was normalized to values measured in standard solution ($I/I_{10}$ mM $Ca^{2+}$, pH 7.3) and plotted versus $[Ca^{2+}]_{ext}$ (used concentrations: 0.1, 0.5, 2, 5, 10, 20, 30, and 50 mM). The line represents the fit obtained using Eq. 2 as described in Results. (C) Superimposed traces measured at 60 mV at 5 mM $[Ca^{2+}]_{ext}$ (black line) and at 20 mM $[Ca^{2+}]_{ext}$ (gray line) measured from the same oocyte. Currents were scaled to the steady-state current at 60 mV. Horizontal bar, 200 ms. (D) Typical currents of ClC-Kb measured at different $Ca^{2+}$ concentrations as indicated. (E) Effect of $[Ca^{2+}]_{ext}$ (concentrations as in B) on ClC-Kb (squares; $n = 5$). Horizontal bars, 200 ms. Vertical bars, 5 µA.

Published August 30, 2010

voltages with slower kinetics compared with ClC-Ka (Estévez et al., 2001; Picollo et al., 2004) (Fig. 1 D).

In the first set of experiments, we applied solutions with different $Ca^{2+}$ concentrations ranging from 0.1 to 50 mM $Ca^{2+}$, keeping the pH fixed at 7.3. ClC-Ka–mediated currents increase with increasing $[Ca^{2+}]_{ext}$ (Estévez et al., 2001), without saturation up to 50 mM (Fig. 1 A). Such high $Ca^{2+}$ concentrations did not induce unspecific endogenous or leak currents in non-injected oocytes (not depicted). An important finding from a mechanistic point of view is that, at a $Ca^{2+}$ concentration of 0.1 mM, ClC-Ka currents are still ~20% of the currents measured in 10 mM $[Ca^{2+}]_{ext}$ (Fig. 1 B). Preliminary experiments showed that reducing $[Ca^{2+}]_{ext}$ to nominally zero did not further reduce currents compared with 0.1 mM $[Ca^{2+}]_{ext}$ (not depicted). However, the development of endogenous currents under these conditions precluded a more systematic investigation. These results suggest that extracellular $Ca^{2+}$ is not strictly essential for opening. As can be seen from the traces in Fig. 1 A, the kinetics—and thus the voltage dependence—are, to a first approximation unaffected by $[Ca^{2+}]_{ext}$. This is illustrated in more detail in Fig. 1 C, where currents recorded from the same oocyte at 5 mM $[Ca^{2+}]_{ext}$ and at 20 mM $[Ca^{2+}]_{ext}$ measured at 60 mV are superimposed and normalized to the steady-state current. ClC-Kb has a qualitatively very similar but slightly less pronounced dependence on $[Ca^{2+}]_{ext}$ (Fig. 1, D and E).

Next, we investigated the pH sensitivity of ClC-Ka and ClC-Kb (Fig. 2). In these experiments, $[Ca^{2+}]_{ext}$ was fixed at 10 mM. ClC-Ka–mediated currents decrease at acidic pH with an almost complete block at pH 6.0 (Fig. 2, A and B). Extracellular pH clearly alters the kinetics and the voltage dependence of gating, as demonstrated by the superposition of traces at pH 8.0 and at 7.0 measured at 60 mV (Fig. 2 C). In fact, protons slightly alter the kinetics of the current relaxation at positive voltages

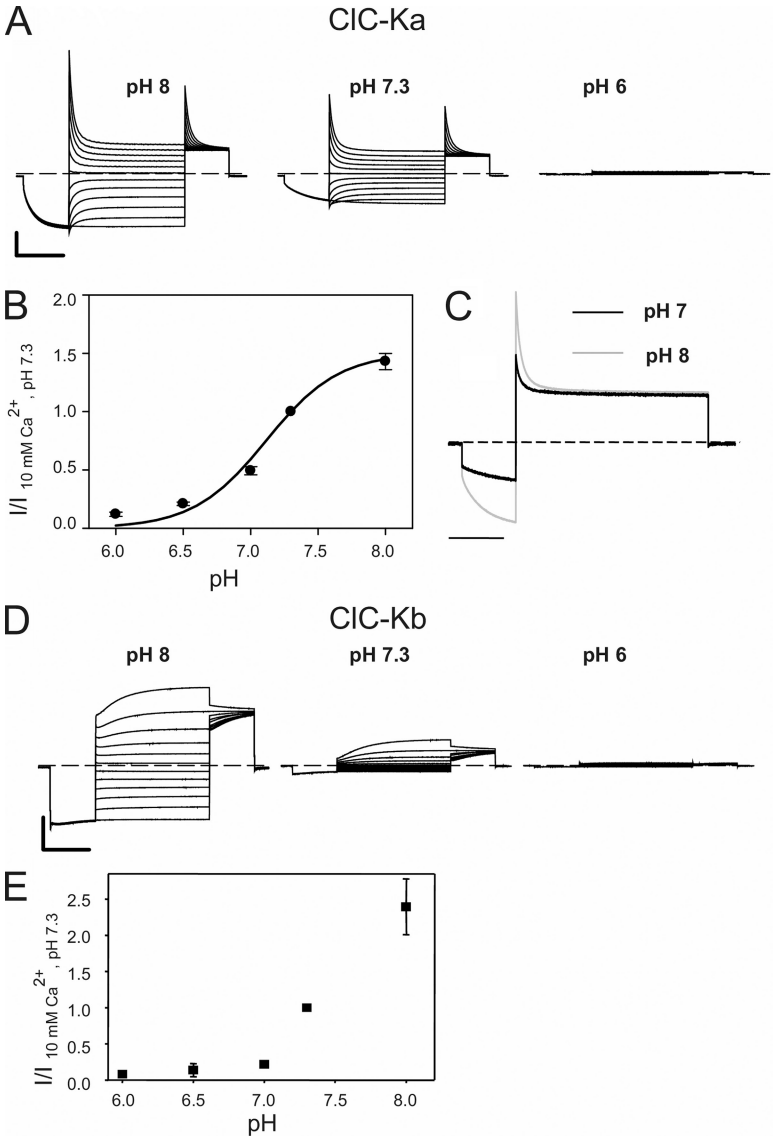


**Figure 2.** $pH_{ext}$ dependence of ClC-Ka and ClC-Kb. (A) Voltage clamp traces of ClC-Ka measured at different pH as indicated, in 10 mM $[Ca^{2+}]_{ext}$. (B) Effect of $pH_{ext}$ on ClC-Ka (circles; $n = 7$). Normalized currents were calculated as for Fig. 1. $I/I_{10}$ mM $Ca^{2+}$, pH 7.3, is plotted versus pH. The line represents the fit obtained using Eq. 1 as described in Results. (C) Superimposed traces measured at pH 7.0 (black line) and pH 8.0 (gray line) measured from the same oocyte. Currents were scaled to the steady-state current at 60 mV. Horizontal bar, 200 ms. (D) Traces of ClC-Kb measured at different pH as indicated, in 10 mM $[Ca^{2+}]_{ext}$. (E) Effect of $pH_{ext}$ on ClC-Kb (squares; $n = 4$). Horizontal bars, 200 ms. Vertical bars, 5 µA.

Published August 30, 2010

and significantly affect the activation at negative voltages. However, we did not study the effect of pH on the kinetics of gating in more detail, mainly because of the well-known problems of voltage clamp studies in *Xenopus* oocytes. ClC-Kb shows a similar behavior, but it appears to be more sensitive to proton block than ClC-Ka (Fig. 2, D and E), and for ClC-Kb, the effect of pH does not seem to saturate. This may be explained by a shift of the apparent pK of the effect toward more alkaline pH. Qualitatively, $Ca^{2+}$ and protons have a similar effect on both CLC-K homologues. Therefore, we focused our attention on ClC-Ka because of its higher expression compared with ClC-Kb.

An important mechanistic question is whether $Ca^{2+}$ and $H^+$ exert their effect by a direct pore-occluding mechanism or if they modulate in an allosteric manner the open probability of the channel that is governed by one or more gating processes. A crude distinction between these two possibilities can be based on a kinetic analysis: allosteric gating regulation is expected to be "slow," whereas a direct occluding effect is expected to be "fast." Rapid perfusion is difficult to achieve in whole oocyte recordings. Therefore, we conducted outside-out patch recordings and used a rapid perfusion system to change the extracellular pH or $Ca^{2+}$ concentration. A typical experiment is shown in Fig. 3 A, in which the current recorded at 60 mV from a patch containing many channels is displayed as a function of time. Upon reduction of external $Ca^{2+}$ from 10 to 1.8 mM, currents decrease reversibly. To test the speed of the perfusion system, a solution without $Cl^-$ was applied at the end of the experiment. The insets in Fig. 3 A (a, b, and c) show the solution changes at an expanded time scale, superimposed with single-exponential fits (red lines). The speed of the solution exchange was on the order of 10 ms (Fig. 3 A, inset c), clearly much faster than the relaxations observed upon changing the $Ca^{2+}$ concentration. Similarly slow relaxations were observed upon switching the extracellular pH from 7.3 to 8 (see Fig. 3 B). Average time constants are shown in Fig. 3 B for $Ca^{2+}$

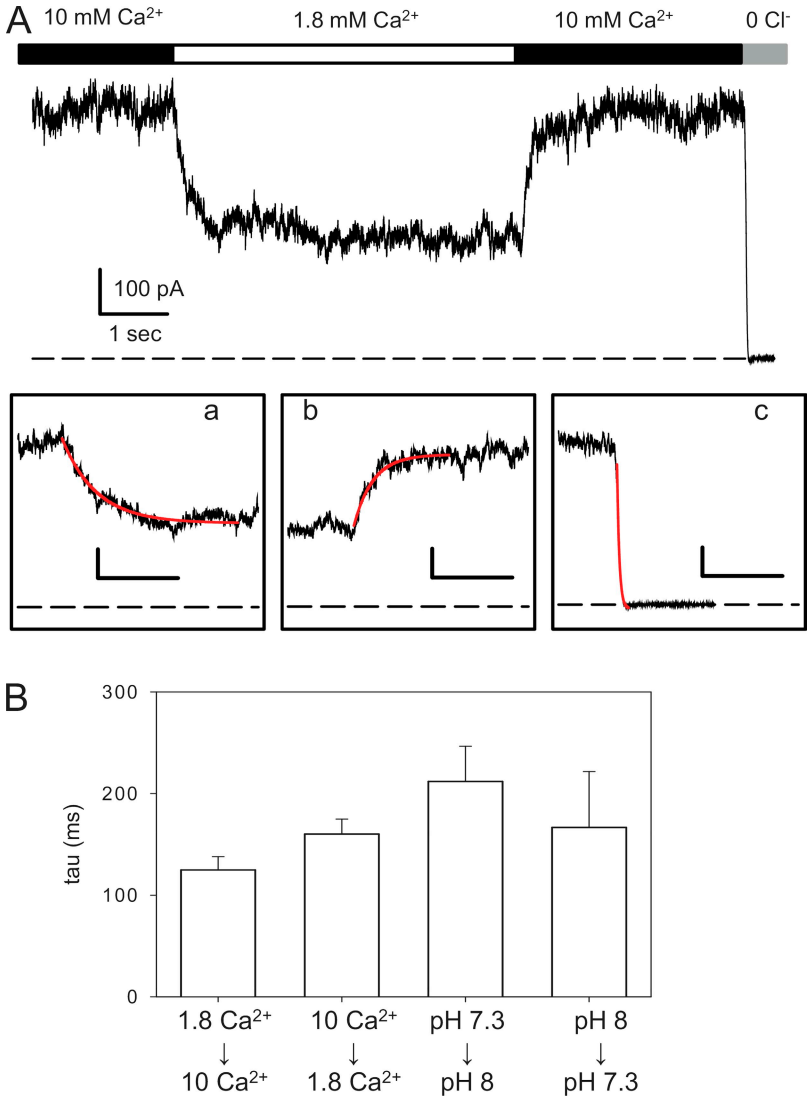


**Figure 3.** Relaxation kinetics upon fast concentration jumps in outside-out patches. (A) Example recording of a patch held at 60 mV in which $[Ca^{2+}]_{ext}$ was switched from 10 to 1.8 mM, and then back to 10 mM. Finally, the patch was exposed to a solution without $Cl^-$ (and without $Ca^{2+}$). The three insets below show the transition regions on an expanded time scale (bar, 500 ms), superimposed with a single-exponential fit (red line). Time constants for the solution exchange (inset c) were on the order of 10 ms. (B) Average time constants ($n > 3$ patches) for the indicated transitions.

Published August 30, 2010

jumps and pH jumps. These kinetic experiments suggest that both $Ca^{2+}$ and protons exert their effects by an allosteric modulation of the channel open probability.

To further exclude a direct effect on ion permeation, we performed nonstationary noise analysis to estimate the single-channel conductance. Typical experiments are shown in Fig. S1. From these experiments, no effect of $Ca^{2+}$ or pH on the single-channel conductance could be detected (Table I).

To find out whether $Ca^{2+}$ and $H^+$ compete for common binding sites, we performed experiments mixing the concentrations of the two cations. First, we applied solutions with various $[Ca^{2+}]_{ext}$, keeping the pH fixed at a value of 8, a condition of maximal stimulation in the range of pH values tested (see Fig. 2 A). Interestingly, ClC-Ka currents still increase without saturation up to 50 mM $Ca^{2+}$ (Fig. 4 A). Also at pH 6.5, a condition at which channel activity is very low (see Fig. 2 B), the effect of $Ca^{2+}$ was still clearly evident (Fig. 4 B). At this pH, measurements at a $[Ca^{2+}]_{ext}$ <2 mM are not reliable due to an increase of leak and endogenous currents after a long exposure to low pH and low $Ca^{2+}$. Next, keeping $[Ca^{2+}]_{ext}$ fixed at 0.5 mM, the pH dependence was very similar to that seen at $[Ca^{2+}]_{ext}$ of 10 mM (Fig. 4 C). These results suggest that extracellular $Ca^{2+}$ and extracellular protons act via independent mechanisms and binding sites. This hypothesis was further scrutinized by kinetic modeling.

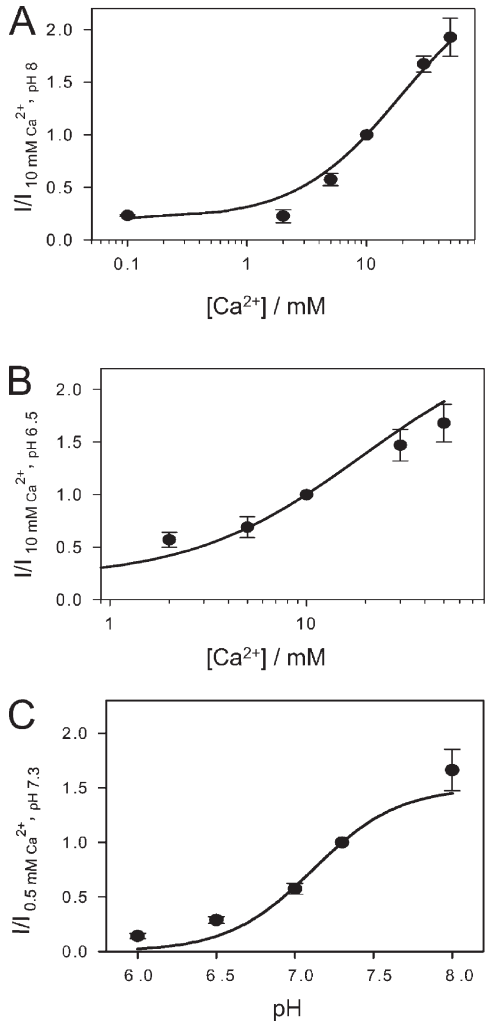


**Figure 4.** $Ca^{2+}$ and pH effects on ClC-Ka at mixed conditions. (A and B) Effect of $[Ca^{2+}]_{ext}$ on ClC-Ka measured at $pH_{ext}$ 8 (A, $n = 6$) and $pH_{ext}$ 6.5 (B, $n = 4$). Currents at 60 mV were normalized to values measured in 10 mM $[Ca^{2+}]_{ext}$ and plotted versus $[Ca^{2+}]_{ext}$. (C) Effect of $pH_{ext}$ on ClC-Ka in 0.5 mM $Ca^{2+}$ ($n = 3$). Currents at 60 mV were normalized to values measured at pH 7.3 and plotted versus $pH_{ext}$. Lines represent the theoretical predictions obtained using Eqs. 1 and 2 as described in Results using the same parameters obtained from the fit in the standard conditions (i.e., pK = 7.11; $K^C$ = 19.6 mM, $K^O$ = 1.5 mM, and $r_0$ = 434).

### Modeling pH and $Ca^{2+}$ modulation of ClC-Ka

Acidic pH practically completely blocks CLC-Ka. We therefore fitted the pH dependence by a simple Michaelis-Menten titration curve,

$$p_u = \frac{1}{1+\left(\frac{[H]}{K_H}\right)^n}, \quad (1)$$

where $p_u$ is the probability of not being blocked by a proton, *[H]* the proton concentration, $K_H$ the apparent binding constant, and $n$ the Hill coefficient. We define $pK = -log_{10}(K_H)$ for convenience. As shown in Fig. 2 C, proton-induced block is voltage dependent. For simplicity, however, we concentrated our analysis on the proton block at 60 mV. The solid line in Fig. 2 B is the best fit of Eq. 1, with $pK = 7.11$ and $n = 1.61$. The Hill coefficient is significantly larger than one suggesting that more than one proton (most likely two) is necessary to block the channel.

Regarding the modeling of the $Ca^{2+}$-induced potentiation, we have to consider that ClC-Ka channels are partially open even in the absence of $Ca^{2+}$. Therefore, a simple two-state mechanism is inadequate. Instead, we are forced to invoke an allosteric model of $Ca^{2+}$ modulation that incorporates an open non-$Ca^{2+}$–bound state. Conceptually, the simplest allosteric model is composed of four states, as shown below.

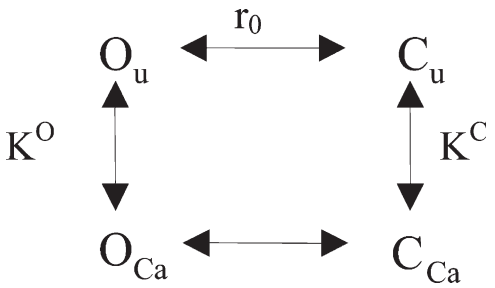


(SCHEME 1)

Published August 30, 2010

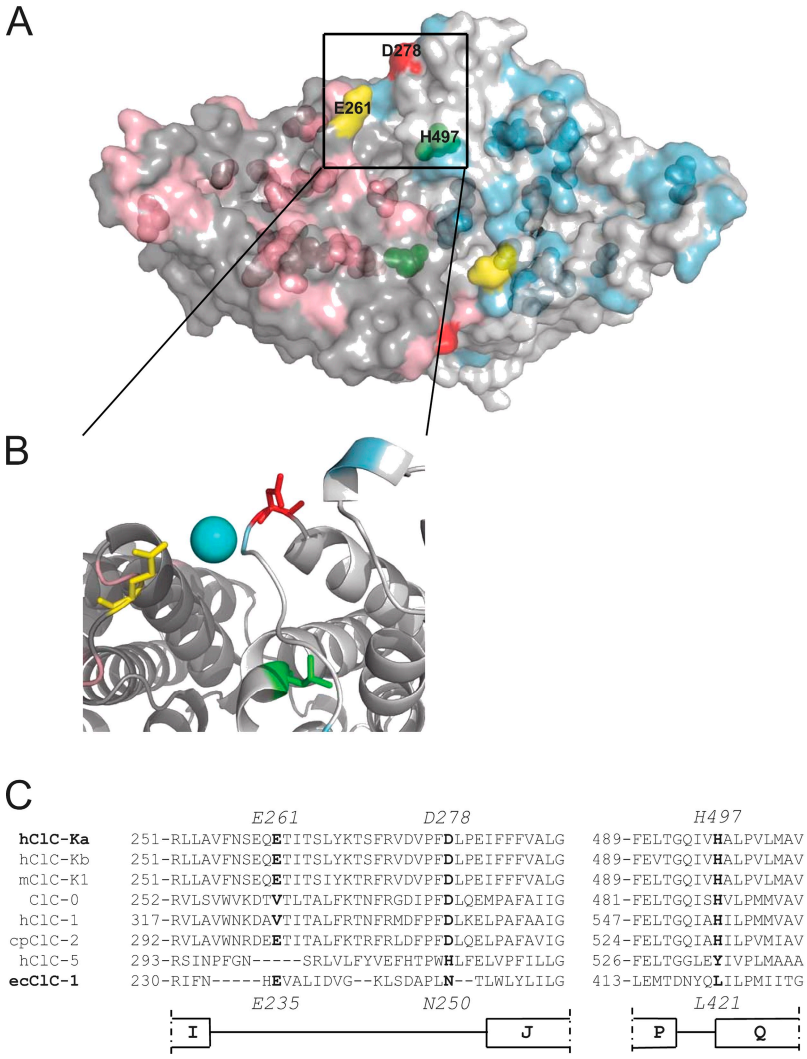


**Figure 5.** Location of mutants mapped on the structure of ecClC-1. (A) A surface representation of the bacterial ecClC-1 (Protein Databank accession no. 1OTS) viewed from the extracellular side is shown. The two subunits that compose ecClC-1 are colored in gray and light gray, respectively. The residues corresponding to those selected for mutation are shown in pink and light blue in the two different subunits, respectively. The transparent surface also allows a glimpse of the internal mutated residues. The residues responsible for $Ca^{2+}$ and $H^+$ sensitivity are shown in different colors: yellow, E261 (corresponding to E235 of ecClC-1); red, D278 (corresponding to N250 of ecClC-1); green, H497 (corresponding to L421 of ecClC-1); the numbers of residues indicated in the figure correspond to those of ClC-Ka. (B) A zoom of a selected region is shown in cartoon representation. The three residues E235, N250, and L421 are highlighted as sticks and colored as in A. A hypothetical $Ca^{2+}$ ion is shown as a light blue sphere between E261 and D278. (C) Alignments around the three residues responsible for $Ca^{2+}$ and proton sensitivity are shown. E261, D278, H497, and the corresponding residues in other CLCs are in bold.

Here, $O_u$ is the open $Ca^{2+}$-free state, and $O_{Ca}$ is the open state bound to $Ca^{2+}$. $C_u$ and $C_{Ca}$ refer similarly to the closed states. $Ca^{2+}$ binding to the open state is governed by the dissociation constant $K^O$, whereas $Ca^{2+}$ binding to the closed state is described by the dissociation constant $K^C$. $r_0$ is the ratio between the probability of being in states $C_u$ and $O_u$ ($r_0 = p(C_u)/p(O_u)$).

For Scheme 1, the open probability is given by the following equation:

$$p_o = \frac{1+\frac{[Ca]}{K^O}}{1+r_0+\frac{[Ca]}{K^O}+r_0\frac{[Ca]}{K^C}}. \quad (2)$$

The solid line in Fig. 1 B is the best fit of Eq. 2, resulting in $K^C$ = 19.6 mM, $K^O$ = 1.5 mM, and $r_0$ = 434. The theoretical prediction of this model nicely fits the experimental data. The value obtained for $r_0$ cannot be considered reliable. In fact, the model predictions are practically independent from the value of $r_0$, as long as it is significantly >1. The precise determination of $r_0$ would imply knowledge about the absolute open probability, clearly an impossible piece of information to be obtained from macroscopic measurements.

To further test if proton-induced block and $Ca^{2+}$ potentiation are independent processes, we compared the experimental results obtained under "mixed conditions" (Fig. 4) with the predictions of the modeling obtained under standard conditions (Figs. 1 and 2). The lines in Fig. 4 were calculated using the same parameters obtained from the fits described above (i.e., pK = 7.11; $K^C$ = 19.6 mM, $K^O$ = 1.5 mM, and $r_0$ = 434). Within the experimental error, these fits provide an adequate

TABLE I

*Single-channel conductance estimated from noise analysis*

| Condition | Conductance (pS) | *n* |
|---|---|---|
| 10 mM $Ca^{2+}$, pH 7.3 | 16.0 ± 1.0 | 5 |
| 2 mM $Ca^{2+}$, pH 7.3 | 16.3 ± 0.7 | 3 |
| 10 mM $Ca^{2+}$, pH 8 | 16.6 ± 0.5 | 5 |

Published August 30, 2010

description of the data, consistent with the idea that $Ca^{2+}$ and $H^+$ act via independent mechanisms.

Thus, the model allows the following conclusions. First, two protons bind to the binding site for protons, and one $Ca^{2+}$ binds to the binding site for $Ca^{2+}$. Second, the analysis reveals that ClC-Ka has an affinity for $Ca^{2+}$ that is 13-fold higher in the open state ($K_{Ca}^{O}$ = 1.5 mM) than in the closed state ($K_{Ca}^{C}$ = 19.6 mM), suggesting that $Ca^{2+}$ promotes the open state of the channel. Proton block occurs with an apparent pK of ~7.11. However, we would like to note that the two-electrode voltage clamp measurements present some technical limitations such as, for example, problems arising from the series resistance and difficulties distinguishing small currents (e.g., in low pH) from endogenous currents. Therefore, additional evidence to support the conclusions from the modeling is desirable.

### Substitution of two externally accessible residues eliminates the sensitivity to $Ca^{2+}$

The structure of the bacterial homologue EcClC-1 has been determined by x-ray crystallography (Dutzler et al., 2002). The bacterial EcClC-1 is significantly homologous to the eukaryotic CLCs (Maduke et al., 2000). In particular, they share the same transmembrane topology and several conserved regions. For this reason, we used the structure of the bacterial transporter as a guide to select and mutate all titratable residues of ClC-Ka that could be accessible from the extracellular side of the pore. In total, we chose and mutated 50 residues that are located between helices B and Q (see legend to Fig. S2). In general, charged residues (Glu, Asp, Arg, Lys, and His) were neutralized. Other titratable residues (Cys and Tyr) were changed with non-titratable residues. In cases where the mutations were not functional,

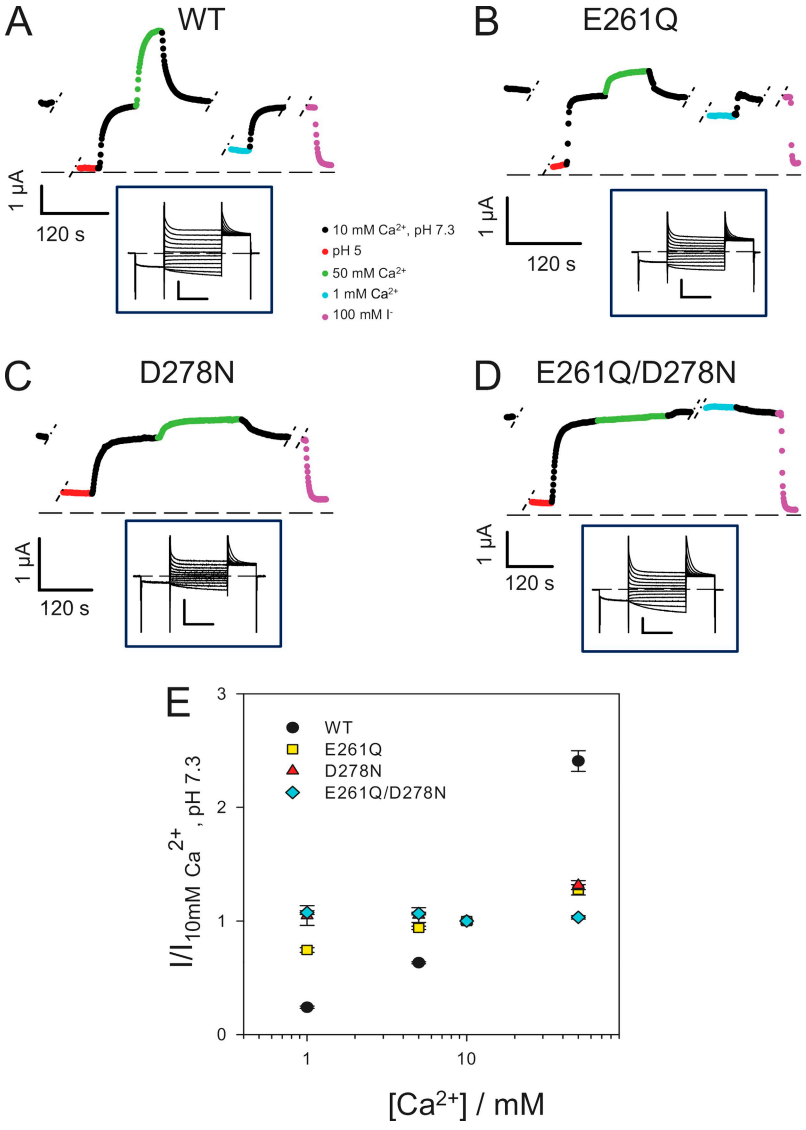


**Figure 6.** Effect of $[Ca^{2+}]_{ext}$ on ClC-Ka WT and its mutants E261Q, D278N, and E261Q/D278N. (A–D) The mean current, shown in color, at 60 mV plotted as a function of time. The type of solution applied is color coded as indicated in the middle inset. Breaks during the experiment are indicated with short dashed lines. Insets display representative current traces evoked by the standard IV-pulse protocol in standard solution. Horizontal bars, 100 ms; vertical bars, 3 µA. (E) Dose–response relationship of the modulation by $Ca^{2+}$ of ClC-Ka WT (black circles; $n$ = 16) and the mutants E261Q (yellow squares; $n$ = 4), D278N (red triangles; $n$ = 5), and E261Q/D278N (light blue rhombi; $n$ = 5). Currents at 60 mV were normalized to values measured in standard solution and plotted versus $[Ca^{2+}]_{ext}$. Data for WT are different compared with Fig. 1 because they were obtained from different oocytes as control measurements in the mutagenic screen. The currents shown for the mutants D278N and E261Q/D278N are from oocytes with exceptionally large expression. On average, the current expression level measured at 60 mV were (in µA ± SD [no. of oocytes]): WT (2 d), 2.5 ± 1.4 (7); WT (3 d), 5.3 ± 1.9 (8); E261Q (1–2 d), 4.3 ± 0.9 (4); D278N (>3 d), 1.1 ± 0.9 (8); E261Q/D278N (>3 d), 2.2 ± 0.9 (7); E261Q/D278N/H497M (>3 d), 0.8 ± 0.3 (15); not injected, 0.17 ± 0.07 (8).

Published August 30, 2010

we tried alternative and more conservative mutations. The extensive mutagenic screen is shown in Fig. 5 A, where we colored the mutated residues in light blue and in pink in the two different subunits. With the exception of H480 and E490, mutations of all other residues led to functionally active protein at least for one amino acid change. The majority of them displayed $Cl^-$ currents that rapidly deactivate at positive voltages and activate at negative voltages, similar to WT currents when measured in standard solution (not depicted). For each of these mutations, we studied the effect of extracellular $Ca^{2+}$ and protons. The results of this screen are shown in Figs. S2 and S3, where normalized currents of the mutants are plotted versus the calcium concentrations and pH, respectively. Although several mutations slightly affected calcium sensitivity (Fig. S2), only E261Q and D278N had a drastically reduced calcium sensitivity (Fig. 6, B and C).

E261Q loses most of the $Ca^{2+}$ sensitivity (Fig. 6, B and E). In fact, at 1 mM $[Ca^{2+}]_{ext}$, currents mediated by E261Q are >50% of the currents measured in 10 mM $[Ca^{2+}]_{ext}$, and when increasing $[Ca^{2+}]_{ext}$ to 50 mM, the currents only slightly increase. For this mutant, the normalized current $I([Ca^{2+}]_{ext})/I(10\ mM)$ varied less than twofold between 1 and 50 mM $[Ca^{2+}]_{ext}$, whereas for WT, the same ratio varied by ∼10-fold (Fig. 6, A and E).

Having identified E261 as being critical for $[Ca^{2+}]_{ext}$ sensitivity, we selected and mutated all residues located nearby, but none of these mutations were significantly different from WT (Fig. S2).

The other mutation, D278N, is even less $Ca^{2+}$ sensitive than E261Q (Fig. 6, C and E). In fact, currents mediated by D278N do not vary between 1 and 10 mM $[Ca^{2+}]_{ext}$, and they only slightly increase at 50 mM $[Ca^{2+}]_{ext}$ (Fig. 6, C and E). These results lead us to suggest that E261 and D278 could be part of a binding site for calcium. In agreement with this hypothesis, the double mutant E261Q/D278N completely abolishes the calcium sensitivity (Fig. 6, D and E).

Residue E261 is conserved in both human CLC-K homologues and also in the rodent isoforms ClC-K1 and ClC-K2, but not in all CLCs. Residue D278 is conserved in all human and rodent CLC-Ks and quite conserved in other CLCs (Fig. 5 C). Both are located in the loop between helices I and J (Fig. 5 C). Based on the alignment of ClC-Ka with EcClC-1, we tentatively assigned the residue in EcClC-1 corresponding to D278 of ClC-Ka to N250 in EcClC-1 (Fig. 5 C). Because of a gap in the bacterial sequence, we could not uniquely align E261 (Fig. 5 C). Tentatively, we assigned the bacterial residue E235 as the one corresponding to E261 (Fig. 5 C). Keeping in mind these limits, we evidenced E235, in yellow, and N250, in red, in a surface representation of EcClC-1 (Fig. 5, A and B). These residues are quite far from each other in the primary sequence. Interestingly, in the 3-D structure of EcClC-1, E235 from one subunit of the homodimer and N250 from the other subunit are relatively close to each other (∼10 Å). Thus, based on the experimental evidence and the structure of EcClC-1, we conclude that E261 and D278 are excellent candidates for forming an intersubunit $Ca^{2+}$-binding site.

### Substitution of an external residue removes the sensitivity to protons

Another objective of our work was to identify the residues of ClC-Ka that are responsible for the sensitivity to protons. Therefore, we investigated the pH sensitivity of all the mutants prepared (Fig. S3). In particular, we paid attention to the residues involved in calcium sensitivity.

E261Q and D278N are still responsive to different pH. Nevertheless, at basic pH, both show a behavior different from WT. In fact, currents mediated by E261Q only slightly increase at pH 8, whereas those mediated by D278N even decrease in the same pH range (Fig. 7 B). These results might point to an indirect involvement of these residues in the binding of protons.

Even though we selected and mutated all external titratable residues, we were not able to identify mutations that abolish the block induced at acidic pH effect. However, we could not obtain functional expression for several mutants of His-497, which corresponds to His-532 of the ClC-2 channel, where it has been shown to be responsible for $H^+$-induced block (Niemeyer et al., 2009). His-497 is located at the N terminus of helix Q in a region that is conserved in most CLC proteins (Fig. 5 C). In ClC-2, the H532F mutation was specifically shown to eliminate $H^+$ block. Unfortunately, the corresponding mutation in ClC-Ka (H497F) did not yield currents. In ClC-1, mutating the corresponding His to Ala was reported to yield normal channel function (Kürz et al., 1999). However, we could not obtain expression of the analogous H497A mutation. Among several other mutations (H497N, H497D, H497E, H497K, H497Y, and H497M), only H497M yielded very small currents that were, however, barely above background (not depicted). H497 corresponds to L421 in EcClC-1 (Fig. 5 C). We highlighted L421 in green in a surface representation of EcClC-1 (Fig. 5, A and B). Interestingly, H497 is localized relatively close to the amino acids E261 and D278, which form the acidic $Ca^{2+}$-binding site (on the same subunit as D278).

The proximity of these three amino acids and their lower $Ca^{2+}$ and $H^+$ sensitivity than WT drove us to prepare the triple mutant E261Q/D278N/H497M. Fortunately, the triple mutant showed bigger currents than H497M, allowing us to investigate its pH sensitivity. The triple mutant E261Q/D278N/H497M completely eliminated $H^+$-induced current block. In fact, currents did not vary significantly between pH 5 and 7.3 (Fig. 7, A and B). As expected, the triple mutant was also completely insensitive to $[Ca^{2+}]_{ext}$ (Fig. 7 A).

Published August 30, 2010

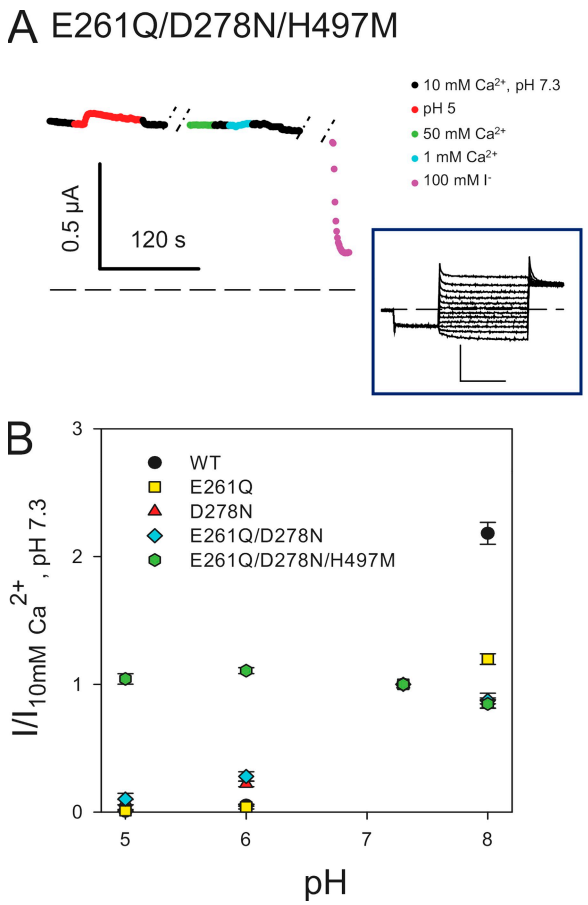


**Figure 7.** Effect of $[H^+]_{ext}$ on ClC-Ka WT and its mutants E261Q, D278N, E261Q/D278N, and E261Q/D278N/H497M. (A) The current at 60 mV, shown in color, of the triple mutant E261Q/D278N/H497M as a function of time (color code as in Fig. 6). Inset in A shows representative current traces of the mutant in standard solution. Horizontal bars, 100 ms; vertical bars, 1 µA. Capacitive transients have been blanked for clarity. (B) Dose–response relationship of the modulation by protons of ClC-Ka WT (black circles; $n = 14$) and the mutants E261Q (yellow squares; $n = 4$), D278N (red triangles; $n = 5$), E261Q/D278N (light blue rhombi; $n = 5$), and E261Q/D278N/E261Q (green hexagons; $n = 5$). Currents at 60 mV were normalized to values measured in standard solution and plotted versus pH. Data for WT are different compared with Fig. 2 because they were obtained from different oocytes as control measurements in the mutagenic screen.

## DISCUSSION

Here, we performed for the first time a detailed analysis of the modulation of CLC-K channels by extracellular $Ca^{2+}$ and protons. Both human homologues, ClC-Ka and ClC-Kb, are enhanced by increasing the extracellular $Ca^{2+}$ concentration and are blocked by increasing the extracellular proton concentration. As shown previously (Estévez et al., 2001), ClC-Kb appears to be slightly more sensitive to pH compared with ClC-Ka. However, we focused on ClC-Ka because of its higher expression compared with ClC-Kb. The relatively slow relaxation kinetics upon stepwise changes of $Ca^{2+}$ or pH in outside-out patch clamp recordings led us to conclude that both ions modulate CLC-K activity by altering the open probability of the channel. In fact, the absolute open probability of ClC-Ka and ClC-Kb in physiological conditions is significantly smaller than unity, allowing for a vast modulation of CLC-K–mediated membrane conductance by various ligands, including niflumic acid (NFA) (Zifarelli et al., 2010). Applying a two-state Michaelis-Menten model for $H^+$ block revealed that the binding of two $H^+$ is probably needed to induce channel closure, with an apparent pK of 7.1. A simple allosteric model for $Ca^{2+}$ modulation was able to reproduce the concentration dependence of the $Ca^{2+}$ modulation, assuming a dissociation constant of 19.6 mM for the closed state and 1.5 mM for the open state. The parameters obtained from the fits at standard conditions could also reasonably well describe $H^+$-induced block at low $[Ca^{2+}]$ and $Ca^{2+}$ modulation at more acidic and more alkaline pH, consistent with the idea that $Ca^{2+}$ and $H^+$ act via separate binding sites.

Next, using the structure of a bacterial CLC protein as a guide, we were able to identify the putative binding sites for both ions. Regarding the $H^+$-binding site, we were aided by recent results obtained for the ClC-2 channel (Niemeyer et al., 2009). ClC-2 is regulated by external pH in a biphasic manner: slightly acidic pH values activate the channel, whereas strong acidic conditions block it (Jordt and Jentsch, 1997; Arreola et al., 2002; Niemeyer et al., 2009). Niemeyer et al. (2009) showed that the potentiation of ClC-2 by external protons is mediated by the protonation of the "gating glutamate" residue that is highly conserved in most CLC proteins. However, in CLC-K channels, this glutamate is exchanged by a not-titratable valine residue. In contrast, the $H^+$-blocking site appears to be similar to the blocking site identified on the ClC-2 channel (Niemeyer et al., 2009). In ClC-2, protonation of His-532 appears to be responsible for $H^+$-induced block, in that the H532F mutation was not blocked at acidic pH (Niemeyer et al., 2009). Unfortunately, most mutations of the corresponding His-497 residue in ClC-Ka resulted in nonfunctional channels. However, we could obtain reasonable currents of the triple mutant E261Q/D278N/H497M that were insensitive to pH in the range of 5 and 8, whereas the E261Q/D278N mutation was fully blocked at pH 5. Based on these results, we cannot completely rule out a certain interdependence of the pH and the $Ca^{2+}$ effects because we could assert the importance of the His-497 residue for $H^+$ block only in the context of a $Ca^{2+}$-insensitive construct (i.e., E261Q/D278N). Nevertheless, these results also suggest that in ClC-K channels, protonation of this histidine residue at the beginning of helix Q is responsible for pH-induced block. As in ClC-2 (Arreola et al., 2002; Niemeyer et al., 2009), $H^+$ block displays a functional stoichiometry of two; i.e., it appears that two $H^+$ are necessary for closing

Published August 30, 2010

the channel, further supporting the assumption of a similar mechanism of pH-induced block in the two channels. It has been speculated that $H^+$ block acts on the "common gate" of the double-barreled channel. However, in the absence of single-channel data, such conclusions are difficult to draw conclusively. It will be interesting to find out if protonation of the corresponding histidine residue in other CLC channels, like ClC-0 or ClC-1, also affects channel function. Regulation by extracellular $Ca^{2+}$ appears to be unique to CLC-K channels. Based on an exhaustive mutagenic screen, we could identify the most likely $Ca^{2+}$-binding site. It is formed by two acidic residues (E261 and D278), both localized in the loop connecting helices I and J. This loop connects the two halves of one pseudosymmetric CLC monomer (Dutzler et al., 2002); i.e., helix I is the last helix of the first half, whereas helix J is the first helix of the second half, which is inserted oppositely into the membrane with respect to the first half. Sequence conservation in the I-J loop is relatively poor among distantly related CLCs, and the *Escherichia coli* sequence is considerably shorter than that of most eukaryotic CLCs, resulting in a certain ambiguity of assigning the residues of the *E. coli* EcClC-1 that correspond to E261 and D278 of ClC-Ka. Based on the alignment shown in Fig. 5, we identified E261-ClC-Ka with E235-ecClC-1 and D278-ClC-Ka with N250-ecClC-1. Interestingly, these two residues of one subunit of ecClC-1 are far from each other, but E235-ecClC-1 of one subunit and N250-ecClC-1 of the neighboring subunit are within ∼10 Å from each other. This distance is clearly too large to form a cation-binding site. However, because the I-J loop of ClC-K channels is considerably longer than that of ecClC-1, we speculate that in this channel, the two residues identified here, E261 and D278, form a millimolar affinity $Ca^{2+}$-binding site between the two subunits. Consequently, two symmetrically located $Ca^{2+}$-binding sites are present on each channel. The modeling of the functional data indicated that occupation of a single binding site is sufficient to promote channel activation. However, we believe that this issue deserves further detailed investigation, using, for example, heteromeric constructs in which only one of the subunits is manipulated.

Whereas D278 is rather conserved among the eukaryotic channel CLCs, E261 is not conserved in ClC-0, ClC-1, and ClC-5. Thus, it is not surprising that these CLCs are $Ca^{2+}$ insensitive. It may be interesting to find out if $Ca^{2+}$ sensitivity can be engineered into other CLC channels or transporters.

Recently, it was described that a mutation in the C-terminal cytosolic region of ClC-Kb (R538P) abolished its $Ca^{2+}$ sensitivity, whereas the same mutation was without effect in ClC-Ka (Martinez and Maduke, 2008). This effect is likely caused indirectly by affecting the gating of ClC-Kb. Furthermore, ClC-Kb–mediated currents are rather small, such that unspecific effects cannot be fully excluded. In fact, in another recent report, the mutation R351W was suggested to abolish the $Ca^{2+}$ and $H^+$ sensitivity of ClC-Kb (Yu et al., 2010). However, in our hands, the similar mutation R351A in ClC-Ka was identical to WT (Figs. S2 and S3). Furthermore, the currents of the R351W mutant reported by Yu et al. (2010) were barely above background, casting serious doubts on the significance of this result.

Regarding the mechanism of the regulation of ClC-K channels by $Ca^{2+}$ (and $H^+$), three major questions have to be addressed in the future. First, what is the precise structure of the binding site? Second, what is the functional and structural nature of the conformational changes induced by $Ca^{2+}$ and/or $H^+$ binding? Lastly, what is the relationship of the modulation of CLC-K channels by $Ca^{2+}/H^+$ and the potentiation by NFA (Liantonio et al., 2006, 2008)? Regarding the latter point, we have previously identified a region on ClC-Ka where mutations strongly affect NFA sensitivity (Zifarelli et al., 2010). This region is distinct from the $Ca^{2+}$-binding site identified here, and the less $Ca^{2+}$-sensitive mutants E261Q and D278 do not affect the NFA sensitivity (Zifarelli et al., 2010). Nevertheless, it is not known whether $Ca^{2+}$ (and $H^+$) affects the same gating processes as does NFA.

A further important question is whether the regulation by $Ca^{2+}$ and pH is of any physiological relevance. The normal plasma $Ca^{2+}$ concentration ranges from 2.25 to 2.65 mM, 50% of which is in ionized form (i.e., the free concentration is ∼1.2–1.3 mM) (Vargas-Poussou et al., 2002). Several mechanisms regulate $Ca^{2+}$ homeostasis. Bone, intestine, and kidney are the organs that determine the plasma $Ca^{2+}$ level. Disorders in $Ca^{2+}$ balance due to several diseases or pathological conditions are highly frequent (Houillier et al., 2006). $Ca^{2+}$ is reabsorbed in the kidney, particularly in the proximal tubule (∼70%) and in the TAL through paracellular pathways (20%) (Frick and Bushinsky, 2003). The driving force for the paracellular flux of $Ca^{2+}$ in the TAL is given by a transepithelial voltage gradient that is created by the basolateral secretion of $Cl^-$ and the apical secretion of $K^+$ (Jeck et al., 2005). An impairment of $Cl^-$ transport leads to an abnormal $Ca^{2+}$ absorption, implicating that $Ca^{2+}$ reabsorption and CLC-K function are interrelated. Because CLC-Ks are modulated in the physiological range of $Ca^{2+}$, and the interstitial $Ca^{2+}$ level may vary in a wide range of conditions, we can speculate that this modulation is of physiological relevance. A critical test if $Ca^{2+}$ regulation of CLC-K channels is physiologically relevant could be the analysis of animals that express $Ca^{2+}$-insensitive CLC-K variants. In this respect, the single E261Q mutation has properties that are most favorable for a knock-in strategy because its overall properties are rather similar to the WT. In contrast, the D278N mutant and the E261Q/D278N double mutant show rather drastically reduced current levels.

Published August 30, 2010

The kidney is also critically involved in the maintenance of the acid-base balance. As for $Ca^{2+}$, protons modulate CLC-Ks in the physiological range of pH. Unfortunately, the pH-insensitive mutation H497M shows a drastically reduced expression level. Thus, a direct test of the physiological relevance of the pH modulation using knock-in technology will be more difficult.

Lacking direct binding data, we can certainly not exclude that the mutations E261Q/D278N and H497M/E261Q/D278N abolish $Ca^{2+}$ and $H^+$ sensitivity of ClC-Ka in an indirect manner, for example, by prohibiting conformational changes associated with $Ca^{2+}$ or $H^+$ binding. However, we believe that our data provide rather strong evidence for a direct involvement of these residues in forming the respective $Ca^{2+}$- and $H^+$-binding sites because our mutational screen of externally accessible titratable or charged residues was exhaustive, without any other positive hits. Thus, if these mutations were not involved in $Ca^{2+}/H^+$ binding, the true binding site must be formed in an unconventional manner: $Ca^{2+}$ would bind to uncharged residues, and $H^+$ would bind to a nontitratable residue. We deem this possibility as unlikely.

In summary, we have identified two symmetrically repeated millimolar affinity $Ca^{2+}$-binding sites on ClC-Ka that are localized at the dimer interface, each with contributions from both subunits. Our results provide a solid starting point for a detailed investigation of the precise structural basis and of the physiological relevance of the $Ca^{2+}$ and pH sensitivity of ClC-K channels.

We thank T. Jentsch for providing all cDNA clones; Consuelo Murgia, Francesca Quartino, and Michela De Bellis for help in constructing some of the mutants; G. Gaggero for help in constructing the recording chamber; and Gianni Zifarelli for critical comments on the manuscript.

This work is supported by Telethon Italy (grant GGP08064) and the Italian "Ministero dell'Istruzione, dell'Università e della Ricerca" (grant MIUR PRIN 20078ZZMZW_002). The Compagnia San Paolo is gratefully acknowledged.

Christopher Miller served as editor.

Submitted: 20 April 2010
Accepted: 14 August 2010

## REFERENCES

Accardi, A., and C. Miller. 2004. Secondary active transport mediated by a prokaryotic homologue of ClC $Cl^-$ channels. *Nature.* 427:803–807.

Accardi, A., and M. Pusch. 2003. Conformational changes in the pore of CLC-0. *J. Gen. Physiol.* 122:277–293.

Arreola, J., T. Begenisich, and J.E. Melvin. 2002. Conformation-dependent regulation of inward rectifier chloride channel gating by extracellular protons. *J. Physiol.* 541:103–112.

Birkenhäger, R., E. Otto, M.J. Schürmann, M. Vollmer, E.M. Ruf, I. Maier-Lutz, F. Beekmann, A. Fekete, H. Omran, D. Feldmann, et al. 2001. Mutation of BSND causes Bartter syndrome with sensorineural deafness and kidney failure. *Nat. Genet.* 29:310–314.

Chen, M.F., and T.Y. Chen. 2001. Different fast-gate regulation by external $Cl^-$ and $H^+$ of the muscle-type ClC chloride channels. *J. Gen. Physiol.* 118:23–32.

Dutzler, R., E.B. Campbell, M. Cadene, B.T. Chait, and R. MacKinnon. 2002. X-ray structure of a ClC chloride channel at 3.0 Å reveals the molecular basis of anion selectivity. *Nature.* 415:287–294.

Dutzler, R., E.B. Campbell, and R. MacKinnon. 2003. Gating the selectivity filter in ClC chloride channels. *Science.* 300:108–112.

Estévez, R., T. Boettger, V. Stein, R. Birkenhäger, E. Otto, F. Hildebrandt, and T.J. Jentsch. 2001. Barttin is a $Cl^-$ channel beta-subunit crucial for renal $Cl^-$ reabsorption and inner ear $K^+$ secretion. *Nature.* 414:558–561.

Frick, K.K., and D.A. Bushinsky. 2003. Molecular mechanisms of primary hypercalciuria. *J. Am. Soc. Nephrol.* 14:1082–1095.

Friedrich, T., T. Breiderhoff, and T.J. Jentsch. 1999. Mutational analysis demonstrates that ClC-4 and ClC-5 directly mediate plasma membrane currents. *J. Biol. Chem.* 274:896–902.

Hamill, O.P., A. Marty, E. Neher, B. Sakmann, and F.J. Sigworth. 1981. Improved patch-clamp techniques for high-resolution current recording from cells and cell-free membrane patches. *Pflugers Arch.* 391:85–100.

Hanke, W., and C. Miller. 1983. Single chloride channels from *Torpedo* electroplax. Activation by protons. *J. Gen. Physiol.* 82:25–45.

Heinemann, S.H., and F. Conti. 1992. Nonstationary noise analysis and application to patch clamp recordings. *Methods Enzymol.* 207:131–148.

Houillier, P., M. Froissart, G. Maruani, and A. Blanchard. 2006. What serum calcium can tell us and what it can't. *Nephrol. Dial. Transplant.* 21:29–32.

Jeck, N., K.P. Schlingmann, S.C. Reinalter, M. Kömhoff, M. Peters, S. Waldegger, and H.W. Seyberth. 2005. Salt handling in the distal nephron: lessons learned from inherited human disorders. *Am. J. Physiol. Regul. Integr. Comp. Physiol.* 288:R782–R795.

Jentsch, T.J. 2005. Chloride transport in the kidney: lessons from human disease and knockout mice. *J. Am. Soc. Nephrol.* 16:1549–1561.

Jentsch, T.J., T. Maritzen, and A.A. Zdebik. 2005. Chloride channel diseases resulting from impaired transepithelial transport or vesicular function. *J. Clin. Invest.* 115:2039–2046.

Jordt, S.E., and T.J. Jentsch. 1997. Molecular dissection of gating in the ClC-2 chloride channel. *EMBO J.* 16:1582–1592.

Kieferle, S., P. Fong, M. Bens, A. Vandewalle, and T.J. Jentsch. 1994. Two highly homologous members of the ClC chloride channel family in both rat and human kidney. *Proc. Natl. Acad. Sci. USA.* 91:6943–6947.

Kürz, L.L., H. Klink, I. Jakob, M. Kuchenbecker, S. Benz, F. Lehmann-Horn, and R. Rüdel. 1999. Identification of three cysteines as targets for the $Zn^{2+}$ blockade of the human skeletal muscle chloride channel. *J. Biol. Chem.* 274:11687–11692.

Liantonio, A., A. Picollo, E. Babini, G. Carbonara, G. Fracchiolla, F. Loiodice, V. Tortorella, M. Pusch, and D.C. Camerino. 2006. Activation and inhibition of kidney CLC-K chloride channels by fenamates. *Mol. Pharmacol.* 69:165–173.

Liantonio, A., A. Picollo, G. Carbonara, G. Fracchiolla, P. Tortorella, F. Loiodice, A. Laghezza, E. Babini, G. Zifarelli, M. Pusch, and D.C. Camerino. 2008. Molecular switch for CLC-K $Cl^-$ channel block/activation: optimal pharmacophoric requirements towards high-affinity ligands. *Proc. Natl. Acad. Sci. USA.* 105:1369–1373.

Maduke, M., C. Miller, and J.A. Mindell. 2000. A decade of CLC chloride channels: structure, mechanism, and many unsettled questions. *Annu. Rev. Biophys. Biomol. Struct.* 29:411–438.

Martinez, G.Q., and M. Maduke. 2008. A cytoplasmic domain mutation in ClC-Kb affects long-distance communication across the membrane. *PLoS One.* 3:e2746.

Matsumura, Y., S. Uchida, Y. Kondo, H. Miyazaki, S.B. Ko, A. Hayama, T. Morimoto, W. Liu, M. Arisawa, S. Sasaki, and F. Marumo. 1999. Overt nephrogenic diabetes insipidus in mice lacking the CLC-K1 chloride channel. *Nat. Genet.* 21:95–98.

Niemeyer, M.I., L.P. Cid, Y.R. Yusef, R. Briones, and F.V. Sepúlveda. 2009. Voltage-dependent and -independent titration of specific residues accounts for complex gating of a ClC chloride channel by extracellular protons. *J. Physiol.* 587:1387–1400.

Picollo, A., and M. Pusch. 2005. Chloride/proton antiporter activity of mammalian CLC proteins ClC-4 and ClC-5. *Nature.* 436:420–423.

Picollo, A., A. Liantonio, M.P. Didonna, L. Elia, D.C. Camerino, and M. Pusch. 2004. Molecular determinants of differential pore blocking of kidney CLC-K chloride channels. *EMBO Rep.* 5:584–589.

Pusch, M., K. Steinmeyer, and T.J. Jentsch. 1994. Low single channel conductance of the major skeletal muscle chloride channel, ClC-1. *Biophys. J.* 66:149–152.

Rickheit, G., H. Maier, N. Strenzke, C.E. Andreescu, C.I. De Zeeuw, A. Muenscher, A.A. Zdebik, and T.J. Jentsch. 2008. Endocochlear potential depends on $Cl^-$ channels: mechanism underlying deafness in Bartter syndrome IV. *EMBO J.* 27:2907–2917.

Rychkov, G.Y., M. Pusch, D.S. Astill, M.L. Roberts, T.J. Jentsch, and A.H. Bretag. 1996. Concentration and pH dependence of skeletal muscle chloride channel ClC-1. *J. Physiol.* 497:423–435.

Saviane, C., F. Conti, and M. Pusch. 1999. The muscle chloride channel ClC-1 has a double-barreled appearance that is differentially affected in dominant and recessive myotonia. *J. Gen. Physiol.* 113:457–468.

Schlingmann, K.P., M. Konrad, N. Jeck, P. Waldegger, S.C. Reinalter, M. Holder, H.W. Seyberth, and S. Waldegger. 2004. Salt wasting and deafness resulting from mutations in two chloride channels. *N. Engl. J. Med.* 350:1314–1319.

Simon, D.B., R.S. Bindra, T.A. Mansfield, C. Nelson-Williams, E. Mendonca, R. Stone, S. Schurman, A. Nayir, H. Alpay, A. Bakkaloglu, et al. 1997. Mutations in the chloride channel gene, CLCNKB, cause Bartter's syndrome type III. *Nat. Genet.* 17: 171–178.

Stühmer, W. 1998. Electrophysiologic recordings from Xenopus oocytes. *Methods Enzymol.* 293:280–300.

Traverso, S., G. Zifarelli, R. Aiello, and M. Pusch. 2006. Proton sensing of CLC-0 mutant E166D. *J. Gen. Physiol.* 127:51–65.

Uchida, S., S. Sasaki, T. Furukawa, M. Hiraoka, T. Imai, Y. Hirata, and F. Marumo. 1993. Molecular cloning of a chloride channel that is regulated by dehydration and expressed predominantly in kidney medulla. *J. Biol. Chem.* 268:3821–3824.

Uchida, S., S. Sasaki, K. Nitta, K. Uchida, S. Horita, H. Nihei, and F. Marumo. 1995. Localization and functional characterization of rat kidney-specific chloride channel, ClC-K1. *J. Clin. Invest.* 95:104–113.

Vargas-Poussou, R., C. Huang, P. Hulin, P. Houillier, X. Jeunemaître, M. Paillard, G. Planelles, M. Déchaux, R.T. Miller, and C. Antignac. 2002. Functional characterization of a calcium-sensing receptor mutation in severe autosomal dominant hypocalcemia with a Bartter-like syndrome. *J. Am. Soc. Nephrol.* 13:2259–2266.

Waldegger, S., N. Jeck, P. Barth, M. Peters, H. Vitzthum, K. Wolf, A. Kurtz, M. Konrad, and H.W. Seyberth. 2002. Barttin increases surface expression and changes current properties of ClC-K channels. *Pflugers Arch.* 444:411–418.

Yu, Y., C. Xu, X. Pan, H. Ren, W. Wang, X. Meng, F. Huang, and N. Chen. 2010. Identification and functional analysis of novel mutations of the CLCNKB gene in Chinese patients with classic Bartter syndrome. *Clin. Genet.* 77:155–162.

Zifarelli, G., and M. Pusch. 2009. Conversion of the 2 Cl(−)/1 H+ antiporter ClC-5 in a NO3(−)/H+ antiporter by a single point mutation. *EMBO J.* 28:175–182.

Zifarelli, G., and M. Pusch. 2010. The role of protons in fast and slow gating of the Torpedo chloride channel ClC-0. *Eur. Biophys. J.* 39:869–875.

Zifarelli, G., A.R. Murgia, P. Soliani, and M. Pusch. 2008. Intracellular proton regulation of ClC-0. *J. Gen. Physiol.* 132:185–198.

Zifarelli, G., A. Liantonio, A. Gradogna, A. Picollo, G. Gramegna, M. De Bellis, A.R. Murgia, E. Babini, D.C. Camerino, and M. Pusch. 2010. Identification of sites responsible for the potentiating effect of niflumic acid on ClC-Ka kidney chloride channels. *Br. J. Pharmacol.* 160:1652–1661.

## 3.3 Dissecting the $Ca^{2+}$ binding site of CLC-K channels

As described in chapter 3.2 "A $Ca^{2+}$ binding site at the subunit interface of CLC-K channels", we have identified the $Ca^{2+}$ binding site of the ClC-Ka channel. Based on the structure of the bacterial homologue EcClC-1 we chose and mutated all external titratable residues. This extensive mutagenic screen combined with voltage clamp measurements performed on *Xenopus* oocytes co-injected with ClC-Ka/barttin led us to identify two acidic residues, E261 and D278, responsible for calcium sensitivity of ClC-Ka channels (chapter 3.2) (Gradogna et al, 2010). Based on the alignment of ClC-Ka with EcClC-1 we tentatively located the corresponding residues in the 3-D bacterial structure. E261 from one subunit and D278 from the neighboring subunit are close each other to form a calcium-binding site at the subunit interface (Gradogna et al, 2010). Moreover, we identified H497 as the residue responsible for proton block. This histidine is not far from the calcium-binding site. Therefore these residues define a novel region involved in the regulation of the gating of a CLC channel (Gradogna et al, 2010). In order to increase the knowledge on this characteristic region, we further investigated the conservation and the specificity of the calcium-binding site. Using the same strategy that combines molecular biology and electrophysiology measurements, we could establish that the calcium-binding site is conserved in all CLC-K channels. In order to explore the specificity of the binding site, we tested the effect of several divalent cations. We found that $Ca^{2+}$, $Ba^{2+}$, $Sr^{2+}$, and $Mn^{2+}$ activate CLC-K channels interacting with the acidic residues E261 and D278. Interestingly the rank order of potency is similar for ClC-Ka and ClC-Kb, but different for ClC-K1. $Mg^{2+}$ does not activate CLC-K channels. Finally $Zn^{2+}$ ions block CLC-K channels with a different unknown mechanism.

### *3.3.1 The calcium-binding site is conserved in CLC-K channels*

The alignment of CLC proteins at the loop between helices I and J including E261 and D278 residues responsible for calcium binding shows a region that is highly conserved in CLC-K channels. ClC-Ka and ClC-Kb share 100% identity, while two substitutions are found in rat ClC-K1 compared with human CLC-K channels (I266 instead of L266, R270 instead of S270) (Fig. 3.1).

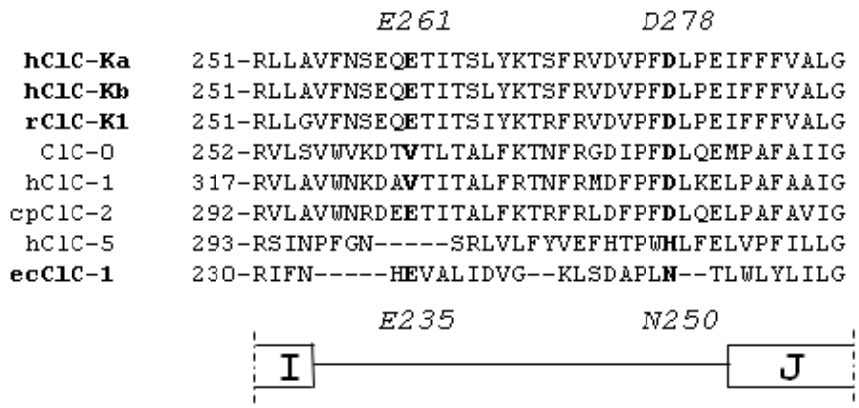


**Fig. 3.1 Alignment of CLC proteins around the residues, E261 and D278 responsible for $Ca^{2+}$ sensitivity**

Similarly to ClC-Ka the currents of ClC-Kb increase with increasing $Ca^{2+}$ concentrations (Estévez et al, 2001; Waldegger et al, 2002), without saturation up to 50 mM (Gradogna et al, 2010) (Fig. 3.2A). We evaluated calcium effect on ClC-K1channel applying solutions with different $Ca^{2+}$ concentrations ranging from nominally 0 to 50 mM $Ca^{2+}$. ClC-K1 is more calcium sensitive than human CLC-K channels. In fact, ClC-K1 currents already at 1 mM $Ca^{2+}$ are ~47% of the maximum level of the currents recorded at high calcium. Moreover they reach saturation at about 10 mM $Ca^{2+}$ (Fig. 3.2B). Similarly to what was previously shown for ClC-Ka and ClC-Kb (Gradogna et al, 2010), $Ca^{2+}$ is not strictly essential for ClC-K1 opening. In fact the currents measured at nominally 0 $Ca^{2+}$ concentration are ~10% of currents at 10 mM $Ca^{2+}$ (Fig. 3.2B). The high sequence identity and the conserved calcium sensitivity suggest that the calcium binding site is a characteristic shared by CLC-K channels. To test this, we inserted E261Q, D278N, E261Q/D278N mutations in ClC-Kb and ClC-K1. Then we assayed the calcium effect on each mutant. Current traces of ClC-Kb and ClC-K1 WT and the mutants are shown in Fig. 3.3 and Fig. 3.4, respectively. Both ClC-Kb and ClC-K1 single mutants lose most of their calcium sensitivity, while the double mutants E261Q/D278N are completely calcium insensitive (Fig. 3.2A and B). In particular, E261Q mutants keep a weakened response to the different calcium concentrations. Instead D278N currents only increase at 50 mM $Ca^{2+}$ (Fig. 3.2A and B). We could conclude that the regulatory calcium binding site formed by E261 and D278 residues from neighboring subunits is conserved in CLC-K channels.

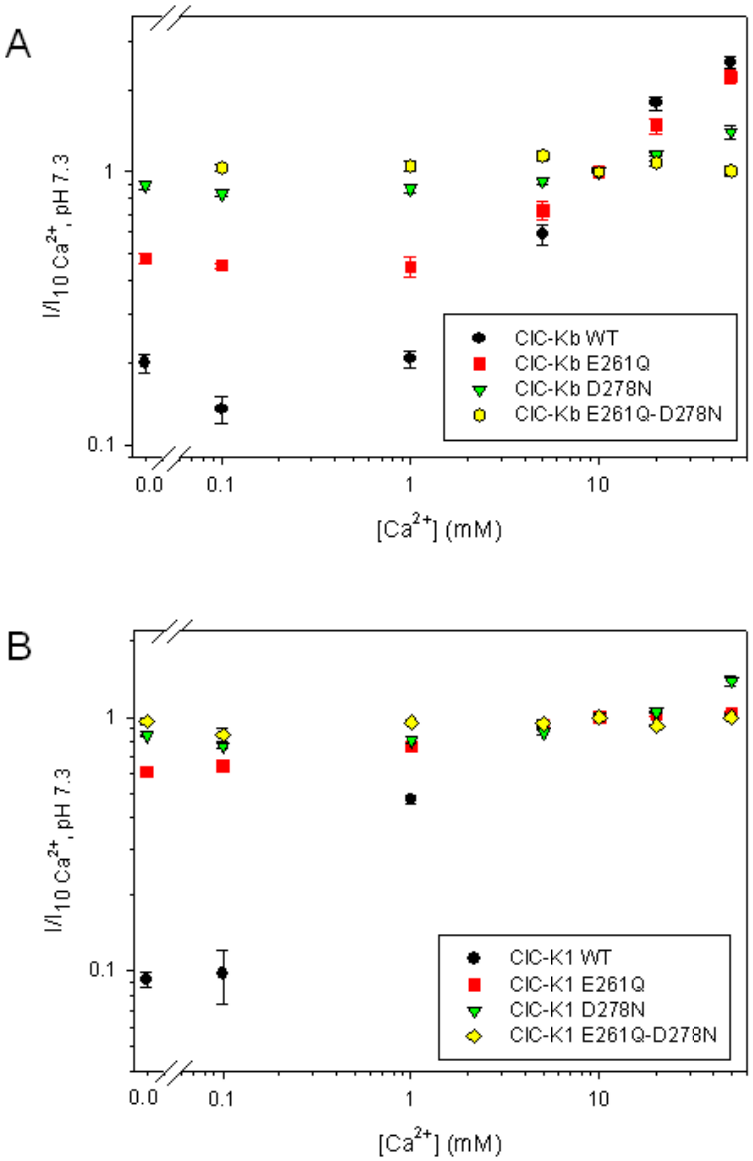


**Fig. 3.2 $Ca^{2+}_{ext}$ dependence of ClC-Kb and ClC-K1 WT and their mutants E261Q, D278N, and E261Q-D278N.** Currents acquired at 60 mV were normalized to the currents measured in standard solution and plotted versus $Ca^{2+}$ concentration. **(A)** Effect of external $Ca^{2+}$ on ClC-Kb WT (black circles) and its mutants E261Q (red squares), D278N (green triangles), and E261Q-D278N (yellow rhombi). **(B)** Effect of external $Ca^{2+}$ on ClC-K1 WT (black circles) and its mutants E261Q (red squares), D278N (green triangles), and E261Q-D278N (yellow rhombi). Error bars indicate SEM.

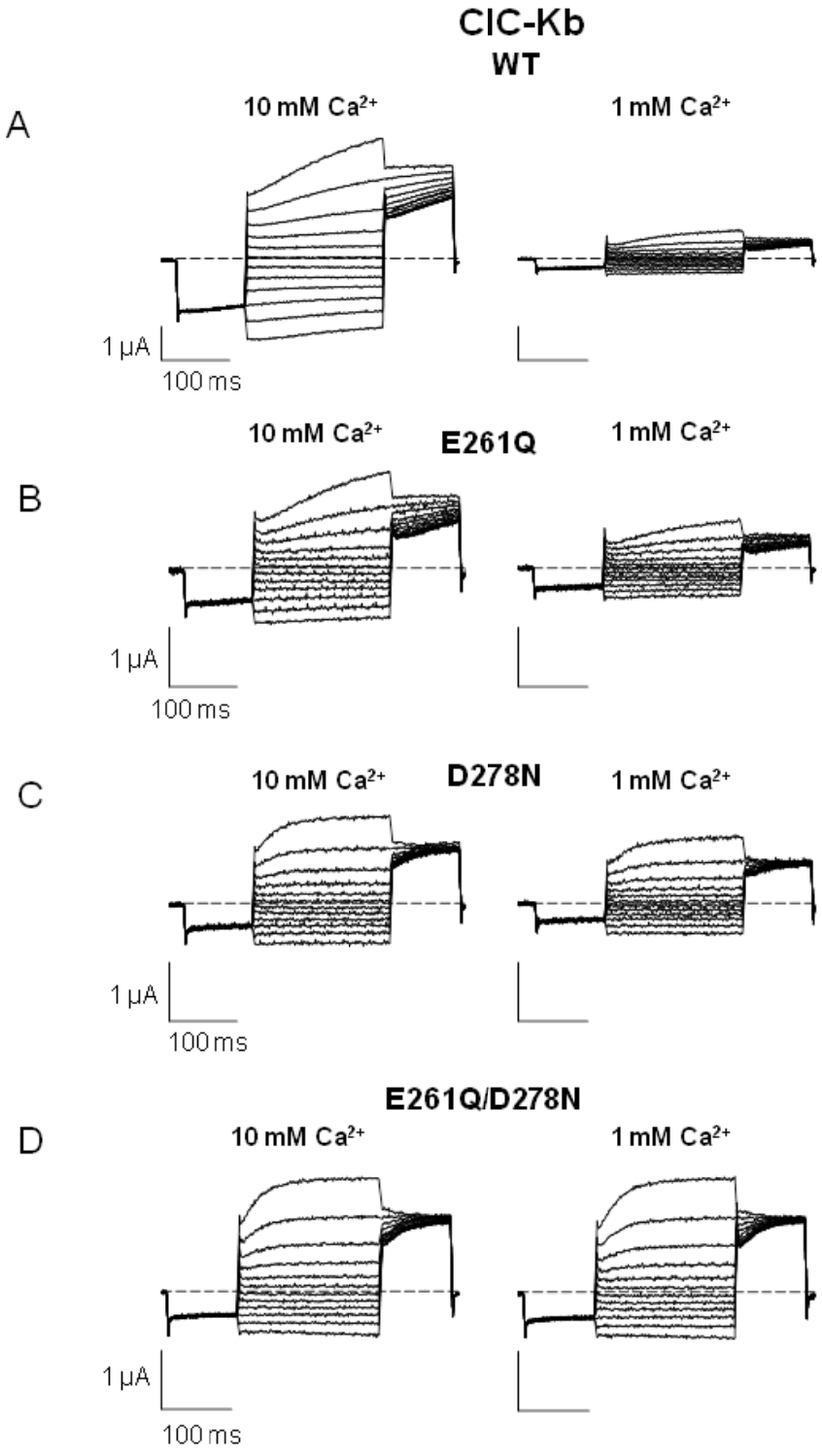


**Fig. 3.3 Current traces of ClC-Kb WT and its mutants E261Q, D278N, and E261Q/D278N.** Current responses of ClC-Kb WT (A) and its mutants E261Q (B), D278N (C), E261Q/D278N (D) to the IV-pulse protocol at 10 and 1 mM $Ca^{2+}$ concentration and pH 7.3.

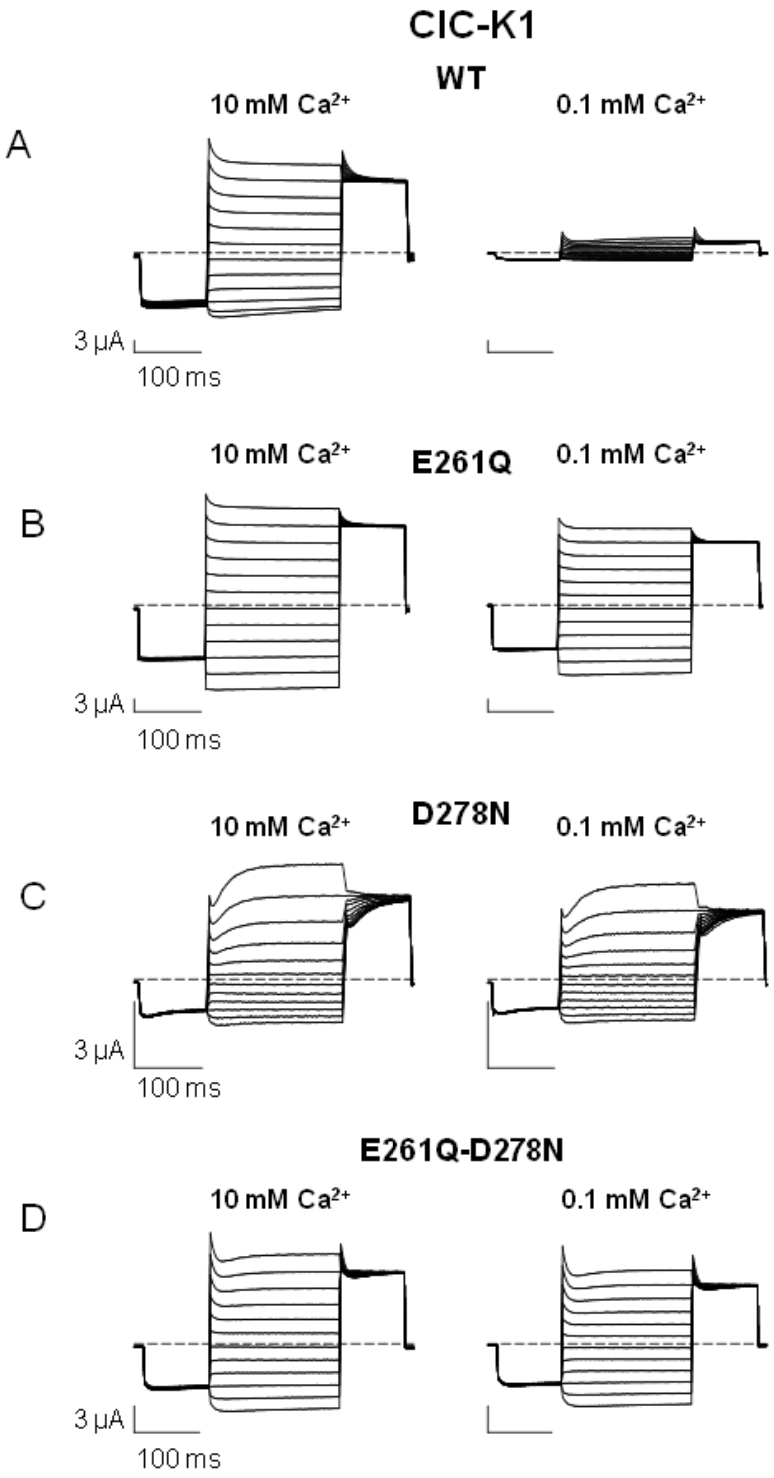


**Fig. 3.4 Current traces of ClC-K1 WT and its mutants E261Q, D278N, and E261Q/D278N.** Current responses of ClC-K1 WT (A) and its mutants E261Q (B), D278N (C), E261Q/D278N (D) to the IV-pulse protocol at 10 and 1 mM $Ca^{2+}$ concentration and pH 7.3.

### *3.3.2 Specificity of the calcium-binding site in ClC-Ka*

Another objective of our work was to investigate the specificity of the $Ca^{2+}$ binding site. We wondered if other ions with similar characteristics to $Ca^{2+}$ could interact with the same binding site and activate CLC-K channels. Hence we decided to test the effects of several divalent cations on WT ClC-Ka and its double mutant E261Q/D278N. In particular, we considered other members belonging to the *alkaline earth metal group*: $Mg^{2+}$, $Sr^{2+}$, and $Ba^{2+}$ that share with $Ca^{2+}$ external electron configuration and reactivity. These easily form complexes with ligands that have carboxyl and carbonyl groups (Elinder & Arhem, 2003). Additionally, we studied the effect of other two metals, Mn and Zn that are mainly in ionized form ($Mn^{2+}$ and $Zn^{2+}$) in physiological solutions and, consequently, can interact with the same amino acids (Elinder & Arhem, 2003). In particular, $Mn^{2+}$ is redox reactive and $Zn^{2+}$ is a strong electron acceptor. Both of them can form a coordination with the imidazole group of histidine and the carboxylate group of glutamate and aspartate. Additionally $Zn^{2+}$ can interact with the S atom of cysteine (Elinder & Arhem, 2003). Hence all these divalent ions can be considered $Ca^{2+}$ mimetic ions and, in theory, they could interact with the residues, E261 and D278 that form the $Ca^{2+}$ binding site. The ionic radii of the studied cations are (in pm): $Mg^{2+}$ (78) $Ca^{2+}$ (106), $Sr^{2+}$ (127), $Ba^{2+}$ (143), $Mn^{2+}$ (91), $Zn^{2+}$ (83) (Elinder & Arhem, 2003). However, we have to keep in mind that in the biological systems the ions have a hydration shell, which is an important feature for the interaction with specific binding sites (Diamond & Wright, 1969).

A typical experiment was carried out in the following way: first, we measured CLC-Ka currents in standard solution (i.e. 10 mM $Ca^{2+}$ and pH 7.3); next we completely replaced $Ca^{2+}$ with another cation until steady state was reached. Lastly we applied an IV protocol. This procedure was repeated for all cations at different concentrations (Fig. 3.5). The main difficulty of these experiments was the availability of very good oocytes able to sustain many changes of solutions and long repetitive stimulation without developing leak currents.

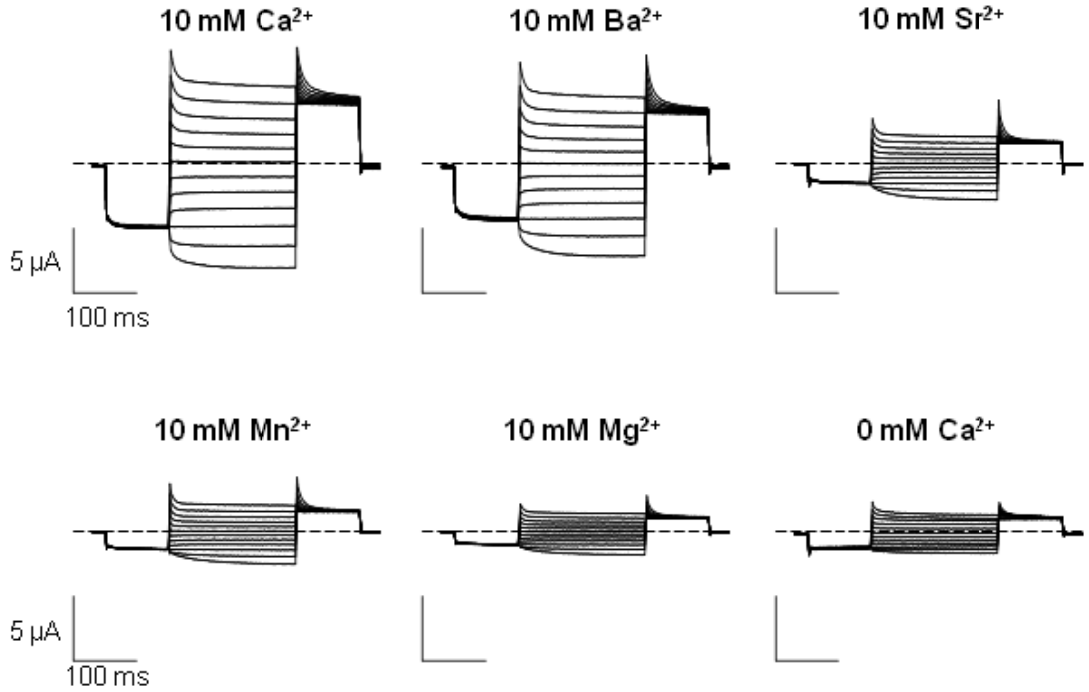


**Fig. 3.5 Current traces of ClC-Ka WT in different cations.** Current responses of ClC-Ka WT to the IV-pulse protocol at 10 mM [cation] concentration and pH 7.3.

I performed these experiments on WT ClC-Ka and its double mutant E261Q/D278N. Because ClC-Ka shows currents even in the absence of $Ca^{2+}$, the current measured at 0 $Ca^{2+}$ was a good evaluation of the functional expression of the channel lacking of activators ions. Based on the data collected we could conclude that $Mg^{2+}$ does not activate CLC-Ka at concentrations up to 50 mM. In contrast, CLC-Ka is activated by $Ba^{2+}$, $Sr^{2+}$, and $Mn^{2+}$. The rank order of potency is $Ca^{2+}$>$Ba^{2+}$>$Sr^{2+}$=$Mn^{2+}$>> $Mg^{2+}$ (Fig. 3.6A). Interestingly, this selectivity sequence is one of those predicted by Diamond and Wright (1969). Moreover, we established that the $Ca^{2+}$ insensitive double mutant E261Q/D278N is also $Ba^{2+}$, $Sr^{2+}$, and $Mn^{2+}$ insensitive (Fig.4.6B). This demonstrates that $Ca^{2+}$, $Ba^{2+}$, $Sr^{2+}$, $Mn^{2+}$ interact with the same binding site formed by E261 and D278 at the subunit interface . The decreasing activation ability likely corresponds to a decreasing affinity of these cations to this binding site.

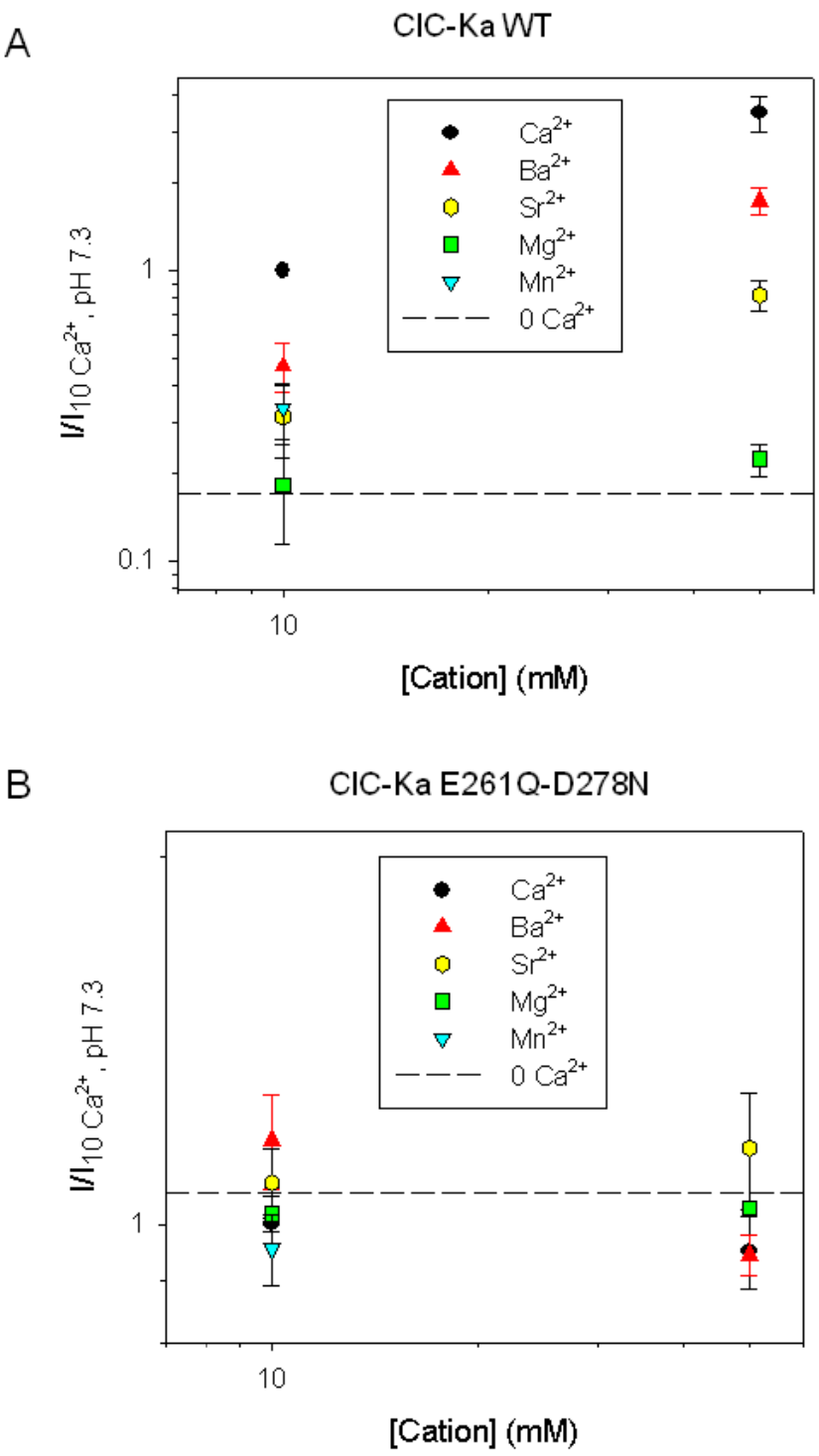


**Fig. 3.6 Effects of various external cations on ClC-Ka WT (A) and its mutant E261Q/D278N (B).** Currents acquired at 60 mV were normalized to the currents measured in standard solution (10 mM $Ca^{2+}$ and pH 7.3) and plotted versus cation concentration. Error bars indicate SD.

Among all the cations studied, we found that $Ba^{2+}$ activates ClC-Ka in a very similar manner as $Ca^{2+}$, even if it is less potent. This could depend on a lower affinity of $Ba^{2+}$ for the binding site or on a lower efficacy of this ion on ClC-Ka compared to $Ca^{2+}$. If the first hypothesis is true, increasing $Ba^{2+}$ concentration Ba-activated currents will be able to reach the same maximum level as Ca-activated currents; if this does not occur $Ba^{2+}$ is less effective than $Ca^{2+}$. To distinguish between these two hypotheses, we performed a dose-response analysis of $Ca^{2+}$ and $Ba^{2+}$ modulation. We measured ClC-Ka currents at 60 mV varying $Ca^{2+}$ concentration in absence of $Ba^{2+}$ and varying $Ba^{2+}$ concentration in absence of $Ca^{2+}$. The results are shown in Fig. 3.7A. Since both Ca- and Ba-activated currents do not reach saturation at 50 mM, we used a model to extrapolate currents at higher $Ca^{2+}$ and $Ba^{2+}$ concentrations. Because ClC-Ka yields currents even in absence of $Ca^{2+}$ and $Ba^{2+}$, we hypothesized an allosteric model composed of six states as shown below:

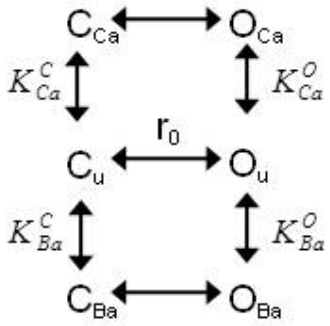


Here $O_U$, $O_{Ca}$ and $O_{Ba}$ indicate unbound, Ca-bound and Ba-bound open states, $C_U$, $C_{Ca}$ and $C_{Ba}$ unbound, Ca-bound and Ba-bound closed states of the channel. $Ca^{2+}$ and $Ba^{2+}$ binding to the open state are governed by the dissociation constants $K_{Ca}^{O}$ and $K_{Ba}^{O}$, respectively, whereas $Ca^{2+}$ and $Ba^{2+}$ binding to the closed state are described by the dissociation constants $K_{Ca}^{C}$ and $K_{Ba}^{C}$, respectively. $r_0$ is here the ratio between the probability of being in states $O_u$ and $C_u$ ($r_0=p(O_u)/p(C_u)$).

At equilibrium, the open probability of the channel is given by the following equation (for details see section 2.9 "Kinetic modeling"):

$$p_0 = \frac{1+\frac{[Ca]}{K_{Ca}^{0}}+\frac{[Ba]}{K_{Ba}^{0}}}{1+\frac{1}{r_0}+[Ca]\left(\frac{1}{r_0 K_{Ca}^{C}}+\frac{1}{K_{Ca}^{0}}\right)+[Ba]\left(\frac{1}{r_0 K_{Ba}^{C}}+\frac{1}{K_{Ba}^{0}}\right)} \quad (3.1)$$

In Fig. 3.7A the solid black line and the dash red line represent the combined best fit of this equation for the $Ca^{2+}$ and $Ba^{2+}$ dependence resulting in $K_{Ca}^{O}$ = 0.62 mM, $K_{Ca}^{C}$ =142 mM, $K_{Ba}^{O}$ =1.6 mM, $K_{Ba}^{C}$ =371 mM, and $r_0 = 1.3 \times 10^{-3}$. The theoretical prediction of this model nicely fits the experimental data. Moreover it provides some useful indications: very high $Ca^{2+}$ and $Ba^{2+}$ concentrations are required so that the currents are in saturation; Ca- and Ba-activated currents reach the same maximum level. This would indicate that barium has a lower affinity for the binding site than calcium, but the same efficacy. However, because the experimental data cover only a restricted little range of the fit curves, we have to consider these results cautiously. To validate the model, we used it to predict the currents in mixed conditions (25 mM $Ca^{2+}$ and 25 mM $Ba^{2+}$). The experimental mean value of the current in mixed conditions was 75% of the mean current at 50 mM $Ca^{2+}$ (0.75±0.029 sem). The relative current value predicted by our model, using the parameters obtained from the best fit, was very similar to the experimental value, i.e. 0.77, (Fig. 3.7B). This confirmed that our model allows predicting ClC-Ka currents at any $Ca^{2+}$ and $Ba^{2+}$ concentrations.

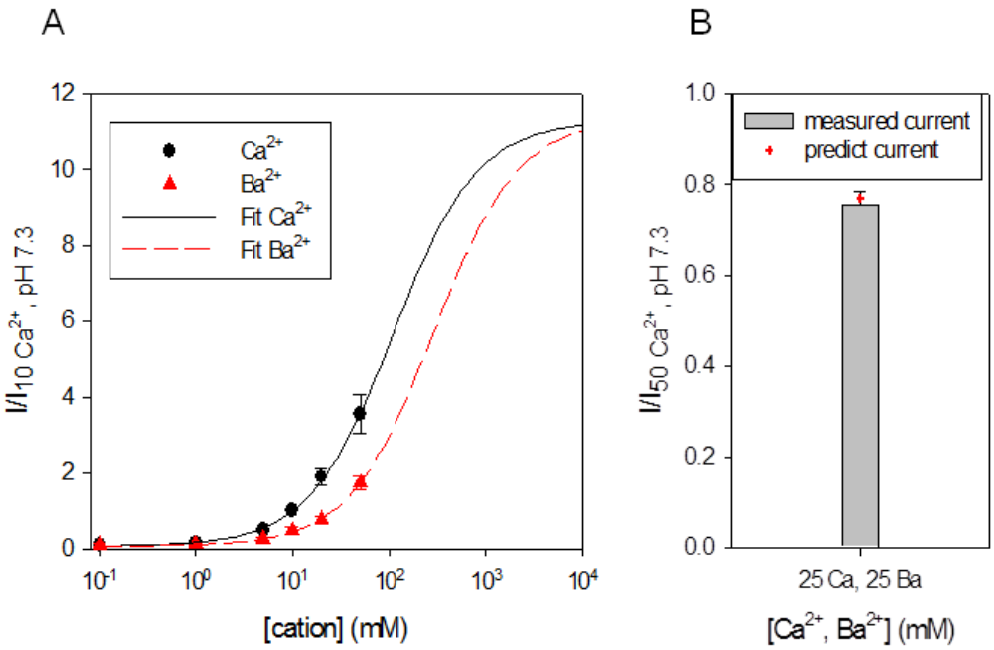


**Fig. 3.7 Effect of external $Ca^{2+}$ and $Ba^{2+}$ on ClC-Ka WT. (A)** Currents acquired at 60 mV were normalized to the currents measured in standard solution (10 mM $Ca^{2+}$ and pH 7.3) and plotted versus $Ca^{2+}$ and $Ba^{2+}$ concentrations (used concentrations: 0.1, 1, 5, 10, 20, and 50 mM). The lines represent the fit obtained using Eq. 3.1 as described above. Error bars indicate SD. **(B)** Current in mixed condition (25 mM $Ca^{2+}$ and 25 mM $Ba^{2+}$) was normalized to the current measured at 50 mM $Ca^{2+}$ and pH 7.3. The red cross represents the value obtained by Eq. 3.1.Error bar indicates SEM.

### *3.3.3 Specificity of the calcium-binding site in ClC-Kb and ClC-K1*

Our experiments performed on ClC-Ka demonstrated that $Ca^{2+}$, $Ba^{2+}$, $Sr^{2+}$, $Mn^{2+}$ interact with the same binding site formed by E261 and D278 residues with the following rank order of potency: $Ca^{2+}$>$Ba^{2+}$>$Sr^{2+}$=$Mn^{2+}$>> $Mg^{2+}$. Next we intended to determine if ClC-K1 and ClC-Kb have a similar specificity as ClC-Ka. Leaving out $Mn^{2+}$ because of its tendency to precipitate, we tested the effects of $Ba^{2+}$, $Sr^{2+}$, and $Mg^{2+}$ on WT ClC-Kb and on WT ClC-K1 and its double mutant E261Q/D278N. The experimental procedure used was the same employed for determine the specificity of ClC-Ka (for the details see section 3.3.2 “Specificity of the calcium-binding site in ClC-Ka”).

$Ba^{2+}$ and $Sr^{2+}$ activate ClC-Kb WT, whereas $Mg^{2+}$ does not active this channel at concentrations up to 50 mM. The rank order of potency is the same as found for

ClC-Ka, i.e. $Ca^{2+}$>$Ba^{2+}$>$Sr^{2+}$>>$Mg^{2+}$. This result is shown for a typical oocyte in Fig. 3.8A and normalized currents are depicted in Fig. 3.8B. Because of the low functional expression of ClC-Kb E261Q/D278N we could not investigate the effects of the cations on it.

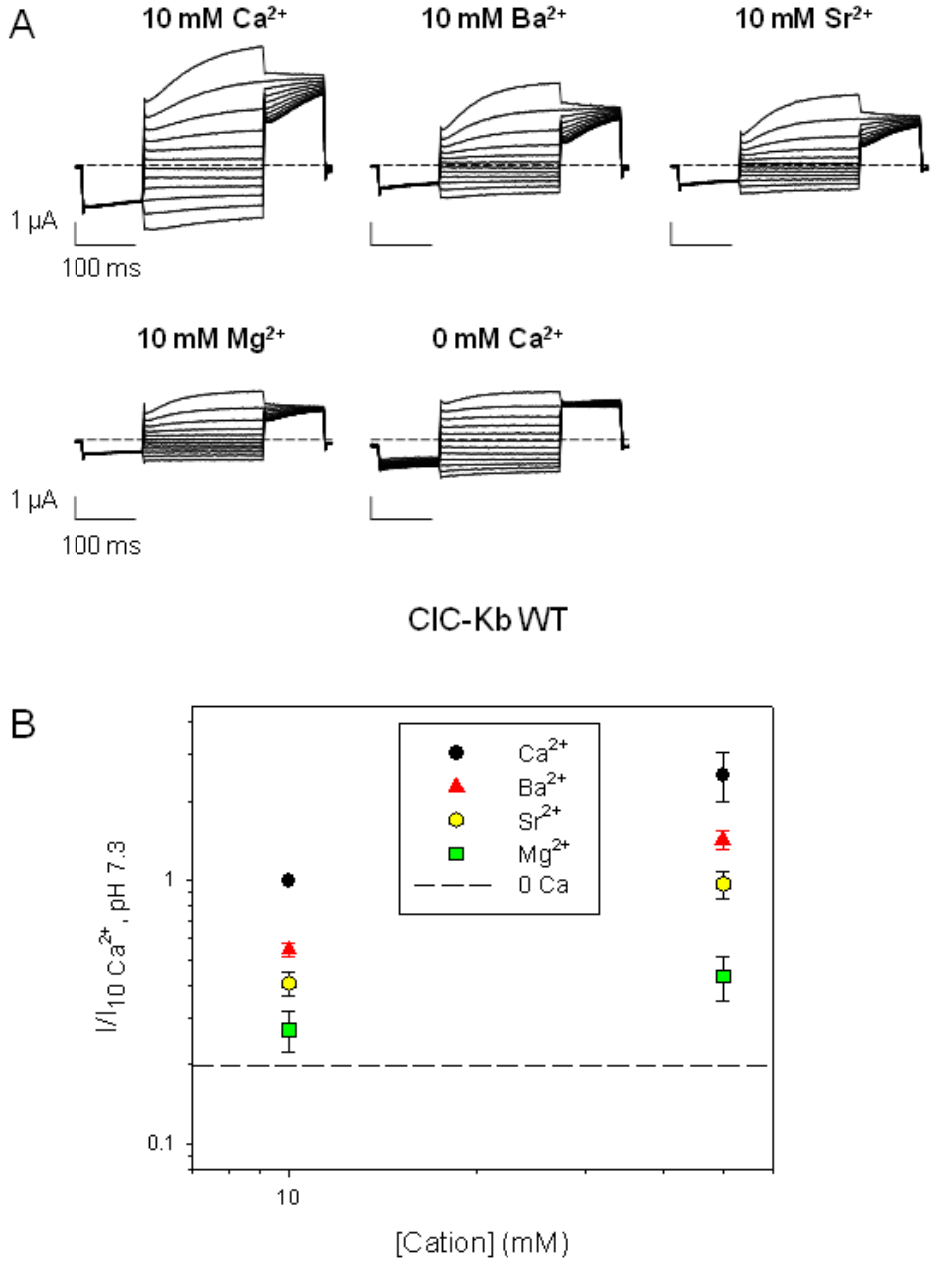


**Fig. 3.8 Effects of various external cations on ClC-Kb WT (A)** Current responses of ClC-Kb WT to the IV-pulse protocol at 10 mM [cation] concentration and pH 7.3. **(B)** Currents acquired at 60 mV were normalized to the currents measured in standard solution (10 mM $Ca^{2+}$ and pH 7.3) and plotted versus cation concentration. Error bars indicate SD.

Next we tested the effects of $Ba^{2+}$, $Sr^{2+}$, and $Mg^{2+}$ on WT ClC-K1. Since ClC-K1 is more calcium sensitive than the human CLC-K channels and its currents are in saturation at ~10 mM $Ca^{2+}$ concentration, we performed the dose-response analysis of the cations at concentrations ranging between 1 and 50 mM. Our experiments demonstrated that $Sr^{2+}$ and $Ba^{2+}$ activate ClC-K1 WT, while $Mg^{2+}$ is ineffective up to a concentration of 50 mM. Surprisingly, the rank order of potency was: $Ca^{2+}>Sr^{2+}>Ba^{2+}>>Mg^{2+}$ unlike the human CLC-K channels (Figs. 4.9 and 4.10). The alignment of the sequence of the loop between helices I and J including E261 and D278 shows two substitutions in the rat ClC-K1 sequence compared with the human CLC-K channels (I266 instead of L266, R270 instead of S270) (Fig. 3.1). Excluding the conservative substitution Iso266Leu, we concentrated on the more drastic substitution Arg270Ser. A plausible hypothesis was that this amino acid could affect the specificity of the calcium-binding site. However, the mutant ClC-Ka S270R had an unchanged specificity compared to WT (Fig. 3.11). Finally, we tested the effects of $Ba^{2+}$, $Sr^{2+}$, and $Mg^{2+}$ on the double mutant E261Q/D278N of ClC-K1. As expected, the Ca-insensitive E261Q/D278N was also Ba- and Sr-insensitive (Fig. 3.9C). This demonstrates that $Ca^{2+}$, $Sr^{2+}$, $Ba^{2+}$ interact with the same binding site formed by E261 and D278 at the subunit interface also in ClC-K1.

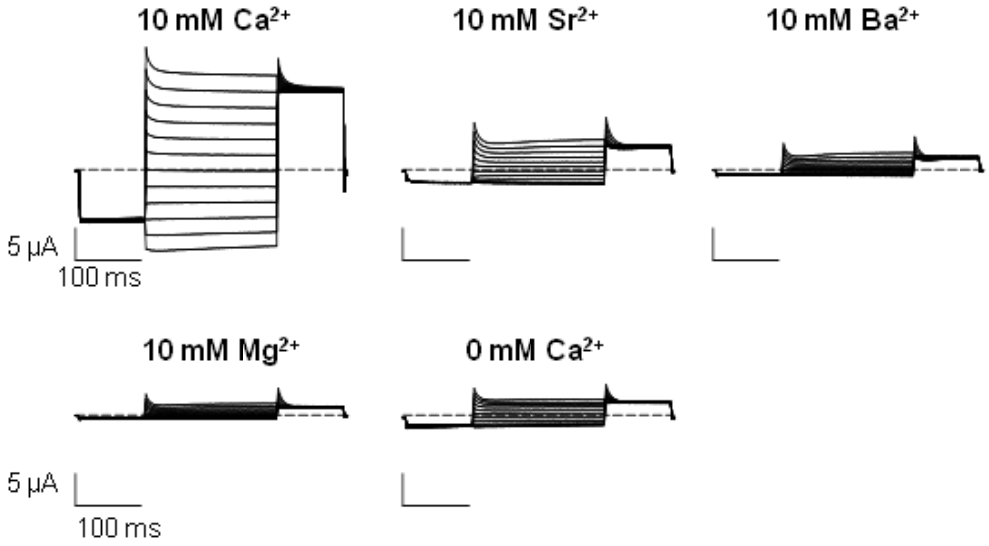


**Fig. 3.9 Current traces of ClC-K1 WT in different cations.** Current responses of ClC-K1 WT to the IV-pulse protocol at 10 mM [cation] concentration and pH 7.3.

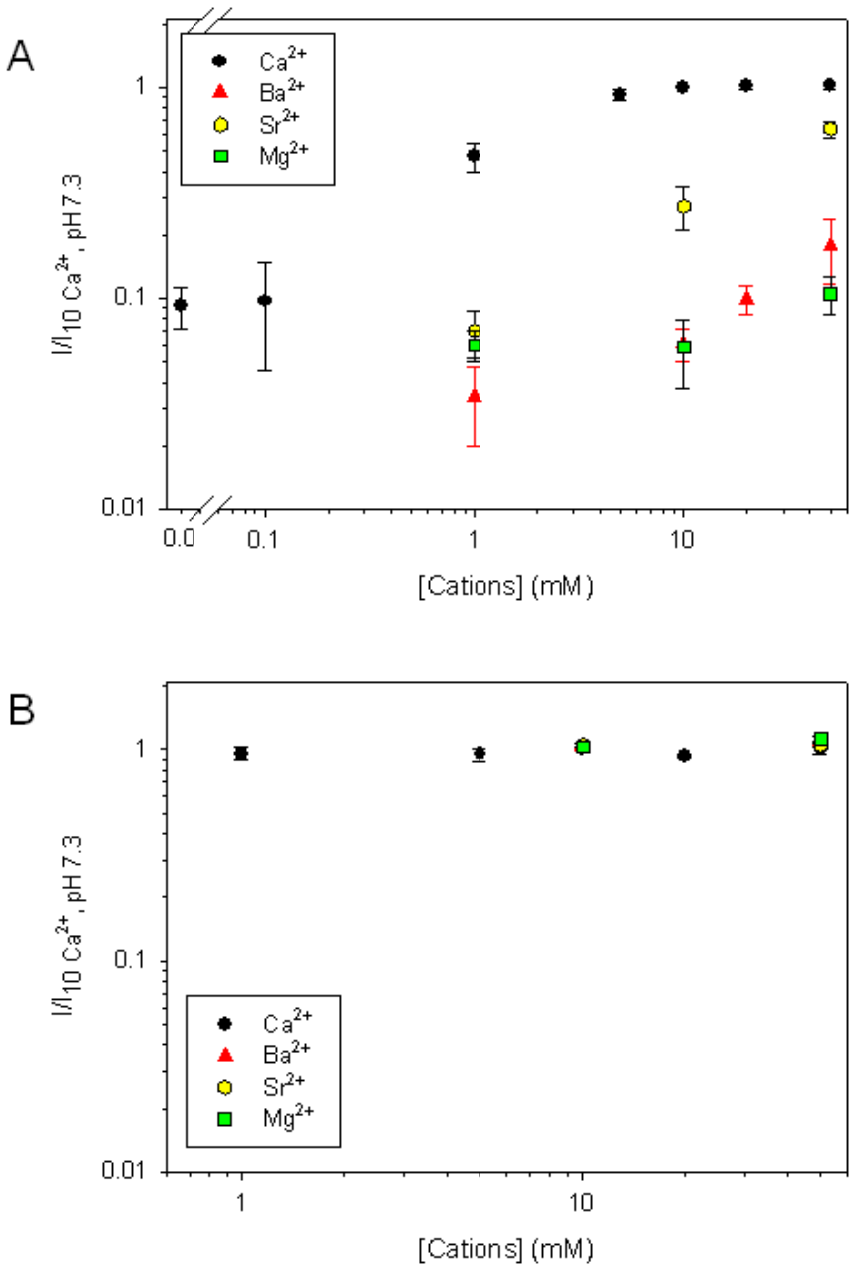


**Fig. 3.10 Effects of various external cations on ClC-K1 WT (A) and its mutant E261Q/D278N (B).** Currents acquired at 60 mV were normalized to the currents measured in standard solution (10 mM $Ca^{2+}$ and pH 7.3) and plotted versus cation concentration. Error bars indicate SD.

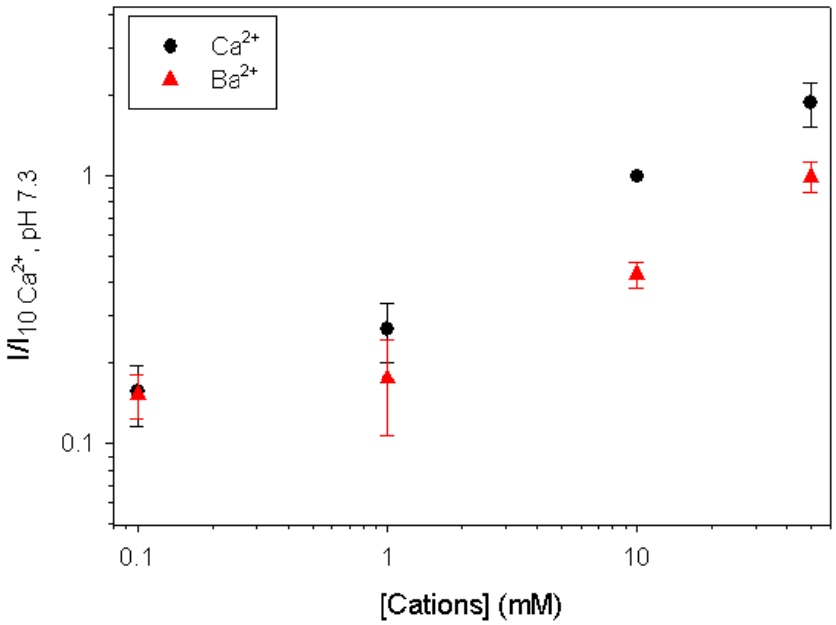


**Fig. 3.11 Effect of external $Ca^{2+}$ and $Ba^{2+}$ on ClC-Ka S270R.** Currents acquired at 60 mV were normalized to the currents measured in standard solution (10 mM $Ca^{2+}$ and pH 7.3) and plotted versus cation concentration. Error bars indicate SD.

### *3.3.4 An outsider ion: $Zn^{2+}$*

Modulation of CLC proteins by $Zn^{2+}$ is very common. Extracellular $Zn^{2+}$ inhibits both $Cl^-$ channels and $Cl^-/H^+$ antiporters (Kürz et al, 1997; Chen, 1998; Clark et al, 1998; Osteen & Mindell, 2008). $Zn^{2+}$ was found to block reversibly ClC-0 (Chen, 1998) and ClC-2 (Clark et al, 1998), while it inhibits irreversibly ClC-1 (Kürz et al, 1997). In particular, $Zn^{2+}$ inhibition of ClC-0 and ClC-1seems to be related to the common gating mechanism that acts by opening and closing of both the pores of these channels (Chen, 1998; Duffield et al, 2005). In fact the mutation C212S in ClC-0 and the equivalent C277S in ClC-1 that blocks these channels in the open state also abolishes $Zn^{2+}$ inhibition (Lin et al, 1999; Duffield et al, 2005). A different mechanism seems to cause $Zn^{2+}$ block of the $Cl^-/H^+$ antiporter ClC-4. ClC-4 is lacking the cysteine corresponding to C212 of ClC-0. Instead three extracellular consecutive histidines were proposed to be involved in $Zn^{2+}$ inhibition (Osteen & Mindell, 2008). This is not so surprising because $Zn^{2+}$ can be coordinated by several residues, preferably by histidine and cysteine, but also by glutamate and aspartate.

We tested the effect of $Zn^{2+}$ on CLC-K channels. As found for the other CLC proteins (see above), ClC-Ka is inhibited by this ion. In fact, at nominally 0 $Ca^{2+}$, ClC-Ka currents at 5 mM $Zn^{2+}$ are ~6% of those measured in the absence of $Zn^{2+}$ (Fig. 3.12A). Because in ClC-K channels a threonine residue (T211) substitutes C212 of ClC-0 and there are no histidine residues corresponding to the histidines involved in $Zn^{2+}$ block of ClC-4 (Osteen & Mindell, 2008), a distinct mechanism of inhibition must be hypothesized for CLC-K channels. A possible hypothesis is that $Zn^{2+}$ could interact with the $Ca^{2+}$ binding site formed by E261 and D278 residues. To investigate this hypothesis, we tested the effect of $Zn^{2+}$ on the double mutant E261Q/D278N of ClC-Ka. However, the currents of the double mutant E261Q/D278N (Fig. 3.12C) and WT ClC-Ka (Fig. 3.12B) are inhibited in a similar way. Thus, we can conclude that $Zn^{2+}$ block is mediated by a different binding site.

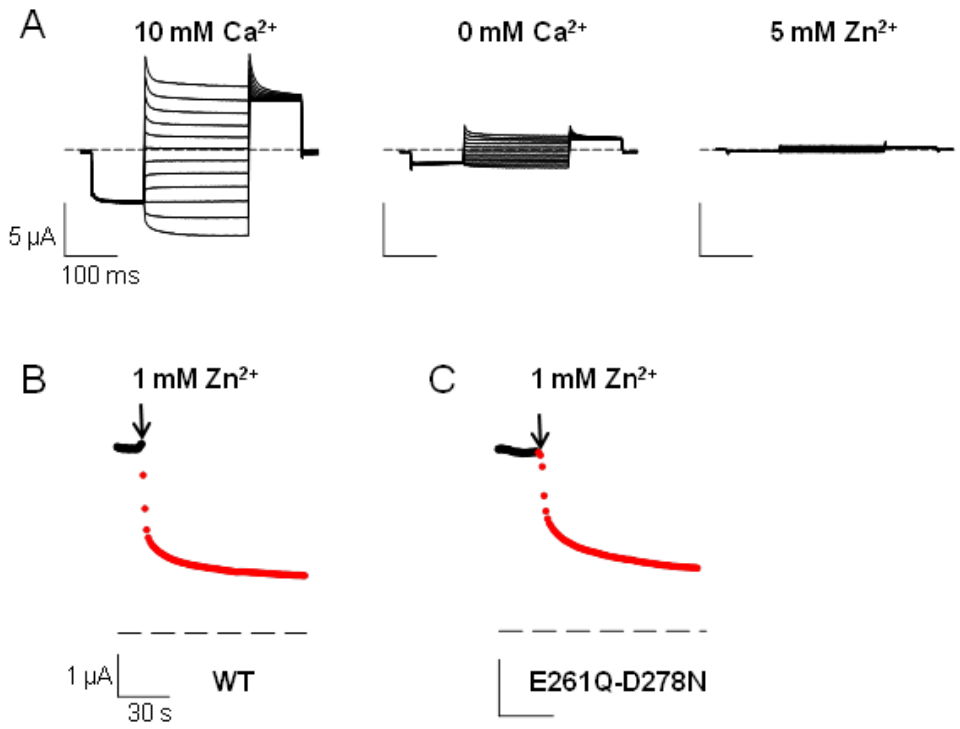


**Fig. 3.12 Effect of $Zn^{2+}$ on CLC-Ka WT and its double mutant E261Q/D278N. (A)** Current responses of ClC-Ka WT to the IV-pulse protocol at 10 mM $Ca^{2+}$, 0 mM $Ca^{2+}$, and 5 mM $Zn^{2+}$. **(B-C)** The mean currents at 60 mV plotted as a function of the time in standard solution (in black) and after perfusion with 1 mM $Zn^{2+}$ (in red).

In the initial experiments on the $Zn^{2+}$-induced inhibition of CLC-Ka we replaced the standard solution (10 $Ca^{2+}$ and pH 7.3) with a solution containing $Zn^{2+}$ in the

absence of $Ca^{2+}$. Consequently, the decrease of the currents may depend on two causes: $Ca^{2+}$ removal and $Zn^{2+}$ addition. To distinct these effects and to isolate the block by $Zn^{2+}$, experiments were performed using solutions containing 5 mM $Zn^{2+}$ and $Ca^{2+}$ at different concentrations (0, 1, 10, or 50 mM). Finally the currents recorded in the presence of $Zn^{2+}$ were normalized to the currents measured at the same $Ca^{2+}$ concentration in the absence of $Zn^{2+}$. These measurements were performed on the double mutant E261Q/D278N and on WT ClC-Ka. Both WT and E261Q /D278N ClC-Ka currents at 5 mM $Zn^{2+}$ and any $Ca^{2+}$ concentration were $\leq$ 10% (± standard error) of the currents recorded at the same $Ca^{2+}$ concentration in the absence of $Zn^{2+}$ (Fig. 3.13). This detailed analysis confirmed our initial results: $Zn^{2+}$ blocks ClC-Ka interacting with a binding site different from the $Ca^{2+}$ binding site formed by E261 and D278.

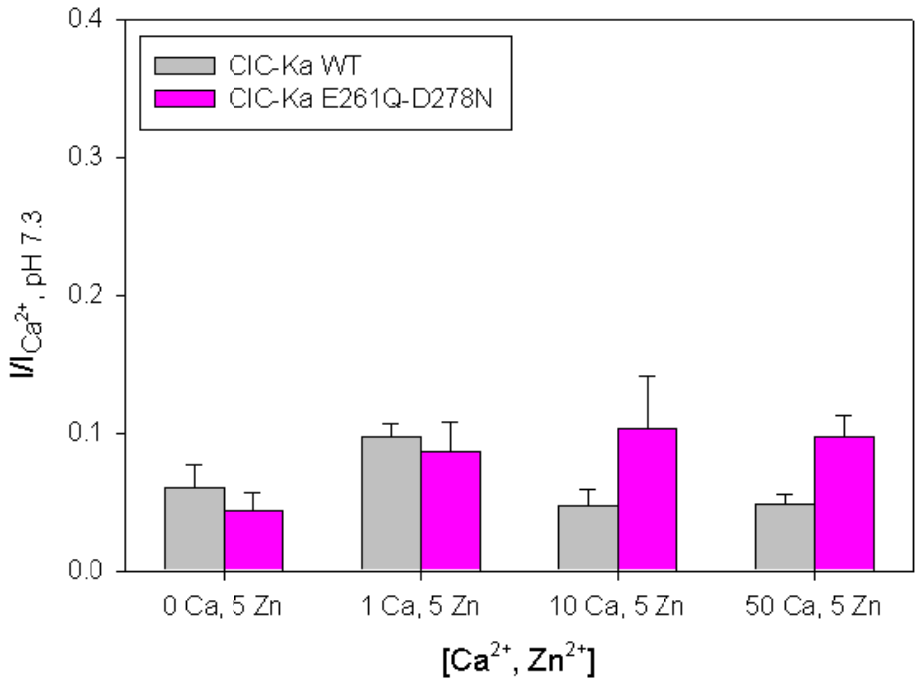


**Fig. 3.13 Effect of $Zn^{2+}$ on CLC-Ka WT and its double mutant E261Q/D278N at different $Ca^{2+}$ concentrations.** Currents recorded at 60 mV in presence of $Zn^{2+}$ were normalized to the currents measured at the same $Ca^{2+}$ concentration in absence of $Zn^{2+}$. The solutions tested contained 0, 1, 10, or 50 $Ca^{2+}$, and 5 mM $Zn^{2+}$. Error bars indicate SEM.

## 3.4 Cloning and expression of a bacterial $K^+$ channel: SynCaK

The gene *sll0993* was identified by an ORF analysis on the genome of the cyanobacterium Synechocistis sp. PCC 6083 (Kaneko et al, 1996). By homology searches based on conserved amino acid sequences of $K^+$ channels, the group of Prof. Ildikò Szabò from the University of Padua highlighted that this gene could encode a putative $Ca^{2+}$ activated $K^+$ channel, called SynCaK. In order to verify this hypothesis, the SynCaK channel was cloned and expressed alone and as an EGFP fusion protein in mammalian cells (CHO). Patch clamp experiments on transfected cells showed outwardly rectifying $K^+$ currents activated by intracellular $Ca^{2+}$. To obtain further information on this channel, we decided to try *Xenopus laevis* oocytes as an alternative expression system.

I obtained two constructs from Prof. Szabò: in one of the constructs the SynCaK ORF was cloned into the pEGFP-N1 vector. The stop codon of SynCaK gene was abolished so that the protein could be expressed as a fusion protein at the N-terminus of EGFP. In the other construct the SynCaK ORF was cloned into the pET28a vector without EGFP. These vectors are optimized for expression in mammalian cells, but not suitable for the expression in oocytes. For this reason, I subcloned the coding sequence of the EGFP fusion protein into the pFrog3 vector, and the coding sequence of SynCaK into the pTLN vector. Both vectors are optimized for the expression in *Xenopus laevis* oocytes. In particular, they use the *Xenopus* β-globin untranslated regions to boost expression of the proteins in oocytes (Lorenz et al, 1996). The SynCaK-EGFP and SynCaK constructs were sequenced and linearized with MluI. Capped cRNA of the SynCaK construct was transcribed *in vitro* using SP6 RNA polymerase, while capped cRNA of the SynCaK-EGFP fusion protein was transcribed with T7 RNA polymerase (mMessage mMachine Kit, Ambion) and injected in *Xenopus* oocytes. Three to five days after injection I performed voltage clamp measurements and fluorescence detection on SynCaK and SynCaK-EGFP injected oocytes.

SynCaK-EGFP injected oocytes (Fig. 3.14A) examined with an inverted fluorescence microscope (excitation 490 nm, emission 515 nm) yielded a significant level of fluorescence compared to not injected oocytes (Fig. 3.14B). This demonstrated that the fusion protein SynCaK-EGFP was expressed in the oocytes.

However we could not establish if the protein is localized in the plasma membrane or in a compartment close to the plasma membrane.

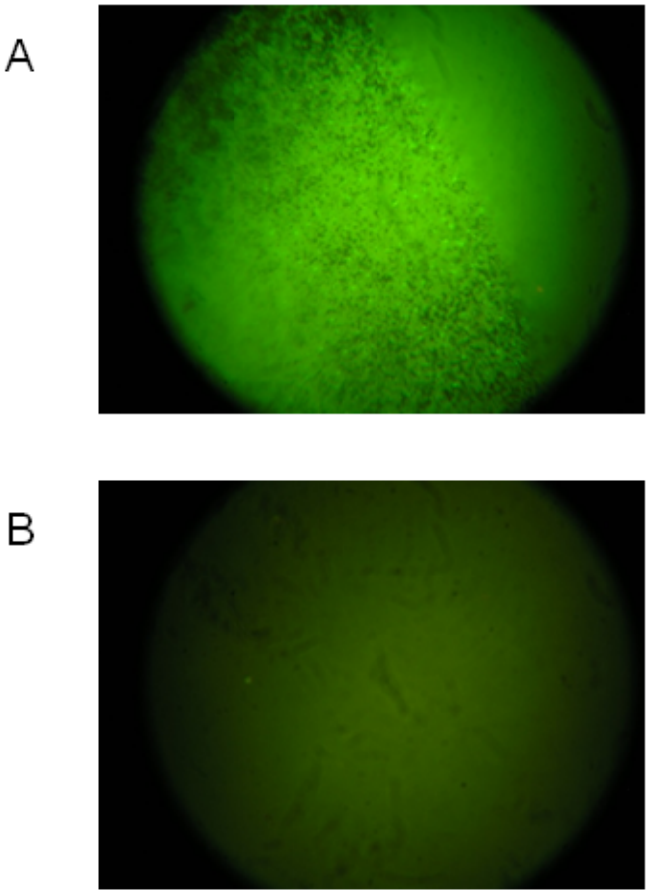


**Fig. 3.14 Detection of fluorescence from a SynCaK injected oocyte (A) and a not injected oocyte (B).**

To test the functional expression of SynCaK and SynCaK-EGFP channels in oocytes, I prepared two solutions at different $Ca^{2+}$ concentration (0 and 5 mM) containing (in mM):

Solution "0 $Ca^{2+}$": 100 NMDG-glutamate, 5 K-Gluconate, 5 $MgSO_4$, 10 Hepes at pH 7.3 (osmolarity: 204 mosm);

Solution "5 $Ca^{2+}$": 100 NMDG-glutamate, 5 K-Gluconate, 5 Ca-$Gluconate_2$, 10 Hepes at pH 7.3 (osmolarity: 204 mosm).

These solutions are deliberately devoid of chloride in order to reduce to a minimum currents mediated by the endogenous calcium activated chloride channel.

To increase intracellular calcium I employed the calcium ionophore A23187 at a concentration of 10 μM.

To verify that the ionophore effectively increases intracellular calcium I applied the following chloride containing solution (in mM):

Solution "100 $Cl^-$", 5 $Ca^{2+}$: 100 NaCl, 5 K-Gluconate, 5 Ca-$Gluconate_2$, 10 Hepes at pH 7.3.

During the voltage clamp experiments the membrane was kept at a holding potential between -55 and -25 mV corresponding to the resting membrane potential in our conditions. To evaluate the presence of current at different potentials, the stimulation protocol comprised a pulse at 60 mV, one at -100 mV and the last at 100 mV (Fig. 3.15A).

A typical voltage clamp experiment was performed in the following way: initially current was acquired in 0 $Ca^{2+}$; in these conditions the channel was expected not to be activated and the recorded current reflects an endogenous conductance (Fig. 3.15B). Next, I replaced the external solution with the "5 $Ca^{2+}$" solution; also in these conditions the channel is expected to be silent because intracellular calcium has not been altered yet. To increase intracellular $Ca^{2+}$, I added the A21387 calcium ionophore. In these conditions (high intracellular $Ca^{2+}$) SyncaK was expected to be activated (Fig. 3.15C). Finally, I replaced the external solution with the "100 $Cl^-$" solution containing the ionophore. This step allowed me to check that the $Ca^{2+}$ concentration in the oocyte was indeed increased by the ionophore. In fact, in these conditions the endogenous $Ca^{2+}$ activated chloride currents mediated by the TMEM16A channel are activated (Fig. 3.15D).

This protocol was applied to both the constructs: SynCaK and SynCaK-EGFP. Unfortunately, both before (Fig. 3.15B) and after the addition of the ionophore (Fig. 3.15C) no current different from background could be detected. Importantly, the high level of current due to TMEM16A channels in 100 mM $Cl^-$ demonstrated that the intracellular $Ca^{2+}$ concentration was effectively increased (Fig. 3.15D). Thus, we concluded that neither construct resulted in functional expression in *Xenopus* oocytes.

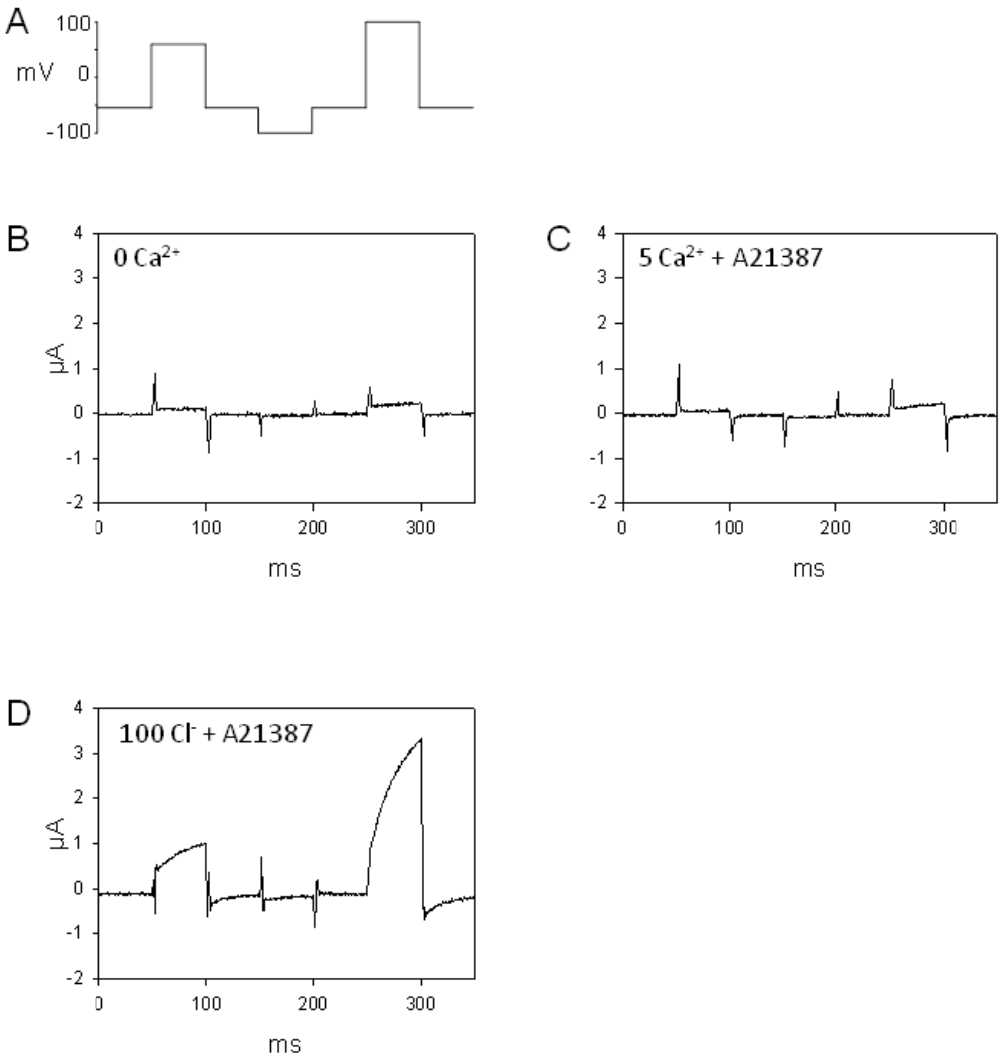


**3.15 Stimulation protocol and corresponding currents recorded from SynCaK-EGFP (oocytes n=6). (A)** Stimulation protocol. **(B)** Current responses to the protocol of the panel A in 0 $Ca^{2+}$. **(C)** Current responses in 5 $Ca^{2+}$ with A21387. **(D)** Current responses in 5 $Ca^{2+}$, 100 $Cl^-$ with A21387.

# 4 Discussion and outlook

## 4.1 Physiological role of CLC-K channels

The human $Cl^-$ channels ClC-Ka and ClC-Kb, as their murine orthologues ClC-K1 and ClC-K2, are expressed in the kidney where they are involved in the mechanism of water and NaCl reabsorption, and in the inner ear where they contribute to the maintenance of a positive endocochlear potential (Rickheit et al, 2008). Mutations in ClC-Kb and barttin cause Bartter's syndrome (type III and type IV, respectively), a kidney disease characterized by severe salt wasting and secondary hypokalemia (Simon et al, 1997). Additional deafness is present in Bartter's syndrome type IV (Birkenhäger et al, 2001). Diseases associated with ClC-Ka mutations are not known, however a digenic defect in the genes encoding ClC-Ka and ClC-Kb results in Bartter's syndrome IV with deafness. This suggests a mutual compensation of CLC-Ka (ClC-K1) and ClC-Kb (ClC-K2) in the inner ear (Schlingmann et al, 2004). Moreover there are hints of the involvement of ClC-K1 (and possibly ClC-Ka) in the urine concentrating mechanism (Matsumura et al, 1999).

Specific modulators of CLC-Ks would be useful tools to treat several pathological conditions. Blockers of CLC-K channels may work as alternative diuretics (Fong, 2004), while activators of these channels may be useful for patients with Bartter's syndrome by enhancing the ClC-Ka activity or increasing the residual activity of ClC-Kb. Because of the important physiological roles of CLC-Ks, the side effects of potential drugs would have to be evaluated carefully. In particular, specific blockers targeted to one of the human ClC-K channels should not impair hearing by maintaining functional the other ClC-K channel. Hence, the identification of potential specific modulators of CLC-Ks is an interesting target of research. On the other hand, the knowledge of the intrinsic mechanisms of modulation of these channels is another intriguing field of study. Extracellular calcium and protons modulate CLC-K channels in the physiological concentration range. In particular, the channels are activated by extracellular calcium and blocked by extracellular protons (Gradogna et al, 2010). Since the kidney has an important role in calcium reabsorption and in the maintenance of acid-base balance (Frick & Bushinsky, 2003;

Jeck et al, 2005), calcium and proton regulation of CLC-K channels is potentially of physiological relevance. The study of the intrinsic modulation of CLC-Ks is important to relate these channels with the physiological processes of the organism; moreover it improves our insight about the mechanisms that regulate the gating processes of CLC proteins.

## 4.2 Niflumic acid (NFA)

Various derivatives of CPP (p-chloro-phenoxy-propionic acid) were found to be potent inhibitors of CLC-Ks (Liantonio et al, 2002; Liantonio et al, 2004; Picollo et al, 2004). In particular, the most potent molecules were MT-189 and RT-93 that block ClC-Ka with apparent $K_D$ values of 7 μM (Liantonio et al, 2008). These compounds could be tested as potential diuretics. Regarding the CLC-K potentiators, NFA represents the most potent activator of the human CLC-K channels described so far. This is quite surprising because NFA is a known inhibitor of $Cl^-$ channels. In fact it blocks ClC-K1(Liantonio et al, 2004; Picollo et al, 2007); instead it increases ClC-Kb currents, and modulates ClC-Ka in a biphasic manner (Liantonio et al, 2006). It was proposed that two different sites are responsible for NFA-induced block and potentiation of ClC-Ka (Picollo et al, 2007). By an extensive site-directed mutagenesis of ClC-Ka combined with electrophysiological measurements, we identified three extracellular residues (L155, G345, and A349) which are involved in the potentiation by NFA (Zifarelli et al, 2010). The extracellular side of helix E (where L155 is situated) and the loop between helices K and L (where G345 and A349 are situated) form a region of ClC-Ka critical for the occurrence of the potentiating effect of NFA. In a surface representation of the structure of the homologous bacterial ClC-ec1 these residues are situated at a distance compatible to form a putative binding site (Zifarelli et al, 2010). Unfortunately, ClC-ec1 and CLC-Ks show low sequence conservation. Hence we cannot predict the arrangement of these residues in ClC-Ka. Further investigations are required to establish if the effect of the mutations identified arises from the lack of an NFA binding site or from conformational changes that are associated with NFA binding. At the present moment we are testing the effect of NFA on other mutants of ClC-Ka. In particular we have concentrated our attention on further mutations that affect the NFA action.

A feature that I would like to underscore is the difficulty in interpretation of the experimental data because of the biphasic nature of the modulation of ClC-Ka by NFA. In fact in our measurements we have to keep in mind the superimposition of two components: the blocking and activating effect of NFA. Even though NFA is the most potent activator of the human CLC-K channels so far, its affinity for these channels is rather low. Moreover it is an anti-inflammatory drug. Hence it can be expected to exert significant side effects. Consequently, we think that further studies should be aimed at identifying more potent activators. Finally, to study the potentiating effect of NFA on murine CLC-K models is not useful because ClC-K1 is blocked by NFA (Gradogna & Pusch, 2010). Keeping in mind the limits of use of this compound, it represents a good model to know the mechanisms that underlie CLC-K activation by potential drugs.

## 4.3 $Ca^{2+}$ and proton modulation

Previous studies demonstrated that ClC-K currents increase by increasing of extracellular $Ca^{2+}$ (Uchida et al, 1995; Sauvé et al, 2000; Waldegger & Jentsch, 2000; Estévez et al, 2001; Waldegger et al, 2002), while acid pH blocks these channels (Uchida et al, 1995; Waldegger & Jentsch, 2000; Estévez et al, 2001; Waldegger et al, 2002). Proton modulation is common in CLC proteins (Friedrich et al, 1999; Accardi & Miller, 2004; Picollo & Pusch, 2005; Zifarelli & Pusch, 2009a), instead $Ca^{2+}$ modulation is not found in other CLC proteins. Interestingly, $Ca^{2+}$ and proton modulation of CLC-K channels occur in physiological concentration ranges. A detailed biophysical analysis of $Ca^{2+}$ and proton regulation of human CLC-K channels allowed us to establish that hCLC-K currents increase with increasing $Ca^{2+}$ concentration without saturation up to 50 mM, while they decrease at acid pH with an almost complete block at pH 6.0 (Gradogna et al, 2010). Kinetic experiments, performed by patch recordings and fast solution exchange, showed that both $Ca^{2+}$ and protons modulate CLC-Ks in an allosteric way. Based on the experimental data, we hypothesized a two state (blocked/unblocked) model for proton modulation, while $Ca^{2+}$ modulation required a four state model because CLC-Ks are open even in the absence of $Ca^{2+}$. The theoretical predictions for proton and $Ca^{2+}$ modulation nicely fitted the experimental data. Moreover a Hill coefficient > 1 suggested that

two protons are required to block the channel. To identify the $Ca^{2+}$ binding site we used a strategy similar to that adopted for NFA. By an extensive site-directed mutagenesis of ClC-Ka combined with electrophysiological measurements, we identified two mutations, E261Q and D278N, which reduced the calcium sensitivity of ClC-Ka. Since E261 from one subunit and D278 from the neighboring subunit are close in the structure of the bacterial homologous ClC-ec1, we hypothesize that they form an intersubunit $Ca^{2+}$ binding site. In fact the double mutant E261D/D278N was completely $Ca^{2+}$-insensitive (Gradogna et al, 2010). Regarding the proton binding site, the identification of the histidine responsible for $H^+$-induced block of the ClC-2 channel (Niemeyer et al, 2009) led us to mutate the corresponding residue of ClC-Ka, H497, in several amino acids. Unfortunately, most mutations resulted in non-functional channels. Because the double mutant E261D/D278N was blocked by acid pH, we prepared the triple mutant E261Q/D278N/H497M. This mutant was insensitive to pH in the range of 5 and 8 demonstrating that H497 is responsible for acid block of CLC-Ka (Gradogna et al, 2010).

## 4.4 A bacterial $Ca^{2+}$-activated $K^+$ channel: SynCaK

The study of the $Ca^{2+}$ modulation of the CLC-K channels has been the main topic of this thesis. Hence when Prof. Ildikò Szabò from the University of Padua proposed to test the functional expression of a novel putative bacterial $K^+$ channel from *Synecocystis* sp. PCC6803 (Kaneko et al, 1996), characterized by the presence of a C-terminal RCK domain, we considered this project an interesting exploration of the $Ca^{2+}$ activation of ion channels in the bacterial world.

I subcloned the coding sequence of the SynCaK-EGFP fusion protein and the coding sequence of SynCaK into vectors optimized for the expression in *Xenopus laevis* oocytes. The significant level of fluorescence yielded by SynCaK-EGFP injected oocytes compared to not injected oocytes demonstrated that the fusion protein SynCaK-EGFP was expressed in the oocytes. However we could not establish if the protein was localized in the plasma membrane or in a compartment close to the plasma membrane. Using the calcium ionophore A23187 to increase intracellular calcium, we performed voltage clamp measurements on SynCaK and SynCaK-EGFP injected oocytes. However, no ionic currents different from that of non-injected

oocytes could be detected. Thus, the *Xenopus* oocyte system appears to be a non-ideal expression system for ion channels from cyanobacteria.

## 4.5 Dissecting the $Ca^{2+}$ binding site

The residues, E261 and D278 that form the $Ca^{2+}$ binding site, are localized in the loop connecting helices I and J. This loop has a particular role in the protein. CLC proteins are dimers formed by two identical subunits. Each subunit in turn is characterized by a pseudo two-fold symmetry axis within the membrane (Dutzler et al, 2002), i.e. each subunit is composed of two halves (α-helices B-I and α-helices J-Q) that are situated in the membrane with opposite orientation. These two halves of each subunit are connected by the I-J loop. Sequence conservation in this loop is relatively poor between the CLC proteins. In particular in the homologous bacterial ClC-ec1 the I-J loop is shorter than in eukaryotic CLC proteins such that the alignment of the sequences of ClC-Ks and that of ClC-ec1 is not univocally determined. Tentatively, we identified E261-ClC-Ka with E235-ClC-ec1 and D278-ClC-Ka with N250-ClC-ec1. In the representation of the bacterial structure, E235 of one subunit and N250 of the neighboring subunit are within ~ 10Å from each other. This distance is too large to form the $Ca^{2+}$ binding site. However the I-J loop of CLC-Ks is longer than that of ClC-ec1.Thus we hypothesize that E261 and D278 do actually form a $Ca^{2+}$ binding site in the ClCK channels. In order to develop a molecular model of the calcium binding site of ClC-Ka, we initiated a collaboration with the group of Dr. Lucy Forrest from the Max-Planck-Institute of Biophysics in Frankfurt/Germany, a group specialized in theoretical structural biophysics. Because $Ca^{2+}$ is often found to be coordinated with carboxylate groups, carbonyl groups, and with oxygen atoms of water molecules, several models could theoretically describe the $Ca^{2+}$ binding site. Based on initial models, we are currently preparing and testing new mutations which will allow choosing the right model among various candidates. Because CLC proteins are homodimers, two symmetrically located $Ca^{2+}$ binding sites are present on each CLC-K channel. The modeling of the experimental data predicted that occupation of a single binding site is sufficient to activate ClC-Ka. To establish if this prediction is true, we are currently preparing heteromeric tandem constructs in which only one of the subunits is manipulated. This will allow us to

study how each residue (glutamate or aspartate) from each subunit contributes to the $Ca^{2+}$ modulation of ClC-Ka.

Another interesting question was if the $Ca^{2+}$ binding site is conserved in CLC-K channels. We performed a dose-response analysis of the calcium effect on the other CLC-K homologues. Human ClC-Kb displays a similar behaviour as ClC-Ka, while rat ClC-K1 is more calcium sensitive than the human CLC-Ks. The high sequence identity and the conserved calcium sensitivity suggest that the calcium binding site is a characteristic shared by all CLC-K channels. The double mutant E261Q/D278N of ClC-Kb and ClC-K1 completely abolished the calcium sensitivity confirming our hypothesis.

Interestingly, calcium sensitivity is a peculiar feature of CLC-Ks. This is not surprising because only one (D278) of the residues that form the $Ca^{2+}$ binding site is conserved in CLC proteins, E261 is not found in most of them. An intriguing issue is if $Ca^{2+}$ sensitivity can be engineered into other CLC proteins. To answer this question, we are preparing a chimeric protein. We decided to insert the I-J loop of ClC-Ka in the background of the ClC-0 channel.

Both ClC-Ka potentiation by NFA and $Ca^{2+}$ activation of CLC-Ks are caused by an increasing of the open probability of these channels. Previously we identified a protein region involved in the binding of NFA (Zifarelli et al, 2010) which is distinct from the $Ca^{2+}$ binding site. Thus, an interesting question is: do $Ca^{2+}$, $H^{+}$, NFA affect the same gating processes? Further studies are required to answer this question.

So far there is no direct evidence for the physiological relevance of the $Ca^{2+}$ sensitivity of CLC-Ks. However some considerations lead us to hypothesize a physiological role for this process. The normal plasma $Ca^{2+}$ concentration ranges from 2.25 to 2.65 mM (the free concentration is ~ 1.2-1.3 mM) (Vargas-Poussou et al, 2002). We detected a consistent activation of the CLC-K channels by $Ca^{2+}$ concentrations ~ 1 mM. $Ca^{2+}$ reabsorption occurs in the kidney, at the level of the proximal tubule and of the TAL trough paracellular pathways (Frick & Bushinsky, 2003). This paracellular flux requires a transepithelial voltage gradient that is generated by the basolateral secretion of $Cl^{-}$, for which CLC-Ks are responsible, and by the apical secretion of $K^{+}$ (Jeck et al, 2005). Consequently, an impairment of $Cl^{-}$ transport causes an abnormal $Ca^{2+}$ absorption. All this suggests that $Ca^{2+}$

reabsorption and $Ca^{2+}$ modulation of CLC-Ks may be interrelated. A way to establish if this hypothesis is true could be the phenotypic analysis of animals that express $Ca^{2+}$-insensitive CLC-K variants.

## 4.6 Specificity of the $Ca^{2+}$ binding site

Another feature to be investigated was the specificity of the $Ca^{2+}$ binding site. The question was: can other ions interact with the same binding site and activate CLC-K channels?

We studied the effect of various divalent cations ($Zn^{2+}$, $Mg^{2+}$, $Ba^{2+}$, $Sr^{2+}$, $Mn^{2+}$) on ClC-Ka, ClC-K1, and ClC-Kb. Both WT ClC-Ka and the double mutant E261Q/D278N, were blocked by 5 mM $Zn^{2+}$ suggesting that $Zn^{2+}$ affects the channel interacting with a separate binding site. Modulation of CLC proteins by $Zn^{2+}$ is very common. Extracellular $Zn^{2+}$ inhibits both $Cl^-$ channels and $Cl^-/H^+$ antiporters (Kürz et al, 1997; Chen, 1998; Clark et al, 1998; Osteen & Mindell, 2008). However all the residues that are found involved in $Zn^{2+}$ block in the other CLC proteins are not conserved in CLC-Ks. Consequently, a distinct mechanism of inhibition must be present in the CLC-K channels. A new topic of study could be the identification of $Zn^{2+}$ binding site.

$Mg^{2+}$ did not activate CLC-K channels at concentrations up to 50 mM. In contrast, CLC-Ka and ClC-Kb were activated by $Ba^{2+}$, $Sr^{2+}$, and $Mn^{2+}$ with a rank order of potency $Ca^{2+}$>$Ba^{2+}$>$Sr^{2+}$. Among all the cations studied, we found that $Ba^{2+}$ activates ClC-Ka in a very similar manner as $Ca^{2+}$, even though it is less potent. By modeling the $Ca^{2+}$- and $Ba^{2+}$-dependence, we could establish that the lower potentiating of $Ba^{2+}$ compared to $Ca^{2+}$ reflects a lower affinity of $Ba^{2+}$ for the binding site. According the theoretical predictions, $Ba^{2+}$ and $Ca^{2+}$ show a similar efficacy on the ClC-Ka channel.

Interestingly, ClC-K1 showed an altered rank order ($Ca^{2+}$> $Sr^{2+}$>> $Ba^{2+}$) compared to the human CLC-K channels. The alignment of the sequence of the loop between helices I and J including E261 and D278 highlights two substitutions in the rat ClC-K1 sequence compared with the human CLC-K channels (I266 instead of L266, R270 instead of S270). We hypothesized that the rather drastic substitution

Arg270Ser could affect the specificity of the calcium-binding site. However, the mutant ClC-Ka S270R has an unchanged specificity compared to WT.

The behavior of ClC-K1 has several peculiar features compared to that of the human CLC-K channels. This channel is blocked by NFA, while NFA activates ClC-Kb and modulates ClC-Ka in biphasic manner. ClC-K1 is more $Ca^{2+}$ sensitive than the human CLC-Ks. Finally the $Ca^{2+}$ binding site of ClC-K1 has a different specificity compared to that of ClC-Ka and ClC-Kb. Based on the high level of functional expression of this channel we can hypothesize that ClC-K1 has a larger open probability than the human ClC-Ka and ClC-Kb. Hence the crucial difference between the CLC-K channels seems to be the regulation of the open probability. What are the gating processes that determine these differences? This is another interesting question for the future.

In all CLC-Ks, the $Ca^{2+}$ insensitive double mutant, E261/D278, was also insensitive to $Ba^{2+}$ and $Sr^{2+}$(Gradogna et al, 2010) demonstrating the specificity of the mechanism of activation of CLC-K channels by $Ca^{2+}$ and the other divalent cations.

# Acknowledgments

I wish to thank:

Dr. Michael Pusch for his invaluable support, help, input and guidance throughout the course of my Ph.D.;

Prof. Ildikò Szabò for the supervision of my work;

Dr. Giovanni Zifarelli for his support and helpful discussion;

and all colleagues of the Institute of Biophysics.

# 5. References


Accardi A & Miller C. 2004. Secondary active transport mediated by a prokaryotic homologue of ClC $Cl^-$ channels. *Nature* 427:803-7

Alekov AK & Fahlke C. 2009. Channel-like slippage modes in the human anion/proton exchanger ClC-4. *J Gen Physiol* 133:485-96

Aromataris EC, Astill DS, Rychkov GY, Bryant SH, Bretag AH & Roberts ML. 1999. Modulation of the gating of ClC-1 by S-(-) 2-(4-chlorophenoxy) propionic acid. *Br J Pharmacol* 126:1375-82

Arreola J, Begenisich T & Melvin JE. 2002. Conformation-dependent regulation of inward rectifier chloride channel gating by extracellular protons. *J Physiol* 541:103-12

Baker M. 2010. Making membrane proteins for structures: a trillion tiny tweaks. *Nat Methods* 7:429-34

Barnard EA, Miledi R & Sumikawa K. 1982. Translation of exogenous messenger RNA coding for nicotinic acetylcholine receptors produces functional receptors in Xenopus oocytes. *Proc R Soc London B Biol Sci* 215:241-6

Bennetts B, Parker MW & Cromer BA. 2007. Inhibition of skeletal muscle CLC-1 chloride channels by low intracellular pH and ATP. *J Biol Chem* 282:32780-91

Bennetts B, Rychkov GY, Ng H-L, Morton CJ, Stapleton D, Parker MW & Cromer BA. 2005. Cytoplasmic ATP-sensing domains regulate gating of skeletal muscle ClC-1 chloride channels. *J Biol Chem* 280:32452-8

Birkenhäger R, Otto E, Schurmann MJ, Vollmer M, Ruf EM, Maier-Lutz I, Beekmann F, Fekete A, Omran H, Feldmann D, Milford DV, Jeck N, Konrad M, Landau D, Knoers NV, Antignac C, Sudbrak R, Kispert A & Hildebrandt F. 2001. Mutation of BSND causes Bartter syndrome with sensorineural deafness and kidney failure. *Nat Genet* 29:310-4

Blanz J, Schweizer M, Auberson M, Maier H, Muenscher A, Hubner CA & Jentsch TJ. 2007. Leukoencephalopathy upon disruption of the chloride channel ClC-2. *J Neurosci* 27:6581-9

Bösl MR, Stein V, Hübner C, Zdebik AA, Jordt SE, Mukhopadhyay AK, Davidoff MS, Holstein AF & Jentsch TJ. 2001. Male germ cells and photoreceptors, both dependent on close cell-cell interactions, degenerate upon ClC-2 Cl(-) channel disruption. *EMBO J* 20:1289-99

Caputo A, Caci E, Ferrera L, Pedemonte N, Barsanti C, Sondo E, Pfeffer U, Ravazzolo R, Zegarra-Moran O & Galietta LJ. 2008. TMEM16A, a membrane protein associated with calcium-dependent chloride channel activity. *Science* 322:590-4

Chen MF & Chen TY. 2001. Different fast-gate regulation by external Cl(-) and H(+) of the muscle- type ClC chloride channels. *J Gen Physiol* 118:23-32

Chen TY. 1998. Extracellular zinc ion inhibits ClC-0 chloride channels by facilitating slow gating. *J Gen Physiol* 112:715-26

Clark S, Jordt SE, Jentsch TJ & Mathie A. 1998. Characterization of the hyperpolarization-activated chloride current in dissociated rat sympathetic neurons. *J Physiol* 506:665-78

De Angeli A, Monachello D, Ephritikhine G, Frachisse JM, Thomine S, Gambale F & Barbier-Brygoo H. 2006. The nitrate/proton antiporter AtCLCa mediates nitrate accumulation in plant vacuoles. *Nature* 442:939-42.

De Angeli A, Moran O, Wege S, Filleur S, Ephritikhine G, Thomine S, Barbier-Brygoo H & Gambale F. 2009. ATP binding to the C terminus of the Arabidopsis thaliana nitrate/proton antiporter, AtCLCa, regulates nitrate transport into plant vacuoles. *J Biol Chem* 284:26526-32

De Luca A, Tricarico D, Wagner R, Bryant SH, Tortorella V & Conte Camerino D. 1992. Opposite effects of enantiomers of clofibric acid derivative on rat skeletal muscle chloride conductance: antagonism studies and theoretical modeling of two different receptor site interactions. *J Pharmacol Exp Ther* 260:364-8

Deschenes G & Fila M. 2011. Primary molecular disorders and secondary biological adaptations in bartter syndrome. *Int J Nephrol* 2011:396209

Diamond JM & Wright EM. 1969. Biological membranes: the physical basis of ion and nonelectrolyte selectivity. *Annu Rev Physiol* 31:581-646

Dong J, Shi N, Berke I, Chen L & Jiang Y. 2005. Structures of the MthK RCK domain and the effect of Ca2+ on gating ring stability. *J Biol Chem* 280:41716-24

Doyle DA, Morais Cabral J, Pfuetzner RA, Kuo A, Gulbis JM, Cohen SL, Chait BT & MacKinnon R. 1998. The structure of the potassium channel: molecular basis of $K^+$ conduction and selectivity. *Science* 280:69-77

Duffield MD, Rychkov GY, Bretag AH & Roberts ML. 2005. Zinc inhibits human ClC-1 muscle chloride channel by interacting with its common gating mechanism. *J Physiol* 568:5-12

Dutzler R, Campbell EB, Cadene M, Chait BT & MacKinnon R. 2002. X-ray structure of a ClC chloride channel at 3.0 Å reveals the molecular basis of anion selectivity. *Nature* 415:287-94

Dutzler R, Campbell EB & MacKinnon R. 2003. Gating the selectivity filter in ClC chloride channels. *Science* 300:108-12

Elinder F & Arhem P. 2003. Metal ion effects on ion channel gating. *Q Rev Biophys* 36:373-427

Estévez R, Boettger T, Stein V, Birkenhäger R, Otto E, Hildebrandt F & Jentsch TJ. 2001. Barttin is a $Cl^-$ channel beta-subunit crucial for renal $Cl^-$ reabsorption and inner ear $K^+$ secretion. *Nature* 414:558-61

Estévez R & Jentsch TJ. 2002. CLC chloride channels: correlating structure with function. *Curr Opin Struct Biol* 12:531-9

Feng L, Campbell EB, Hsiung Y & Mackinnon R. 2010. Structure of a eukaryotic CLC transporter defines an intermediate state in the transport cycle. *Science* 330:635-41

Ferrera L, Caputo A & Galietta LJ. 2010. TMEM16A protein: a new identity for Ca(2+)-dependent Cl channels. *Physiology (Bethesda)* 25:357-63

Fischer M, Janssen AG & Fahlke C. 2010. Barttin activates ClC-K channel function by modulating gating. *J Am Soc Nephrol* 21:1281-9

Fisher SE, Black GC, Lloyd SE, Hatchwell E, Wrong O, Thakker RV & Craig IW. 1994. Isolation and partial characterization of a chloride channel gene which is expressed in kidney and is a candidate for Dent's disease (an X-linked hereditary nephrolithiasis). *Hum Mol Genet* 3:2053-9

Fong P. 2004. CLC-K channels: if the drug fits, use it. *EMBO Rep* 5:565-6.
Forge A & Wright T. 2002. The molecular architecture of the inner ear. *Br Med Bull* 63:5-24
Frick KK & Bushinsky DA. 2003. Molecular mechanisms of primary hypercalciuria. *J Am Soc Nephrol* 14:1082-95
Friedrich T, Breiderhoff T & Jentsch TJ. 1999. Mutational analysis demonstrates that ClC-4 and ClC-5 directly mediate plasma membrane currents. *J Biol Chem* 274:896-902
Gradogna A, Babini E, Picollo A & Pusch M. 2010. A regulatory calcium-binding site at the subunit interface of CLC-K kidney chloride channels. *J Gen Physiol* 136:311-23
Gradogna A & Pusch M. 2010. Molecular pharmacology of kidney and inner ear CLC-K chloride channels. *Frontiers in Pharmacology* 1:130
Hanke W & Miller C. 1983. Single chloride channels from *Torpedo* electroplax. Activation by protons. *J Gen Physiol* 82:25-45
Hartzell C, Putzier I & Arreola J. 2005. Calcium-activated chloride channels. *Ann Rev Physiol* 67:719-58
Heginbotham L, Lu Z, Abramson T & MacKinnon R. 1994. Mutations in the K+ channel signature sequence. *Biophys J* 66:1061-7
Hille B. 2001. Ion channels of excitable membranes. Vol. 3rd edition. Sinauer, Sunderland, Mass. xviii, 814 , [8] of plates pp.
Hodgkin AL, Huxley AF & Katz B. 1952. Measurement of current-voltage relations in the membrane of the giant axon of Loligo. *J Physiol* 116:424-48
Jayaram H, Robertson JL, Wu F, Williams C & Miller C. 2011. Structure of a slow CLC $Cl^-/H^+$ antiporter from a Cyanobacterium. *Biochemistry* 50:788-94
Jeck N, Schlingmann KP, Reinalter SC, Komhoff M, Peters M, Waldegger S & Seyberth HW. 2005. Salt handling in the distal nephron: lessons learned from inherited human disorders. *Am J Physiol Regul Integr Comp Physiol* 288:R782-R95
Jentsch TJ. 2008. CLC chloride channels and transporters: from genes to protein structure, pathology and physiology. *Crit Rev Biochem Mol Biol* 43:3-36
Jentsch TJ, Friedrich T, Schriever A & Yamada H. 1999. The CLC chloride channel family. *Pflügers Arch* 437:783-95
Jentsch TJ, Stein V, Weinreich F & Zdebik AA. 2002. Molecular structure and physiological function of chloride channels. *Physiol Rev* 82:503-68
Jentsch TJ, Steinmeyer K & Schwarz G. 1990. Primary structure of *Torpedo marmorata* chloride channel isolated by expression cloning in *Xenopus* oocytes. *Nature* 348:510-4
Jiang Y, Lee A, Chen J, Cadene M, Chait BT & MacKinnon R. 2002. Crystal structure and mechanism of a calcium-gated potassium channel. *Nature* 417:515-22
Jiang Y, Pico A, Cadene M, Chait BT & MacKinnon R. 2001. Structure of the RCK domain from the E. coli K+ channel and demonstration of its presence in the human BK channel. *Neuron* 29:593-601
Jordt SE & Jentsch TJ. 1997. Molecular dissection of gating in the ClC-2 chloride channel. *Embo J* 16:1582-92
Kaneko T, Sato S, Kotani H, Tanaka A, Asamizu E, Nakamura Y, Miyajima N, Hirosawa M, Sugiura M, Sasamoto S, Kimura T, Hosouchi T, Matsuno A,

Muraki A, Nakazaki N, Naruo K, Okumura S, Shimpo S, Takeuchi C, Wada T, Watanabe A, Yamada M, Yasuda M & Tabata S. 1996. Sequence analysis of the genome of the unicellular cyanobacterium Synechocystis sp. strain PCC6803. II. Sequence determination of the entire genome and assignment of potential protein-coding regions (supplement). *DNA Res* 3:109-36

Kieferle S, Fong P, Bens M, Vandewalle A & Jentsch TJ. 1994. Two highly homologous members of the ClC chloride channel family in both rat and human kidney. *Proc Natl Acad Sci U S A* 91:6943-7

Kobayashi K, Uchida S, Mizutani S, Sasaki S & Marumo F. 2001. Intrarenal and cellular localization of CLC-K2 protein in the mouse kidney. *J Am Soc Nephrol* 12:1327-34

Kobayashi K, Uchida S, Okamura HO, Marumo F & Sasaki S. 2002. Human CLC-KB gene promoter drives the EGFP expression in the specific distal nephron segments and inner ear. *J Am Soc Nephrol* 13:1992-8

Koeppen BM. 2009. The kidney and acid-base regulation. *Adv Physiol Educ* 33:275-81

Kornak U, Kasper D, Bösl MR, Kaiser E, Schweizer M, Schulz A, Friedrich W, Delling G & Jentsch TJ. 2001. Loss of the ClC-7 chloride channel leads to osteopetrosis in mice and man. *Cell* 104:205-15

Kürz L, Wagner S, George AL, Jr. & Rüdel R. 1997. Probing the major skeletal muscle chloride channel with $Zn^{2+}$ and other sulfhydryl-reactive compounds. *Pflügers Arch* 433:357-63

Lang F. 2010. Modulation of ClC-K channel function by the accessory subunit barttin. *J Am Soc Nephrol* 21:1238-9

Lange PF, Wartosch L, Jentsch TJ & Fuhrmann JC. 2006. ClC-7 requires Ostm1 as a beta-subunit to support bone resorption and lysosomal function. *Nature* 440:220-3

Leisle L, Ludwig CF, Wagner FA, Jentsch TJ & Stauber T. 2011. ClC-7 is a slowly voltage-gated 2Cl(-)/1H(+)-exchanger and requires Ostm1 for transport activity. *Embo J* 30:2140-52

Li X, Shimada K, Showalter LA & Weinman SA. 2000. Biophysical properties of ClC-3 differentiate it from swelling-activated chloride channels in Chinese hamster ovary-K1 cells. *J Biol Chem* 275:35994-8

Liantonio A, Accardi A, Carbonara G, Fracchiolla G, Loiodice F, Tortorella P, Traverso S, Guida P, Pierno S, De Luca A, Camerino DC & Pusch M. 2002. Molecular requisites for drug binding to muscle CLC-1 and renal CLC-K channel revealed by the use of phenoxy-alkyl derivatives of 2-(p-chlorophenoxy)propionic acid. *Mol Pharmacol* 62:265-71

Liantonio A, Picollo A, Babini E, Carbonara G, Fracchiolla G, Loiodice F, Tortorella V, Pusch M & Camerino DC. 2006. Activation and inhibition of kidney CLC-K chloride channels by fenamates. *Mol Pharmacol* 69:165-73

Liantonio A, Picollo A, Carbonara G, Fracchiolla G, Tortorella P, Loiodice F, Laghezza A, Babini E, Zifarelli G, Pusch M & Camerino DC. 2008. Molecular switch for CLC-K $Cl^-$ channel block/activation: Optimal pharmacophoric requirements towards high-affinity ligands. *Proc Natl Acad Sci U S A* 105:1369-73

Liantonio A, Pusch M, Picollo A, Guida P, De Luca A, Pierno S, Fracchiolla G, Loiodice F, Tortorella P & Conte Camerino D. 2004. Investigations of

pharmacologic properties of the renal CLC-K1 chloride channel co-expressed with barttin by the use of 2-(p-Chlorophenoxy)propionic acid derivatives and other structurally unrelated chloride channels blockers. *J Am Soc Nephrol* 15:13-20

Lin YW, Lin CW & Chen TY. 1999. Elimination of the slow gating of ClC-0 chloride channel by a point mutation. *J Gen Physiol* 114:1-12

Lloyd SE, Pearce SH, Fisher SE, Steinmeyer K, Schwappach B, Scheinman SJ, Harding B, Bolino A, Devoto M, Goodyer P, Rigden SP, Wrong O, Jentsch TJ, Craig IW & Thakker RV. 1996. A common molecular basis for three inherited kidney stone diseases. *Nature* 379:445-9

Lobet S & Dutzler R. 2006. Ion-binding properties of the ClC chloride selectivity filter. *Embo J* 25:24-33

Lorenz C, Pusch M & Jentsch TJ. 1996. Heteromultimeric CLC chloride channels with novel properties. *Proc Natl Acad Sci U S A* 93:13362-6

Ludewig U, Pusch M & Jentsch TJ. 1996. Two physically distinct pores in the dimeric ClC-0 chloride channel. *Nature* 383:340-3

MacKinnon R. 2003. Potassium channels. *FEBS Lett* 555:62-5

Maduke M, Miller C & Mindell JA. 2000. A decade of CLC chloride channels: structure, mechanism, and many unsettled questions. *Annu Rev Biophys Biomol Struct* 29:411-38

Markovic S & Dutzler R. 2007. The structure of the cytoplasmic domain of the chloride channel ClC-Ka reveals a conserved interaction interface. *Structure* 15:715-25

Marmont G. 1949. Studies on the axon membrane; a new method. *J Cell Physiol* 34:351-82

Matsumura Y, Uchida S, Kondo Y, Miyazaki H, Ko SB, Hayama A, Morimoto T, Liu W, Arisawa M, Sasaki S & Marumo F. 1999. Overt nephrogenic diabetes insipidus in mice lacking the CLC-K1 chloride channel. *Nat Genet* 21:95-8

Meyer S, Savaresi S, Forster IC & Dutzler R. 2007. Nucleotide recognition by the cytoplasmic domain of the human chloride transporter ClC-5. *Nat Struct Mol Biol* 14:60-7

Middleton RE, Pheasant DJ & Miller C. 1996. Homodimeric architecture of a ClC-type chloride ion channel. *Nature* 383:337-40

Miledi R, Parker I & Sumikawa K. 1982. Properties of acetylcholine receptors translated by cat muscle mRNA in Xenopus oocytes. *Embo J* 1:1307-12

Miller C. 1982. Open-state substructure of single chloride channels from *Torpedo* electroplax. *Philos Trans R Soc Lond B Biol Sci* 299:401-11

Miller C & Richard EA. 1990. The voltage-dependent chloride channel of *Torpedo* Electroplax. Intimations of molecular structure from quirks of single-channel function. In Chloride Channels and Carriers in Nerve, Muscle and Glial Cells. Vol. F.J. Alvarez-Leefmans, and J.M. Russell, editors. Plenum, New York. 383-405.

Miller C & White MM. 1980. A voltage-dependent chloride conductance channel from *Torpedo* electroplax membrane. *Ann NY Acad Sci* 341:534-51

Neagoe I, Stauber T, Fidzinski P, Bergsdorf EY & Jentsch TJ. 2010. The late endosomal ClC-6 mediates proton/chloride countertransport in heterologous plasma membrane expression. *J Biol Chem* 285:21689-97

Niemeyer MI, Cid LP, Yusef YR, Briones R & Sepúlveda FV. 2009. Voltage-dependent and -independent titration of specific residues accounts for complex gating of a ClC chloride channel by extracellular protons. *J Physiol* 587:1387-400

Osteen JD & Mindell JA. 2008. Insights into the ClC-4 transport mechanism from studies of Zn2+ inhibition. *Biophys J* 95:4668-75

Pau VP, Smith FJ, Taylor AB, Parfenova LV, Samakai E, Callaghan MM, Abarca-Heidemann K, Hart PJ & Rothberg BS. 2011. Structure and function of multiple Ca2+-binding sites in a K+ channel regulator of K+ conductance (RCK) domain. *Proc Natl Acad Sci U S A* 108:17684-9

Picollo A, Liantonio A, Babini E, Camerino DC & Pusch M. 2007. Mechanism of interaction of niflumic acid with heterologously expressed kidney CLC-K chloride channels. *J Membr Biol* 216:73-82

Picollo A, Liantonio A, Didonna MP, Elia L, Camerino DC & Pusch M. 2004. Molecular determinants of differential pore blocking of kidney CLC-K chloride channels. *EMBO Rep* 5:584-9

Picollo A, Malvezzi M & Accardi A. 2010. Proton block of the CLC-5 $Cl^-/H^+$ exchanger. *J Gen Physiol* 135:653-9

Picollo A, Malvezzi M, Houtman JC & Accardi A. 2009. Basis of substrate binding and conservation of selectivity in the CLC family of channels and transporters. *Nat Struct Mol Biol* 16:1294-301

Picollo A & Pusch M. 2005. Chloride/proton antiporter activity of mammalian CLC proteins ClC-4 and ClC-5. *Nature* 436:420-3

Poët M, Kornak U, Schweizer M, Zdebik AA, Scheel O, Hoelter S, Wurst W, Schmitt A, Fuhrmann JC, Planells-Cases R, Mole SE, Hübner CA & Jentsch TJ. 2006. Lysosomal storage disease upon disruption of the neuronal chloride transport protein ClC-6. *Proc Natl Acad Sci U S A* 103:13854-9

Pusch M, Liantonio A, Bertorello L, Accardi A, De Luca A, Pierno S, Tortorella V & Camerino DC. 2000. Pharmacological characterization of chloride channels belonging to the ClC family by the use of chiral clofibric acid derivatives. *Mol Pharmacol* 58:498-507

Pusch M, Ludewig U, Rehfeldt A & Jentsch TJ. 1995. Gating of the voltage-dependent chloride channel CIC-0 by the permeant anion. *Nature* 373:527-31

Rickheit G, Maier H, Strenzke N, Andreescu CE, De Zeeuw CI, Muenscher A, Zdebik AA & Jentsch TJ. 2008. Endocochlear potential depends on Cl(-) channels: mechanism underlying deafness in Bartter syndrome IV. *Embo J* 2:2

Riordan JR, Rommens JM, Kerem B, Alon N, Rozmahel R, Grzelczak Z, Zielenski J, Lok S, Plavsic N, Chou JL, Drumm ML, Iannuzzi MC, Collins FS & Tsui L-C. 1989. Identification of the cystic fibrosis gene: cloning and characterization of complementary DNA. *Science* 245:1066-73

Rychkov GY, Pusch M, Astill DS, Roberts ML, Jentsch TJ & Bretag AH. 1996. Concentration and pH dependence of skeletal muscle chloride channel ClC-1. *J Physiol* 497:423-35

Sauvé R, Cai S, Garneau L, Klein H & Parent L. 2000. pH and external Ca(2+) regulation of a small conductance Cl(-) channel in kidney distal tubule. *Biochim Biophys Acta* 1509:73-85

Scheel O, Zdebik AA, Lourdel S & Jentsch TJ. 2005. Voltage-dependent electrogenic chloride/proton exchange by endosomal CLC proteins. *Nature* 436:424-7

Schild L, Lu Y, Gautschi I, Schneeberger E, Lifton RP & Rossier BC. 1996. Identification of a PY motif in the epithelial Na channel subunits as a target sequence for mutations causing channel activation found in Liddle syndrome. *Embo J* 15:2381-7

Schlingmann KP, Konrad M, Jeck N, Waldegger P, Reinalter SC, Holder M, Seyberth HW & Waldegger S. 2004. Salt wasting and deafness resulting from mutations in two chloride channels. *N Engl J Med* 350:1314-9

Scholl U, Hebeisen S, Janssen AG, Müller-Newen G, Alekov A & Fahlke C. 2006. Barttin modulates trafficking and function of ClC-K channels. *Proc Natl Acad Sci U S A* 103:11411-6.

Schroeder BC, Cheng T, Jan YN & Jan LY. 2008. Expression cloning of TMEM16A as a calcium-activated chloride channel subunit. *Cell* 134:1019-29

Scott JW, Hawley SA, Green KA, Anis M, Stewart G, Scullion GA, Norman DG & Hardie DG. 2004. CBS domains form energy-sensing modules whose binding of adenosine ligands is disrupted by disease mutations. *J Clin Invest* 113:274-84

Simon DB, Bindra RS, Mansfield TA, Nelson-Williams C, Mendonca E, Stone R, Schurman S, Nayir A, Alpay H, Bakkaloglu A, Rodriguez-Soriano J, Morales JM, Sanjad SA, Taylor CM, Pilz D, Brem A, Trachtman H, Griswold W, Richard GA, John E & Lifton RP. 1997. Mutations in the chloride channel gene, CLCNKB, cause Bartter's syndrome type III. *Nat Genet* 17:171-8

Simon DB, Karet FE, Hamdan JM, Pietro AD, Sanjad SA & Lifton RP. 1996a. Bartter's syndrome, hypokalaemic alkalosis with hypercalciuria, is caused by mutations in the Na-K-2CI cotransporter NKCC2. *Nat Genet* 13:183-8

Simon DB, Karet FE, Rodriguez-Soriano J, Hamdan JH, DiPietro A, Trachtman H, Sanjad SA & Lifton RP. 1996b. Genetic heterogeneity of Barter's syndrome revealed by mutations in the $K^+$ channel, ROMK. *Nat Genet* 14:152-6

Stauber T & Jentsch TJ. 2010. Sorting motifs of the endosomal/lysosomal CLC chloride transporters. *J Biol Chem* 285:34537-48

Steinmeyer K, Ortland C & Jentsch TJ. 1991. Primary structure and functional expression of a developmentally regulated skeletal muscle chloride channel. *Nature* 354:301-4

Stobrawa SM, Breiderhoff T, Takamori S, Engel D, Schweizer M, Zdebik AA, Bösl MR, Ruether K, Jahn H, Draguhn A, Jahn R & Jentsch TJ. 2001. Disruption of ClC-3, a chloride channel expressed on synaptic vesicles, leads to a loss of the hippocampus. *Neuron* 29:185-96

Thiemann A, Gründer S, Pusch M & Jentsch TJ. 1992. A chloride channel widely expressed in epithelial and non-epithelial cells. *Nature* 356:57-60

Traverso S, Zifarelli G, Aiello R & Pusch M. 2006. Proton sensing of CLC-0 mutant E166D. *J Gen Physiol* 127:51-66

Tseng P-Y, Bennetts B & Chen T-Y. 2007. Cytoplasmic ATP inhibition of CLC-1 is enhanced by low pH. *J Gen Physiol* 130:217-21

Uchida S, Sasaki S, Furukawa T, Hiraoka M, Imai T, Hirata Y & Marumo F. 1993. Molecular cloning of a chloride channel that is regulated by dehydration and expressed predominantly in kidney medulla. *J Biol Chem* 268:3821-4

Uchida S, Sasaki S, Nitta K, Uchida K, Horita S, Nihei H & Marumo F. 1995. Localization and functional characterization of rat kidney-specific chloride channel, ClC-K1. *J Clin Invest* 95:104-13

Vargas-Poussou R, Huang C, Hulin P, Houillier P, Jeunemaitre X, Paillard M, Planelles G, Dechaux M, Miller RT & Antignac C. 2002. Functional characterization of a calcium-sensing receptor mutation in severe autosomal dominant hypocalcemia with a Bartter-like syndrome. *J Am Soc Nephrol* 13:2259-66

Waldegger S, Jeck N, Barth P, Peters M, Vitzthum H, Wolf K, Kurtz A, Konrad M & Seyberth HW. 2002. Barttin increases surface expression and changes current properties of ClC-K channels. *Pflügers Arch* 444:411-8

Waldegger S & Jentsch TJ. 2000. Functional and structural analysis of ClC-K chloride channels involved in renal disease. *J Biol Chem* 275:24527-33

Weinreich F & Jentsch TJ. 2001. Pores formed by single subunits in mixed dimers of different CLC chloride channels. *J Biol Chem* 276:2347-53

Wellhauser L, Kuo HH, Stratford FL, Ramjeesingh M, Huan LJ, Luong W, Li C, Deber CM & Bear CE. 2006. Nucleotides bind to the C-terminus of ClC-5. *Biochem J* 398:289-94

White MM & Miller C. 1979. A voltage-gated anion channel from the electric organ of *Torpedo californica*. *J Biol Chem* 254:10161-6

Yang YD, Cho H, Koo JY, Tak MH, Cho Y, Shim WS, Park SP, Lee J, Lee B, Kim BM, Raouf R, Shin YK & Oh U. 2008. TMEM16A confers receptor-activated calcium-dependent chloride conductance. *Nature* 455:1210-5

Zanetti M, Teardo E, La Rocca N, Zulkifli L, Checchetto V, Shijuku T, Sato Y, Giacometti GM, Uozumi N, Bergantino E & Szabo I. 2010. A novel potassium channel in photosynthetic cyanobacteria. *PLoS One* 5:e10118

Zdebik AA, Wangemann P & Jentsch TJ. 2009. Potassium ion movement in the inner ear: insights from genetic disease and mouse models. *Physiology (Bethesda)* 24:307-16

Zdebik AA, Zifarelli G, Bergsdorf EY, Soliani P, Scheel O, Jentsch TJ & Pusch M. 2008. Determinants of anion-proton coupling in mammalian endosomal CLC proteins. *J Biol Chem* 283:4219-27

Zifarelli G, Liantonio A, Gradogna A, Picollo A, Gramegna G, De Bellis M, Murgia AR, Babini E, Camerino DC & Pusch M. 2010. Identification of sites responsible for the potentiating effect of niflumic acid on ClC-Ka kidney chloride channels. *Br J Pharmacol* 160:1652-61

Zifarelli G, Murgia AR, Soliani P & Pusch M. 2008. Intracellular proton regulation of ClC-0. *J Gen Physiol* 132:185-98

Zifarelli G & Pusch M. 2007. CLC chloride channels and transporters: a biophysical and physiological perspective. *Rev Physiol Biochem Pharmacol* 158:23-76

Zifarelli G & Pusch M. 2009a. Conversion of the 2 Cl(-)/1 H(+) antiporter ClC-5 in a NO(3)(-)/H(+) antiporter by a single point mutation. *Embo J* 28:175-82

Zifarelli G & Pusch M. 2009b. Intracellular regulation of human ClC-5 by adenine nucleotides. *EMBO Rep* 10:1111-6

Zifarelli G & Pusch M. 2010. The role of protons in fast and slow gating of the Torpedo chloride channel ClC-0. *Eur Biophys J* 39:869-75